Differences in toxicity, mitochondrial function and miRNome in human cells exposed in vitro to Cd as CdS quantum dots or ionic Cd

Elsevier Editorial System(tm) for Journal of Hazardous Materials

Manuscript Draft

Manuscript Number: HAZMAT-D-19-04345R2

Title: Differences in toxicity, mitochondrial function and miRNome in human cells exposed in vitro to Cd as CdS quantum dots or ionic Cd

Article Type: Research Paper

Keywords: miRNA; quantum dot; HepG2; THP-1; cadmium

Corresponding Author: Professor Nelson Marmiroli,

Corresponding Author's Institution: University of Parma

First Author: Laura Paesano

Order of Authors: Laura Paesano; Marta Marmiroli; Massimiliano G Bianchi; Jason C White; Ovidio Bussolati; Andrea Zappettini; Marco Villani; Nelson Marmiroli

Abstract: Cadmium is toxic to humans, although Cd-based quantum dots exerts less toxicity. Human hepatocellular carcinoma cells (HepG2) and macrophages (THP-1) were exposed to ionic Cd, Cd(II), and cadmium sulfide quantum dots (CdS QDs), and cell viability, cell integrity, Cd accumulation, mitochondrial function and miRNome profile were evaluated. Cell-type and Cd form-specific responses were found: CdS QDs affected cell viability more in HepG2 than in THP-1; respective IC20 values were ~3 and ~50 µgml-1. In both cell types, Cd(II) exerted greater effects on viability.
Mitochondrial membrane function in HepG2 cells was reduced 70% with 40 µgml-1 CdS QDs but was totally inhibited by Cd(II) at corresponding amounts. In THP-1 cells, CdS QDs has less effect on mitochondrial function; 50 µgml-1 CdS QDs or equivalent Cd(II) caused 30% reduction or total inhibition, respectively. The different in vitro effects of CdS QDs were unrelated to Cd uptake, which was greater in THP-1 cells.
For both cell types, changes in the expression of miRNAs (miR-222, miR-181a, miR-142-3p, miR-15) were found with CdS QDs, which may be used as biomarkers of hazard nanomaterial exposure. The cell-specific miRNome profiles were indicative of a more conservative autophagic response in THP-1 and as apoptosis as in HepG2.

Cover Letter

Dear Editor,

we wish to thank you and the Reviewer #1 for the helpful suggestions.

We have prepared accordingly a modified version of the paper '*Differences in toxicity, mitochondrial function and miRNome in human cells exposed in vitro to Cd as CdS quantum dots or ionic Cd'*, that we hope it is now suitable with the requests and publishable on *Journal of Hazardous Materials*. Please also found enclosed separately a 'Response to Reviewer' for your considerations.

Thank you again because we are certain the procedure has enriched our paper.

With best regards

Nelson Marmiroli

Director of CINSA
Emeritus Professor
University of Parma

Response to Reviewer

Reviewer #1

	Response
1. The abstract needs work and inclusion of the objectives and specific results.	The authors accept the reviewer suggestion. Therefore, the abstract has been modified: [*Cadmium is toxic to humans, although Cd-based quantum dots exerts less toxicity. Human hepatocellular carcinoma cells (HepG2) and macrophages (THP-1) were exposed to ionic Cd, Cd(II), and cadmium sulfide quantum dots (CdS QDs), and cell viability, cell integrity, Cd accumulation, mitochondrial function and miRNome profile were evaluated.* *Cell-type and Cd form-specific responses were found: CdS QDs affected cell viability more in HepG2 than in THP-1; respective IC_{20} values were ~ 3 and ~ 50 µg ml^{-1}. In both cell types, Cd(II) exerted greater effects on viability.* *Mitochondrial membrane function in HepG2 cells was reduced 70% with 40 µg ml^{-1} CdS QDs but was totally inhibited by Cd(II) at corresponding amounts. In THP-1 cells, CdS QDs has less effect on mitochondrial function; 50 µg ml^{-1} CdS QDs or equivalent Cd(II) caused 30% reduction or total inhibition, respectively. The different in vitro effects of CdS QDs were unrelated to Cd uptake, which was greater in THP-1 cells.* *For both cell types, changes in the expression of miRNAs (miR-222, miR-181a, miR-142-3p, miR-15) were found with CdS QDs, which may be used as biomarkers of hazard nanomaterial exposure. The cell-specific miRNome profiles were indicative of a more conservative autophagic response in THP-1 and as apoptosis as in HepG2.*]
2. I cannot find the data to support that the NPs aggregate/agglomerate size were characterized in cell media.	Details on the characterization in cell media are now reported in Paragraph 2.1, **lines 124 - 131** (pages 6) [*… Average particle size (dh) of the aggregates and zeta potential in deionized water were estimated 178.7 nm and +15.0 mV, respectively. The zeta potential of CdS QDs were comparable in water and in the culture medium used: QDs have approximately neutral charge. The hydrodynamic diameters of CdS QDs were comparable in water; the difference observed in the experimental systems is due to the presence of divalent cations and serum protein that characterizes the culture medium…*] and in Appendix A. Comparison of data in water and in culture medium are reported in Table A.9.
3. Line 25 abstract: two human cell lines	The change was not made because the abstract was modified as suggested by the reviewer.
4. Line 37 abstract: changes in the expression of miRNAs	Change made. Line **39** (page 2): […*For both cell types, changes in the expression of miRNAs…*].

5. Line 70: damaging? Nucleic acid membranes	Change made. Line **71** (page 3): […*indirectly affecting integrity of proteins, nucleic acid and membranes*…].
6. Line 75: allowed for the identification	Change made. Line **76** (page 4): […*has allowed for the identification*…].
7. Line 75-79: The transcriptomic approach has allowed for the identification of molecular mechanisms of CdS QDs exposure, highlighting potential candidates for exposure biomarkers. This paper describes the miRNA profiles as a consequence of exposure to either ionic Cd or CdS QDs and reveals several miRNAs that have the potential to be early biomarkers of exposure to these toxicants.	Change made. Line **76 – 80** (page 4): […*The transcriptomic approach has allowed for the identification of molecular mechanisms of CdS QDs exposure, highlighting potential candidates for exposure biomarkers. This paper describes the miRNA profiles as a consequence of exposure to either ionic Cd or CdS QDs and reveals several miRNAs that have the potential to be early biomarkers of exposure to these toxicants*…].
8. Line 98: For example, Titanium dioxide	Change made. Line **100** (page 5): […*For example, titanium dioxide*…].
9. Line 102: cell lines	Change made. Line **104** (page 5): […*cell lines used were*…].

Differences in toxicity, mitochondrial function and miRNome in human cells exposed *in vitro* to Cd as CdS quantum dots or ionic Cd

Laura Paesano[a], *Marta Marmiroli*[a], *Massimiliano G. Bianchi*[b], *Jason C. White*[c], *Ovidio Bussolati*[b], *Andrea Zappettini*[d], *Marco Villani*[d], *Nelson Marmiroli*[a,e]*

[a]University of Parma, Department of Chemistry, Life Sciences and Environmental Sustainability, Parco Area delle Scienze 11/A, 43124 Parma, Italy

[b]University of Parma, Department of Medicine and Surgery, Laboratory of General Pathology, Via Volturno 39, 43125 Parma, Italy

[c]Department of Analytical Chemistry, The Connecticut Agricultural Experiment Station (CAES), New Haven, Connecticut 06504, United States

[d]Institute of Materials for Electronics and Magnetism (IMEM-CNR), Parco Area delle Scienze 37/A, 43124 Parma, Italy

[e]National Interuniversity Consortium for Environmental Sciences (CINSA), Parco Area delle Scienze 93/A, 43124 Parma, Italy Parma, Italy

[*]*Corresponding Author*:

Email address: nelson.marmiroli@unipr.it

Phone: +39 0521 905606

ABSTRACT

Cadmium is toxic to humans, although Cd-based quantum dots exerts less toxicity. Human hepatocellular carcinoma cells (HepG2) and macrophages (THP-1) were exposed to ionic Cd, Cd(II), and cadmium sulfide quantum dots (CdS QDs), and cell viability, cell integrity, Cd accumulation, mitochondrial function and miRNome profile were evaluated.

Cell-type and Cd form-specific responses were found: CdS QDs affected cell viability more in HepG2 than in THP-1; respective IC_{20} values were ~ 3 and ~ 50 μg ml^{-1}. In both cell types, Cd(II) exerted greater effects on viability.

Mitochondrial membrane function in HepG2 cells was reduced 70% with 40 μg ml^{-1} CdS QDs but was totally inhibited by Cd(II) at corresponding amounts. In THP-1 cells, CdS QDs has less effect on mitochondrial function; 50 μg ml^{-1} CdS QDs or equivalent Cd(II) caused 30% reduction or total inhibition, respectively. The different *in vitro* effects of CdS QDs were unrelated to Cd uptake, which was greater in THP-1 cells.

For both cell types, changes in the expression of miRNAs (miR-222, miR-181a, miR-142-3p, miR-15) were found with CdS QDs, which may be used as biomarkers of hazard nanomaterial exposure. The cell-specific miRNome profiles were indicative of a more conservative autophagic response in THP-1 and as apoptosis as in HepG2.

Keywords. miRNA; quantum dot; HepG2; THP-1; cadmium.

Abbreviations.

Δψm, mitochondrial membrane potential;

Cd(II), $CdSO_4$ 8/3 -hydrate;

CdS QDs, cadmium sulfide quantum dots;

DMEM, Dulbecco's Modified Eagle's Medium;

ENMs, engineered nanomaterials;

FBS, fetal bovine serum;

FCCP, carbonyl cyanide 4-(trifluoromethoxy) phenylhydrazone;

JC1, tetraethylbenzimidazolylcarbocyanine iodide;

PMA, phorbol 12-myristate 13-acetate;

QDs, quantum dots;

SS, side scatter.

1. Introduction

Quantum dots (QDs) have medical applications including fluorescence imaging, biosensing and targeted drug delivery to treat inflammation or drug-resistant cancer cells [1–3]; QDs conjugated with antibodies have been used to distinguish normal from cancerous cells [4]. There is an increasing interest in developing nano-theranostic platforms for simultaneous sensing, imaging and therapy [5]. Given the growing demand for and use of QDs, there is a clear need to understand potential toxicity for organisms and the environment [6]. The likely hazards posed by QDs in the biomedical field are not yet fully understood, although some studies have sought to address this issue [7]. The toxicity associated with cadmium (Cd)-containing QDs has been shown to be higher than for other QDs. This has been assumed to be related to the presence of Cd, leading to the production of excessive reactive oxygen species (ROS), indirectly affecting integrity of proteins, nucleic acid and membranes [8–10]. HepG2 cells, a human hepatocellular carcinoma cell line used as a model for human hepatic tissue [11], have been shown to respond to cadmium sulfide quantum

dots (CdS QDs) exposure by altering the abundance of gene transcripts encoding products associated with apoptosis, oxidative stress response and autophagy [12]. The transcriptomic approach has allowed for the identification of molecular mechanisms of CdS QDs exposure, highlighting potential candidates for exposure biomarkers. This paper describes the miRNA profiles as a consequence of exposure to either ionic Cd or CdS QDs and reveals several miRNAs that have the potential to be early biomarkers of exposure to these toxicants [13,14].

MiRNAs are short (19 - 23 nucleotides) non-coding sequences that are ubiquitous in all life forms. Their biological significance lies in their regulatory control over a wide range of cellular processes, achieved either by targeting the degradation of complementary mRNAs or by repressing the process of translation. There is also evidence to suggest that certain miRNAs can interact with sequences in the 5' and 3' untranslated region of their target mRNA, resulting in an enhancement rather than a reduction in translation [15]. Changes in cellular miRNA profiles have been associated with a number of conditions in humans, including cancer, viral infection, immune disorders and cardiovascular diseases [16–18]. In the plant kingdom, miRNA involvement has been described in the response to heavy metal exposure, including Cd and Cu [19,20]. In yeast (*Saccharomyces cerevisiae*), several miRNAs have been associated with the expression of Cd tolerance [21]. A number of epigenetic effects have been shown to be induced by Cd exposure, including DNA methylation, the post-translational modification of histone tails, and the packaging of DNA around the nucleosome; all have been correlated with the abundances of specific miRNAs [22]. Increasing evidence indicates that *in vitro* and *in vivo* exposure of human cells to environmental organic contaminants and metals can alter miRNA expression [23]. It has been demonstrated that the relative abundance of certain miRNAs is responsive

to nanomaterials, although the global effect of this exposure is not understood [24]. For example, titanium dioxide, zinc oxide and gold nanoparticles change miRNAs expression [25,26].

This study examined the changes in the miRNome of two widely studied human cell lines exposed to various levels of Cd, presented as either CdS QDs or Cd(II). The cell lines used were HepG2, hepatocellular carcinoma cells, and THP-1, human macrophage-like cells. While the literature contains numerous descriptions of therapeutic uses of miRNAs [16], their potential as biomarkers for xenobiotic exposure remains unknown; this is in spite of the fact that miRNAs have been reported to be mediators of cellular responses to environmental contaminants [27]. Moreover, the US Food and Drug Administration (USFDA) considers changes in miRNA levels as a possible genome biomarker [13,14]. MiRNAs could be useful not only as potential biomarkers of several diseases but also as key mediators of the mechanisms linking environmental exposure to toxicity and disease development [28]. The present toxicogenomic study on human cell lines was carried out to assess an *in vitro* (non-animal) test for health risk assessment [29] for exposure to ionic- and nanoscale-Cd. In addition, the study was intended to determine whether CdS QDs could represent a less toxic form of Cd in diagnostic medicine [30].

2. Materials and methods

2.1 Preparation of CdS QDs suspension medium

CdS QDs were synthesized at IMEM-CNR (Parma, Italy), as described elsewhere [31]. They were characterized in deionized water by transmission electron microscopy (Hitachi HT7700, Hitachi High Technologies America, Pleasanton, CA). Major details are described in Paesano *et al.* [32]. Their structure is crystalline with a

mean static diameter of 5 nm with approximately 78% Cd. Average particle size (d_h) of the aggregates and zeta potential in deionized water were estimated 178.7 nm and +15.0 mV, respectively (Zetasizer Nano Series ZS90, Malvern Instruments, Malvern, UK) [33]. The zeta potential of CdS QDs were comparable in water and in the culture medium used: QDs have approximately neutral charge. For hydrodynamic diameters, difference observed in the experimental systems is due to the presence of divalent cations and serum protein that characterizes the culture medium. Characterization details are given in Appendix A. The CdS QDs were suspended in Milli-Q water at a concentration of 100 μg ml^{-1}, and pulsed probe sonication was used to minimize aggregation. For cell treatment, the stock particle suspension was vortexed and sonicated for 30 min, and then diluted as appropriate into complete culture medium.

2.2 Cell Culture, Treatments and Cell Viability Assay

Cells were cultured in Dulbecco's Modified Eagle's Medium (DMEM) containing 10% fetal bovine serum (FBS), 100 μg ml^{-1} streptomycin, 100 U ml^{-1} penicillin, 4 mM glutamine; for THP-1 cells, the glutamine concentration was reduced to 2 mM. Cells were cultured in 10-cm Petri dishes under a humidified atmosphere in the presence of 5% CO_2. Prior to treatment, THP-1 cells were differentiated into macrophages through an incubation with 0.1 μM of phorbol 12-myristate 13-acetate (PMA) for 3 days.

Cells in complete culture medium were seeded into either 96-well plates, at a density of 15×10^3 cells/well, or 10-cm diameter dishes at 3×10^6 cells/dish. The medium was replaced after 24 h with fresh medium containing either CdS QDs or Cd(II) (as $CdSO_4$ 8/3 -hydrate). HepG2 cells were treated with a range of Cd concentration, either as CdS QDs or Cd(II), from 0 to 93.6 μg ml^{-1}; the THP-1 cells were treated with

149 a range of Cd doses from 0 to 124.8 µg ml^{-1}. Details of all the Cd treatments are
150 given in Table A.1. Each treatment was carried out in triplicate (biological replicates)
151 and each replicate was measured three times (technical replicates). Cell viability was
152 evaluated after 24 h of incubation in the presence of Cd using the resazurin method
153 [34]. Briefly, the culture medium was replaced with a solution of resazurin (44 µM,
154 Sigma-Aldrich, Saint Louis, MO, USA) in serum-free medium. After 30 min,
155 fluorescence was measured at 572 nm with a multimode plate reader (Perkin Elmer
156 Enspire, Waltham, MA, USA). Potential interference in this assay was excluded by
157 measuring fluorescence of the dye mixed with CdS QDs. The treatment time of 24 h
158 was chosen from literature reports about the internalisation time of QDs [35].
159
160 *2.3 Mitochondrial Membrane Function Assay*
161 Mitochondrial membrane potential (Δψm) was estimated using the JC-1 kit (Abcam
162 Ltd, Cambridge, UK) according to the manufacturer's instructions. The assay relies
163 on the accumulation of the cationic dye tetraethylbenzimidazolylcarbocyanine iodide
164 (JC-1) in energized mitochondria. When the Δψm is low, JC-1 is present mostly in
165 monomeric form, which can be detected through its emission of green fluorescence
166 (530±15 nm). Conversely, when the Δψm is high, the dye polymerizes, resulting in
167 the emission of red to orange fluorescence (590±17.5 nm). Therefore, a decrease in
168 red fluorescence and an increase in green fluorescence are indicative of
169 depolarization in the mitochondrial membrane. Carbonyl cyanide 4-
170 trifluoromethoxyphenylhydrazone (FCCP), an H^+ ionophore uncoupler of oxidative
171 phosphorylation, was used as a Δψm-depolarization positive control. HepG2 or THP-
172 1 cells were seeded into 96-well plates at a density of 7.5×10^4 cells per well and
173 were incubated for 24 h to allow adhesion. Cells were then exposed to a range of Cd

treatments (Table A.1) for 24 h in the form of either CdS QDs or Cd(II). After extensive washing in phosphate buffered saline (PBS) to remove adherent particles or QDs aggregates, cells were incubated in the JC-1 solution for 30 min at 37°C in the dark. Following a further PBS rinse, fluorescence emitted by the cells was determined by a multimode plate reader (Perkin Elmer Enspire). Individual experiments were run in triplicate; data were expressed as the relative fluorescence unit (RFU) with respect to the control.

2.4 Confocal Microscopy

HepG2 and THP-1 cells were seeded into four-well chamber slides at a density of 5 × 10^4 cells ml^{-1}. After treatment with either CdS QDs or Cd(II) (see Table A.1), cells were transferred to a medium containing 5 µM JC-1 for 30 minutes. Following the staining procedure, the cells were rinsed in complete culture medium, incubated at 37°C and 5% CO_2 in a Kit Cell Observer (Carl Zeiss, Jena, Germany) and imaged using an inverted LSM 510 Meta laser scanning microscope (Carl Zeiss). Excitation at 633 nm and reflectance were used to visualize CdS QDs. The status of the JC-1 dye was recorded by excitation at 480 nm and the emission was passed through a 535-595 nm filter. In selected experiments, nuclei were counterstained with DRAQ5™ (Alexis Biochemicals, San Diego, California, USA). In these instances, 5 µM DRAQ5™ was added together with JC-1 and cells were visualized with excitation at 633 nm with emission through a 670 nm long pass filter.

The cytoplasm of THP-1 cells exposed to 50 µg ml^{-1} CdS QDs for 24 h was visualized by incubation with 1 µM calcein-AM (Millipore Merck, Burlington, MA, USA) for 2 h; calcein-loaded cells were excited at 488 nm and fluorescence was measured through a 515-540 nm band pass filter.

199

200 *2.5 Cellular Uptake of Cadmium*

201 The entry of CdS QDs into THP-1 cells exposed to 50 µg ml^{-1} of the nanomaterial for
202 either 4 and 24 h was estimated with a cytofluorimetric assay [12]. After exposure,
203 cells were first harvested by trypsin treatment and centrifugation (800 x *g*, 5 min),
204 after which they were suspended in PBS containing 1% (v/v) FBS. The presence of
205 CdS QDs was revealed by flow cytometry (NovoCyte, ACEA Biosciences, San
206 Diego, CA, USA); specifically, CdS QDs uptake was associated with a higher side
207 scatter (SS) intensity. The experiment involved three biological replicates, each
208 represented by three technical replicates. A similar analysis of Cd entry into HepG2
209 cells has been reported previously [12]. The cells were thoroughly washed to remove
210 any surface-attached agglomerates of CdS QDs and quantification of Cd
211 accumulated by the cells was then obtained using inductively coupled plasma mass
212 spectrometry (ICP-MS) as described by Peng *et al.* [36]. Confocal microscopy
213 showed that agglomerates of CdS QDs were absent from these preparations. HepG2
214 or THP-1 cells, exposed to various doses of CdS QDs or Cd(II) (Table A.1) for 24 h,
215 were rinsed three times in PBS, harvested by trypsinization prior to counting, and
216 then digested with 67% HNO_3 at 165°C for 3 h. The solution obtained was diluted by
217 adding 2 volumes of water prior to ICP-MS analysis.

218

219 *2.6 RNA Isolation and miRNAs Quantification*

220 To avoid compromising RNA integrity, extractions from HepG2 and THP-1 cells
221 exposed to Cd in the form of either CdS QDs or Cd(II) were performed using a
222 mirVANA™ column-based kit (Life Technologies, Carlsbad, CA, USA). RNA
223 concentration and integrity were monitored by spectrophotometry and gel

electrophoresis, respectively. The abundance of each miRNA was obtained using a TaqMan® Array Human MicroRNA A+B Card Set v3.0 (Applied Biosystems, Foster City, CA, USA), which quantifies 754 miRNAs. A 1-µg aliquot of RNA was reverse-transcribed using Megaplex™ RT Primers (Applied Biosystems), and the subsequent PCR array was run using a 7900HT Fast Real Time PCR system (Applied Biosystems) following the MegaPlex™ Pool Protocol (PN 4399721 RevC). Each sample was analyzed in duplicate. The raw data were analyzed using RQ Manager 1.2 software (Applied Biosystems) and relative abundances were calculated using the $2^{-\Delta\Delta Ct}$ method [37]. The selected reference sequence was non-coding U6 small nuclear RNA. The fold-change threshold applied to define significant changes in abundance was 2 (for increased miRNAs) and 0.5 (for decreased miRNAs).

2.7 In vitro analysis of autophagy: Western blot assay

Total cell lysates were obtained as described elsewhere [38]. The monolayers were rinsed with ice-cold PBS and then covered with 60 µl of Lysis buffer (20 mM Tris–HCl, pH 7.5, 150 mM NaCl, 1 mM EDTA, 1 mM EGTA, 1% Triton, 2.5 mM sodium pyrophosphate, 1 mM β-glycerophosphate, 1 mM Na_3VO_4, 1 mM NaF, 2 mM imidazole) supplemented with a protease inhibitor cocktail (Complete, Mini, EDTA-free, Roche, Monza, Italy). Equal amounts of proteins from each sample were separated by 4-20% SDS-polyacrylamide gels and transferred to PVDF membranes (Immobilon-P, Millipore, Millipore Merck Corporation, MA, USA); membranes were then incubated in TBS with 10% blocking solution (Western Blocking Reagent, Roche) for 1h and exposed overnight at 4°C to primary antibodies against LC3II (microtubule–associated protein light chain 3, Cell Signaling Technology, Danvers, MA, USA), p62 (ubiquitin-binding protein p62, Abcam Ltd) or tubulin (Sigma-Aldrich)

diluted in TBS-T with 5% BSA. After three washes of 10 min each in TBS-T (50mM Tris Base, 150mM NaCl, pH 7.5), membranes were exposed to the HRP-conjugated secondary anti-rabbit or anti-mouse IgG antibodies for 1h at room temperature (HRP, Cell Signaling Technology). Visualization of protein bands was performed using Immobilon Western Chemiluminescent HRP Substrate (Millipore, Merck). The expression of tubulin was used for loading control. Individual experiment were run in triplicate.

2.8 Statistic and Bioinformatics Analysis

The software package SPSS Statistics® v.21 (IBM, Armonk, NY, USA) was used to compare control and treatment effects. Levene, Shapiro-Wilk and Kolmogorov-Smirnov tests were applied to ascertain data normality and variance homogeneity. One-way analysis of variance, followed by the Tukey test was used to identify and order means differing significantly from one another. The significance threshold probability was set at 0.05. To visualize transcriptomic data, hierarchical clustering was performed using the heatmap.2 routine implemented in the R software (www.R-project.org/). Genes targeted by differentially abundant miRNAs were identified using the DIANA-Tarbase v.7 database (diana.imis.athena-innovation.gr/DianaTools/index.php?r=tarbase/index)[39]. The KEGG pathway enrichment of these target genes was derived from an analysis based on DIANA-mirPath software [40]. The p-value threshold was set 0.05 and FDR correction was applied. miRTargetLink [41] was used to identify interaction networks among the target genes using information documented in the miRTarBase. Only strong interactions (backed up by strong experimental methods such as the 'reporter gene assay') were taken into consideration. PANTHER (pantherdb.org/) software was used

to search for gene enrichment, and the Gene Ontology database provided functional annotation for the genes targeted by differentially abundant miRNAs.

3. Results and Discussion

Experiments were designed to compare the responses of HepG2 and THP-1 cells to Cd exposure in the form of either CdS QDs or Cd(II). Some of the distinguishing features of the two cell types are listed in Table A.2. THP-1 were compared with HepG2 cells because of their different role relative to *in vivo* exposure to Cd. In the body, engineered nanoparticles may be recognized and processed by immune cells, among which macrophages play a crucial role. Macrophages act as the first line of defense against invading agents, including QDs [42]. Hepatocytes are instead involved in the attempt to dispose the eventual toxicant in the liver, which is the major human organ which accumulates both Cd^{2+} and Cd-containing QDs [43].

3.1 Cell viability

When exposed to Cd(II), the viability of both cell types was dose-dependent, as reported elsewhere [44,45]. Specifically, the estimated IC_{50} for HepG2 cells was ~ 4 μg ml^{-1} Cd as Cd(II) and ~ 15 μg ml^{-1} Cd as CdS QDs (corresponding to ~ 20 μg ml^{-1} CdS QDs) (Fig. A.1a). The IC_{20} for CdS QDs was calculated at 3 μg ml^{-1} (~ 2.3 μg ml^{-1} Cd). Measurements taken after a 14-day immersion of CdS QDs in the growth medium showed that the release of Cd^{2+} into solution reached a maximum of approximately 1 – 2%, consistent with previous reports [46,47]. This value occurs for all the growth and treatment conditions reported throughout the paper.

For THP-1 cells, the susceptibility to Cd(II) was comparable, whereas the IC_{20} for CdS QDs was nearly 50 μg ml^{-1}, and at ~ 120 μg ml^{-1} viability was still more than

299 60% (Fig. A.1b). Thus, the sub-toxic dose (IC_{20}) of CdS QDs for THP-1 cells was
300 established at 50 µg ml^{-1} (39 µg ml^{-1} Cd). From the literature and from our study, an
301 equivalent dose of Cd^{2+} drastically reduces cell viability [48].
302
303 *3.2 Mitochondrial Function and Cell Morphology*
304 Mitochondrial function is one of the main targets of QDs [49,50]. In HepG2 cells, 2.3
305 µg ml^{-1} of Cd as CdS QDs at IC_{20} (3 µg ml^{-1} CdS QDs) had a minimal effect on
306 mitochondrial membrane potential; an inhibition of ~ 50% was observed at 31.2 µg
307 ml^{-1} of Cd (40 µg ml^{-1} CdS QDs) (Fig. 1a). In contrast, mitochondrial function was
308 significantly inhibited in the presence of 2.3 µg ml^{-1} Cd as Cd(II) (Fig. 1b). THP-1
309 cells responded in similar fashion but were largely unaffected by CdS QDs exposure
310 even at 50 µg ml^{-1} (39 µg ml^{-1} Cd) (Fig. 1c), although they were quite susceptible to
311 Cd(II), the dose totally inhibiting mitochondrial membrane potential being 7.8 µg ml^{-1}
312 Cd as Cd(II) (Fig. 1d). Therefore, Cd strongly inhibited mitochondrial function in both
313 cell lines when present as Cd(II) but not as CdS QDs, which caused only a partial
314 inhibition.
315 Confocal images of JC-1-labeled HepG2 cells exposed to 3 µg ml^{-1} of CdS QDs are
316 shown in Fig. A.2. This condition (IC_{20}) failed to induce any significant reduction in
317 JC-1 aggregation; the amount of JC-1 monomer was not altered (Fig. A.2), indicating
318 that mitochondrial function was unaffected by the treatment. In this condition, the cell
319 shapes were also normal. Treatment with 2.3 µg ml^{-1} Cd as Cd(II) led to a significant
320 decrease in JC-1 aggregates (data not shown). In contrast, micrographs of THP-1
321 cells exposed to 5 µg ml^{-1} Cd in the form of either Cd(II) or CdS QDs (Fig. 2), show a
322 significant alteration in mitochondrial function after exposure to Cd(II). When THP-1
323 cells were exposed to 50 µg ml^{-1} of CdS QDs, a more significant reduction in JC-1

aggregates was observed (Fig. 2), but cell morphology appeared to be substantially unaffected.

3.3 Cd Uptake

Internalization of QDs in human cells occurs *in vitro* within 24 h from exposure [51]. A cytofluorimetric assay was used to demonstrate the capacity of HepG2 and THP-1 cells to accumulate CdS QDs. CdS QDs uptake by HepG2 cells was reported in a previous paper [12]. The same method was applied here for the THP-1 cell line. A significant increase in side scatter (SS) was observed when cells were exposed to 50 μg ml^{-1} of CdS QDs for 4 h and 24 h (Fig. 3), consistent with QDs entry. Separate ICP-MS measurements of cells exposed to CdS QDs for 24 h, with subsequent thorough washing to remove any CdS QDs remaining on the surface, demonstrated a dose-dependent increase in cellular Cd levels (Table A.3). Interestingly, HepG2 cells accumulated greater amounts of Cd upon exposure to CdS QDs than to equivalent amounts of Cd as Cd(II). THP-1 cells accumulated more Cd than HepG2 cells, possibly a result of their phagocytic competence. Also in this case the uptake of Cd as CdS QDs was higher than for Cd as Cd(II). Therefore, the larger negative impacts on viability and mitochondrial function reported for Cd(II) are not due to a greater uptake of Cd.

To evaluate the interaction of THP-1 cells with CdS QDs, calcein-loaded macrophages were treated with 50 μg ml^{-1} of CdS QDs: the majority of the CdS QDs formed aggregates that were clearly evident in reflectance mode (see the grey pseudocolor in the confocal images in Fig. A.3a). The orthogonal projections and 3-D reconstruction indicate that the CdS QDs were grouped in aggregates in close

contact with the cell surface, with images indicating the formation of deep, shallow invaginations in the cell membrane, highly suggestive of internalization (Fig. A.3b).

3.4 miRNAs Expression Profiling: Comparison Between CdS QDs and Cd(II)

Significant changes have been reported for miRNAs of human cells exposed to engineered nanomaterials (ENMs) [25]. Table A.4 gives a summary of the effect of Cd exposure on HepG2 and THP-1 miRNomes (the number of assayed miRNAs was 754). For HepG2 cells exposed to 3 μg ml^{-1} CdS QDs or 5.2 μg ml^{-1} Cd(II), the number of miRNAs with significantly increased or decreased abundance are reported in Fig. 4a as Venn diagrams. Heatmaps showed the abundances of three miRNAs (miR-1267, miR-200a-5p, 26b-3p) which were increased by CdS QDs, but reduced by Cd(II); the opposite trend was evident for three other miRNAs (miR-218-5p, miR-548b-3p, miR-589-3p) (Fig. 5a). A more extensive heatmap is presented in Fig. 1 in Paesano *et al.* (Data in Brief). The analysis demonstrates that exposure to CdS QDs or to Cd(II) had markedly different effects on the HepG2 miRNome. The response of THP-1 cells was more complex, with markedly different effects of high dose CdS QDs (39 μg ml^{-1} Cd) or Cd(II) (5 μg ml^{-1} Cd) on miRNAs abundance (Fig. 6a). Heatmap representations of these data are given in Fig. 2a in Paesano *et al.* (Data in Brief). When THP-1 cells were exposed to lower doses of Cd (5 μg ml^{-1}), equivalent to 6.4 μg ml^{-1} CdS QDs or 11.4 μg ml^{-1} Cd(II), the effects on miRNAs levels were different: only six common miRNAs were found up-modulated while one down-modulated (Fig. 4b). CdS QDs induced a general increase in miRNAs levels, while Cd(II) produced a decrease (heatmap with individual variations is reported in Fig. 2b in Paesano *et al.* (Data in Brief)). Thus, at this lower level of stress, the two forms of

372 Cd also had very different effects on the miRNome in THP-1 and HepG2 cells; Cd(II)
373 led to more dramatic consequences as compared with CdS QDs.
374
375 *3.5 Comparison between the Cell Line Responses to Cd*
376 Figs 4c, d and 5b, c show a comparison of the miRNomes for HepG2 and THP-1
377 cells when exposed to CdS QDs and Cd(II).
378 Exposure of THP-1 cells to 50 μg ml^{-1} CdS QDs had a similar suppressive effect on
379 cell viability as did exposure of 3 μg ml^{-1} CdS QDs on HepG2 cells (Fig. A.1).
380 However, there was little similarity with respect to the effect of the exposure on the
381 miRNome. Specifically, there was no overlap between the sets of miRNAs that
382 increased in abundance, although there were 17 suppressed miRNAs in common
383 between the two cell types (Fig. 6b). Conversely, 13 of the miRNAs responded
384 differentially, either increasing in abundance in THP-1 cells while decreasing in
385 HepG2 cells, or *vice versa*. Analysis of the relevant heatmaps (Fig. 5b and Fig. 3a in
386 Paesano *et al.* (Data in Brief)) suggests that the two cell types deployed different
387 strategies to maintain viability in response to Cd exposure. Molecular responses to a
388 comparable level of CdS QDs-imposed stress (3 μg ml^{-1} for HepG2 and 6.4 μg ml^{-1}
389 for THP-1 cells) were also quite distinct: 10 miRNAs increased in both cell types, and
390 2 decreased (Fig. 4c). In THP-1 cells, exposure to the lower dose of CdS QDs mostly
391 increased miRNAs levels. When the stress was imposed by Cd(II), the responses of
392 the two cell types were similar in the number of miRNAs down-modulated, with 39 of
393 these in common (Fig. 4d). The heatmaps presented in Figs 5b, c presents an
394 overview of the effect of the lower dose of CdS QDs and Cd(II) on the miRNome. A
395 comparison between the two cell lines each challenged with CdS QDs at lower (3 or
396 6.4 μg ml^{-1}) and THP-1 at higher dose (50 μg ml^{-1}) is shown in Fig. 3b in Paesano *et*

al. (Data in Brief). For both THP-1 and HepG2 the lower doses result primarily in up-modulation, whereas THP-1 at 50 μg ml^{-1} is largely down-modulated. A global comparison between the responses of the two cell lines to CdS QDs-imposed stress is also given in Fig. 6c. For THP-1 cells, 130 miRNAs were modulated exclusively in response to 50 μg ml^{-1} of CdS QDs treatment but at 6.4 μg ml^{-1}, that value was only 45. For HepG2 cells, 26 miRNAs responded exclusively to 3 μg ml^{-1} CdS QDs. In conclusion, the miRNomes of the two cell lines reacted differently to QDs exposure; however, exposure to Cd(II) caused mainly a reduction in miRNA abundances in both cell lines.

3.6 In silico analysis: Pathways, GO and Networks Analysis

The pathways potentially impacted by miRNA modulation under Cd-induced stress were identified using the DIANA-mirPath algorithm [40]. In the case of the HepG2 cell line, Tables A.5 and A.6 show the cellular pathways more likely affected by 3 μg ml^{-1} CdS QDs or 5.2 μg ml^{-1} Cd(II). An equivalent analysis was conducted for THP-1 cells exposed to either 6.4 μg ml^{-1} CdS QDs or 11.4 μg ml^{-1} Cd(II) (Tables A.7 and A.8). Although a rather similar set of pathways was impacted in the two cell types, it is noteworthy that the miRNAs involved were markedly different for the two forms of Cd. An *in silico* analysis on the biological significance of the differentially abundant miRNAs was also performed using miRTargetLink and PANTHER software. Gene ontology (GO) enrichment analysis from PANTHER gave results shown summarized below and reported in details in Fig. 4 in Paesano *et al.* (Data in Brief) for HepG2 cells, treated with either CdS QDs or Cd(II). Fig. 5 in Paesano *et al.* (Data in Brief) shows results for THP-1 cells treated with 50 μg ml^{-1} CdS QDs, and Fig. 6 in Paesano *et al.* (Data in Brief) reports THP-1 cells exposed to the lower dose of CdS

422 QDs or to Cd(II). A comparison for HepG2 showed that in the treatment with CdS
423 QDs the major GO categories involved were: ‘miRNA mediated inhibition of
424 translation’, ‘regulation of RNA polymerase II transcriptional preinitiation complex
425 assembly’ and ‘regulation of gene silencing by miRNA’. In the case of Cd(II) the
426 major target genes were associated with apoptosis, stress response, gene silencing
427 and mitochondrial depolarization.
428 For THP-1 exposed to the lower dose of CdS QDs (6.4 µg ml^{-1}), the main GO
429 categories were ‘positive regulation of cell-cycle phase transition’, ‘regulation of cell-
430 cycle G1/S phase transition’ and ‘positive regulation of production of miRNAs
431 involved in gene silencing by miRNA’. In the case of Cd(II) the gene targets belonged
432 to: ‘regulation of B cell apoptotic process’, ‘release of cytochrome c from
433 mitochondria’, ‘positive regulation of protein insertion into mitochondrial membrane
434 involved in programmed cell death’ and ‘leukocyte apoptotic process’. For THP-1,
435 GO categories related to mitochondrial function were more evident when treated with
436 Cd(II) or with CdS QDs at the higher dose. Indeed, when THP-1 were treated with
437 the higher dose of CdS QDs (50 µg ml^{-1}) most of the regulated miRNA belonged to
438 GO categories: ‘regulation of production of miRNAs involved in gene silencing by
439 miRNA’, ‘extrinsic apoptotic signaling pathway in absence of ligand’, ‘regulation of
440 mitochondrial membrane potential’ and ‘cellular response to mechanical stimulus’. A
441 comparison of the GO categories of the target genes in the two cell types revealed
442 for treatment with CdS QDs some commonalities, notably 'epidermal growth factor
443 receptor signaling', 'positive regulation of mitotic cell cycle phase transition' and
444 'negative regulation of extrinsic apoptosis' (see Fig. 7 in Paesano *et al.* (Data in
445 Brief)). Some common categories were also evident from comparison between the
446 response of cells exposed to CdS QDs and those exposed to Cd(II) (see Fig. 7 in

447 Paesano *et al.* (Data in Brief)). Although the two cell lines responded differently to
448 CdS QDs, this analysis has highlighted that some targets of regulated miRNAs
449 belong to the same classes of GO, suggesting that they are involved in the same
450 cellular processes. All similarities and differences in response to CdS QDs and to
451 Cd(II) was markedly different both in HepG2 and in THP-1 are shown in Fig. 7 in
452 Paesano *et al.* (Data in Brief).
453 miRTargetLink software was used to generate regulatory networks using miRNAs
454 modulated in response to CdS QDs in HepG2 and THP-1 cells. From these data, a
455 network was created considering mainly autophagic and apoptotic pathways. The
456 network summarized the response of the two cell types to CdS QDs. Overall, the
457 autophagic pathway seemed activated in THP-1 cells exposed to the higher, but not
458 to the lower dose of CdS QDs. In contrast, in HepG2 cells, exposure to QDs led to
459 activation of the apoptotic process. These networks are illustrated in Figs 8a, b in
460 Paesano *et al.* (Data in Brief).
461
462 *3.7 Activation of miRNA Response*
463 One notable feature of the response of THP-1 cells to 50 μg ml^{-1} CdS QDs was the
464 high number of miRNAs with a decreased abundance. The major pathways likely
465 affected by this response were apoptosis, DNA repair, cell cycling, xenobiotic
466 metabolism and autophagy. In particular, Fig. 7 illustrates a reconstruction *in silico* of
467 miRNAs involved in the regulation of autophagy in the response of THP-1 to the
468 higher dose of CdS QDs (50 μg ml^{-1}); however, the same pathway appears to be
469 largely unaffected in THP-1 cells exposed to the lower dose of CdS QDs (6.4 μg ml^{-1},
470 Fig. 9 in Paesano *et al.* (Data in Brief)). *MTOR* transcript was likely repressed, given
471 that the abundance of miR-101, miR-199a, miR-30a and miR-7 was enhanced. At the

same time, the vesicle elongation phase could be repressed by up-regulated miRNAs including miR-101, miR-30a, miR-885-3p and miR-181a. Moreover, miR-30a, which is involved in the repression of Beclin-1, was up-regulated, thus pointing to autophagy suppression. Several other miRNAs that responded positively to exposure also have gene targets that encode proteins involved in autophagy (Fig. 9 in Paesano *et al.* (Data in Brief)). This hypothesis is confirmed by *in vitro* analysis with autophagy markers (LC3II and p62). LC3II is recruited from the cytosol and associates with the phagophore early in autophagy. This localization serves as a general marker for autophagic membranes and for monitoring the process as it develops [53]. p62 is a receptor for cargo destined to be degraded by autophagy, including ubiquitinated protein aggregates destined for clearance. The p62 protein is able to bind ubiquitin and also to LC3II, thereby targeting the autophagosome and facilitating clearance of ubiquitinated proteins [54]. As shown in Fig. 8, the induction of autophagy in THP-1 cells treated with Cd as CdS QDs was confirmed by an increase in LC3II and a constant p62 levels, while the increase in p62 and LC3II levels after exposure to 5 μg ml^{-1} of Cd as Cd(II) (11.4 μg ml^{-1}) suggests a blockage of the autophagic flow. Conversely, the miRNAs responding in the CdS QDs-exposed HepG2 cells had little or no association with the regulation of autophagy but were, instead, associated with apoptosis (Fig. 9). In this case, the exposure to QDs does not cause an increase in LC3II, suggesting a normal condition of the autophagic flow (Fig. 8). Thus, autophagy seemed to be preferentially activated over apoptosis in THP-1 cells exposed to the highest dose of Cd (Fig. 10 in Paesano *et al.* (Data in Brief)). Instead, THP-1 cells exposed to the lower dose of CdS QDs did not activate the apoptotic process (Fig. 11 in Paesano *et al.* (Data in Brief)), which was, however,

triggered by the exposure to the equivalent dose of Cd as Cd(II) (Fig. 12 in Paesano *et al.* (Data in Brief)).

A previous analysis of the HepG2 response to CdS QDs exposure had suggested that a number of genes associated with apoptosis were among those up-regulated by the stress [12,55]. The current work demonstrates that exposure to CdS QDs reduced the abundance of both miR-32 and miR-149, which would have favored the release of cytochrome c, mitochondria-related apoptosis inducing factor and endonuclease G and, hence, promoted apoptosis [56,57]. The response to Cd(II) suggests that both the intrinsic and the extrinsic apoptotic pathways were activated, pointing to a larger alteration and damage of cell viability (Fig. 13 in Paesano *et al.* (Data in Brief)). The response of THP-1 cells to CdS QDs exposure was quite different in term of cell viability, mitochondrial function and in the number of miRNAs up- or down-modulated. This may explain why these cells appeared to be less susceptible to the stress than HepG2 cells: autophagy is obviously less clearly indicative of a death process than the triggering of apoptosis. Moreover, at the lower dose of CdS QDs, THP-1 cells do not activate either autophagy or apoptosis, relying on subtler rescue mechanisms (see Figs 9 and 10 in Paesano *et al.* (Data in Brief)).

An overview of the differences and commonalities between the miRNomes of the two cell types in response to the lower or to the higher level of CdS QDs is shown in Table 1 and in Figs 14a, b in Paesano *et al.* (Data in Brief). Of note, two cancer-associated miRNAs, miR-191-3p and miR-133a-3p, are increased in abundance.

Table 1 catalogs the miRNAs that were most responsive to the various treatments, including Cd(II), along with functional information regarding their likely target genes [58,59]. miRNAs belonging to the let-7 family were particularly responsive to Cd exposure; these miRNAs have been described as tumor suppressors, given that their

521 abundance is often much lower in cancerous than in healthy tissues [29,60]. In the
522 THP-1 cells, seven let-7 miRNAs were reduced in abundance after exposure to 50 µg
523 ml^{-1} CdS QDs, whereas there was no effect in cells exposed to the lower dose.
524 Meanwhile, exposure to 11.4 µg ml^{-1} Cd(II) reduced the abundance of eight let-7
525 miRNAs. Note that in HepG2 cells exposed to 5.2 µg ml^{-1} Cd(II), only three let-7
526 miRNAs were reduced. In THP-1 cells, miR-15b, which has also been implicated as a
527 tumor suppressor because it affects apoptosis through its targeting of gene *BCL-2*
528 [61], was also reduced by 50 µg ml^{-1} CdS QDs. A low dose of CdS QDs in HepG2
529 cells reduced expression of miR-15b in HepG2 cells but a comparable dose had no
530 effect on THP-1 cells.
531
532 **4. Conclusion**
533 *In vitro* studies on cellular models have clearly shown the molecular effects of ENMs
534 such as QDs and suggested possible modes of action in relation to their intrinsic
535 physico-chemical properties [62]. This information may be important for defining their
536 hazardous properties, a critical step in the identification of suitable biomarkers of
537 exposure. For similar QDs the metal (e.g. Cd) is largely responsible for the toxicity
538 [63]. *In vivo* evidence shows QDs cause pulmonary inflammation and hepatic toxicity
539 [64,65]. MiRNAs have been suggested as potential biomarkers of exposure to toxins
540 with some having important roles in multiple signaling pathways and apoptosis [28].
541 One function of miRNAs seems to cover a critical aspect of the general stress
542 response [66] with involvement in the formation of stress-induced response complex
543 (SIRC) which shuttles miRNAs into the nucleus [67]. Some proteins responsive to
544 metal-containing QDs, including metallothionein 1A, cytochrome P450 1A and heme
545 oxygenase, can be used as sensitivity biomarkers [68], but other events and

546 molecules would be useful to track exposure to QDs. After the oxidative stress which
547 follows ROS production and mitochondrial stress, additional glutathione is
548 synthesized and redistributed via MPAK-Nrf2. In addition TFEB is activated which
549 may promote lysosome formation and stabilization, helping to clear damaged
550 organelles [69]. If the stress continues there can be different types of cell damage
551 [10] including autophagy [70], apoptosis [71] and necrosis [72].
552 Different studies propose miRNAs as biomarkers of adverse exposure to metal-
553 based nanomaterials [25]. Moreover, the USFDA has recently accepted the use of
554 miRNAs as ‘genome biomarkers’.
555 Although miRNA profiling has been used to detect the response of different types of
556 cells and organisms to metals and to nanomaterials such as CdTe QDs [73], no
557 available study reports a direct comparison between exposure to the same
558 metal/element as a salt and as a QD constituent. A number of studies have
559 correlated the level of toxicant exposure to the induction of miRNAs in blood [13,14]
560 but there are several potential drawbacks of using miRNA changes to detect any
561 possible ‘genome biomarkers’ of exposure, including molecular instability [74]. The
562 assay of miRNAs expression we used here was based on 'array' quantitative PCR
563 with specific primers and TaqMan probes, which constitutes a gold-standard method
564 for quantitative transcriptional analysis [75]. Exposure to cadmium-based QDs and
565 changes in miRNAs have been correlated and used to explain cytotoxicity in
566 mammalian NIH/3T3 cells [73], in zebrafish liver cells [76], and in the brain of
567 Alzheimer's disease patients [77]. Altering the level of a single miRNA can trigger a
568 cascade of signaling events, potentially culminating in a major effect, either
569 stimulatory or inhibitory, on cell proliferation, apoptosis or other processes. In
570 principle, this raises the possibility of clinical interventions based on the modulation of

571 specific miRNAs by exposure to inhibitors or enhancers. The data presented here
572 showed that nanosized Cd, rather than ionic Cd, has a ‘soft’ regulatory effect on
573 miRNomes in human cells that is quite different from the ‘toxic’ inhibitory impact of
574 ionic Cd. There are three possible levels of response of human cells to nanomaterials
575 such as CdS QDs. The first of these is cell-type specific, as evidenced in a meta-
576 analysis of Cd-containing QDs [35]. Macrophages appear to be less susceptible to
577 toxicity than hepatocytes, even though they accumulate QDs more readily. The
578 second is physiological, as exemplified by differences in the capacity to maintain
579 mitochondrial structure and function when exposed to the stress agent. The final
580 level relates to the response of the miRNome, which has an impact on the
581 expression of various genes associated with defense or response to damage. It is
582 known that CdS QDs enter HepG2 cells. Previous studies had shown this was
583 followed by entry into lysosomes, triggering lysosomal enzymes with production of
584 ROS and initiation of autophagy [78] or apoptosis [79]. In our work HepG2 cells seem
585 to be programmed for apoptosis when exposed to CdS QDs, whereas for THP-1 cells
586 the outcome is autophagy. Some nanomaterials induce autophagy in cancer cells
587 which could lead to cancer cell death, enabling specific cancer therapies [80].
588 Autophagy induced by QDs can be seen as an attempt to degrade what is perceived
589 as foreign [81], but, in some instances, as for HepG2 cells, it can lead to apoptosis
590 and cell death [82]. MiRNAs associated with mitochondria [83,84] and cytosolic
591 miRNAs can be transferred into the mitochondria (or generated inside) and initiate
592 this deregulation processes [85]. Mitochondria are known as ROS generators and
593 also targets of ROS [49]. ROS cause mitochondrial swelling, inhibition of respiration
594 and mitochondrial permeability transition [86]. In the cells we studied, mitochondrial
595 function was particularly sensitive to Cd(II) but less sensitive to QDs. In particular, the

relative tolerance of THP-1 cells favors the idea that this cell type is more capable to maintain a stable level of cellular homeostasis employing autophagy. Another potentially significant impact is the activation of miRNAs of the tumor-suppressing let-7 family which were down-regulated by Cd(II) but not by equivalent doses of Cd QDs. The relative low cytotoxicity exhibited by CdS QDs could be of interest in the context of their potential use as carriers of clinically active compounds such as antibiotics [87] or antibodies [88] or in gene delivery, as in gene therapy [89, 90].

Appendix A. Supplementary data

Acknowledgments

This work has been supported by the CINSA (National Interuniversity Consortium for Environmental Sciences). The University of Parma, Local Founds (FIL) has also supported OB. Institute of Materials for Electronics and Magnetism – National Research Council (IMEM-CNR) has supported the work of AZ and MV in the preparation analysis and characterization of CdS QDs utilized in this paper. The confocal images were obtained in the Laboratory of Confocal Microscopy of the Department of Medicine and Surgery of the University of Parma. Real Time-PCR analysis were performed using an equipment of SITEIA-Parma, Region Emilia Romagna Tecnopole (Interdepartmental Center on Safety and Technology in the Agro-Food Industry).

Declaration of Competing Interest

The authors declare no competing financial interest.

Author Contributions

The manuscript was written with contributions from all authors who have given approval to the final version of the manuscript.

References

[1] Y.P. Zhang, P. Sun, X.R. Zhang, W.L. Yang, C.S. Si, Synthesis of CdTe quantum dot-conjugated CC49 and their application for in vitro imaging of gastric adenocarcinoma cells, Nanoscale Res. Lett. 8 (2013) 1–9. https://doi.org/10.1186/1556-276X-8-294.

[2] K. V. Chakravarthy, B.A. Davidson, J.D. Helinski, H. Ding, W.C. Law, K.T. Yong, P.N. Prasad, P.R. Knight, Doxorubicin-conjugated quantum dots to target alveolar macrophages and inflammation, Nanomedicine Nanotechnology, Biol. Med. 7 (2011) 88–96. https://doi.org/10.1016/j.nano.2010.09.001.

[3] G. Zhang, L. Shi, M. Selke, X. Wang, CdTe quantum dots with daunorubicin induce apoptosis of multidrug-resistant human hepatoma HepG2/ADM cells: in vitro and in vivo evaluation, 2011. https://doi.org/10.1186/1556-276X-6-418.

[4] Y. Wang, M. Tang, Review of in vitro toxicological research of quantum dot and potentially involved mechanisms, Sci. Total Environ. 625 (2018) 940–962. https://doi.org/10.1016/j.scitotenv.2017.12.334.

[5] C.T. Matea, T. Mocan, F. Tabaran, T. Pop, O. Mosteanu, C. Puia, C. Iancu, L. Mocan, Quantum dots in imaging, drug delivery and sensor applications, Int. J. Nanomedicine. 12 (2017) 5421–5431. https://doi.org/10.2147/IJN.S138624.

[6] D. Mo, L. Hu, G. Zeng, G. Chen, J. Wan, Z. Yu, Z. Huang, K. He, C. Zhang, M. Cheng, Cadmium-containing quantum dots: properties, applications, and toxicity, Appl. Microbiol. Biotechnol. 101 (2017) 2713–2733. https://doi.org/10.1007/s00253-017-8140-9.

[7] B.B. Manshian, J. Jiménez, U. Himmelreich, S.J. Soenen, Personalized medicine and follow-up of therapeutic delivery through exploitation of quantum dot toxicity, Biomaterials. 127 (2017) 1–12. https://doi.org/10.1016/j.biomaterials.2017.02.039.

[8] N. Chen, Y. He, Y. Su, X. Li, Q. Huang, H. Wang, X. Zhang, R. Tai, C. Fan, The cytotoxicity of cadmium-based quantum dots, Biomaterials. 33 (2012) 1238–1244. https://doi.org/10.1016/j.biomaterials.2011.10.070.

[9] T. Zhang, Y. Hu, M. Tang, L. Kong, J. Ying, T. Wu, Y. Xue, Y. Pu, Liver Toxicity of Cadmium Telluride Quantum Dots (CdTe QDs) Due to Oxidative Stress in Vitro and in Vivo., Int. J. Mol. Sci. 16 (2015) 23279–99. https://doi.org/10.3390/ijms161023279.

[10] K. He, X. Liang, T. Wei, N. Liu, Y. Wang, L. Zou, J. Lu, Y. Yao, L. Kong, T. Zhang, Y. Xue, T. Wu, M. Tang, DNA damage in BV-2 cells: An important supplement to the neurotoxicity of CdTe quantum dots, J. Appl. Toxicol. 39 (2019) 525–539. https://doi.org/10.1002/jat.3745.

[11] S. Kato, K. Itoh, T. Yaoi, T. Tozawa, Y. Yoshikawa, H. Yasui, N. Kanamura, A. Hoshino, N. Manabe, K. Yamamoto, S. Fushiki, Organ distribution of quantum dots after intraperitoneal administration, with special reference to area-specific distribution in the brain, Nanotechnology. 21 (2010) 335103. https://doi.org/10.1088/0957-4484/21/33/335103.

[12] L. Paesano, A. Perotti, A. Buschini, C. Carubbi, M. Marmiroli, E. Maestri, S. Iannotta, N. Marmiroli, Markers for toxicity to HepG2 exposed to cadmium sulphide quantum dots; damage to mitochondria, Toxicology. 374 (2016) 18–28. https://doi.org/10.1016/j.tox.2016.11.012.

[13] H. Food and Drug Administration, International Conference on Harmonisation; Guidance on E15 Pharmacogenomics Definitions and Sample Coding; Availability. Notice., Fed. Regist. 73 (2008) 19074–6. http://www.ncbi.nlm.nih.gov/pubmed/18677821 (accessed September 4, 2018).

[14] H. Food and Drug Administration, International Conference on Harmonisation; Guidance on E16 Biomarkers Related to Drug or Biotechnology Product Development: Context, Structure, and Format of Qualification Submissions; availability. Notice., Fed. Regist. 76 (2011) 49773–4. http://www.ncbi.nlm.nih.gov/pubmed/21834216 (accessed September 4, 2018).

[15] Y. Bai, Y. Xue, X. Xie, T. Yu, Y. Zhu, Q. Ge, Z. Lu, The RNA expression signature of the HepG2 cell line as determined by the integrated analysis of miRNA and mRNA expression profiles, Gene. 548 (2014) 91–100. https://doi.org/10.1016/j.gene.2014.07.016.

[16] Y. Chen, D.-Y. Gao, L. Huang, In vivo delivery of miRNAs for cancer therapy: challenges and strategies., Adv. Drug Deliv. Rev. 81 (2015) 128–41. https://doi.org/10.1016/j.addr.2014.05.009.

[17] F. Bignami, E. Pilotti, L. Bertoncelli, P. Ronzi, M. Gulli, N. Marmiroli, G. Magnani, M. Pinti, L. Lopalco, C. Mussini, R. Ruotolo, M. Galli, A. Cossarizza, C. Casoli, Stable changes in CD4+ T lymphocyte miRNA expression after exposure to HIV-1, Blood. 119 (2012) 6259–6267.

https://doi.org/10.1182/blood-2011-09-379503.

[18] L.A. Genovesi, D. Anderson, K.W. Carter, K.M. Giles, P.B. Dallas, Identification of suitable endogenous control genes for microRNA expression profiling of childhood medulloblastoma and human neural stem cells, BMC Res. Notes. 5 (2012). https://doi.org/10.1186/1756-0500-5-507.

[19] A. Tripathi, K. Goswami, N. Sanan-Mishra, Role of bioinformatics in establishing microRNAs as modulators of abiotic stress responses: the new revolution., Front. Physiol. 6 (2015) 286. https://doi.org/10.3389/fphys.2015.00286.

[20] A.B. Mendoza-Soto, F. Sánchez, G. Hernández, MicroRNAs as regulators in plant metal toxicity response., Front. Plant Sci. 3 (2012) 105. https://doi.org/10.3389/fpls.2012.00105.

[21] D. Hosiner, S. Gerber, H. Lichtenberg-Frané, W. Glaser, C. Schüller, E. Klipp, Impact of Acute Metal Stress in Saccharomyces cerevisiae, PLoS One. 9 (2014) e83330. https://doi.org/10.1371/journal.pone.0083330.

[22] B. Wang, Y. Li, C. Shao, Y. Tan, L. Cai, Cadmium and Its Epigenetic Effects, Curr. Med. Chem. 19 (2012) 2611–2620. https://doi.org/10.2174/092986712800492913.

[23] M.A. Burgos-Aceves, A. Cohen, G. Paolella, M. Lepretti, Y. Smith, C. Faggio, L. Lionetti, Modulation of mitochondrial functions by xenobiotic-induced microRNA: From environmental sentinel organisms to mammals, Sci. Total Environ. 645 (2018) 79–88. https://doi.org/10.1016/j.scitotenv.2018.07.109.

[24] H.J. Eom, N. Chatterjee, J. Lee, J. Choi, Integrated mRNA and micro RNA

715 profiling reveals epigenetic mechanism of differential sensitivity of Jurkat T
716 cells to AgNPs and Ag ions, Toxicol. Lett. 229 (2014) 311–318.
717 https://doi.org/10.1016/j.toxlet.2014.05.019.

718 [25] J. Ndika, U. Seemab, W.L. Poon, V. Fortino, H. El-Nezami, P. Karisola, H.
719 Alenius, Silver, titanium dioxide, and zinc oxide nanoparticles trigger
720 miRNA/isomiR expression changes in THP-1 cells that are proportional to their
721 health hazard potential, Nanotoxicology. (2019).
722 https://doi.org/10.1080/17435390.2019.1661040.

723 [26] Y. Huang, X. Lü, Y. Qu, Y. Yang, S. Wu, MicroRNA sequencing and molecular
724 mechanisms analysis of the effects of gold nanoparticles on human dermal
725 fibroblasts, Biomaterials. 37 (2015) 13–24.
726 https://doi.org/10.1016/j.biomaterials.2014.10.042.

727 [27] K. Vrijens, V. Bollati, T.S. Nawro, MicroRNAs as Potential Signatures of
728 Environmental Exposure or Effect:, Env. Heal. Perspect. 123 (2015) 399–411.
729 https://doi.org/http://dx.doi.org/10.1289/ehp.1408459.

730 [28] R. Machtinger, V. Bollati, A.A. Baccarelli, miRNAs and lncRNAs as Biomarkers
731 of Toxicant Exposure, in: Toxicoepigenetics, Elsevier, 2019: pp. 237–247.
732 https://doi.org/10.1016/b978-0-12-812433-8.00010-1.

733 [29] M. Fabbri, C. Urani, M.G. Sacco, C. Procaccianti, L. Gribaldo, Whole genome
734 analysis and microRNAs regulation in HepG2 cells exposed to cadmium.,
735 ALTEX. 29 (2012) 173–82. https://doi.org/10.14573/altex.2012.2.173.

736 [30] Z. Liu, W. Jiang, J. Nam, J.J. Moon, B.Y.S. Kim, Immunomodulating
737 Nanomedicine for Cancer Therapy, Nano Lett. 18 (2018) 6655–6659.

https://doi.org/10.1021/acs.nanolett.8b02340.

[31] M. Villani, D. Calestani, L. Lazzarini, L. Zanotti, R. Mosca, A. Zappettini, Extended functionality of ZnO nanotetrapods by solution-based coupling with CdS nanoparticles, J. Mater. Chem. 22 (2012) 5694. https://doi.org/10.1039/c2jm16164h.

[32] L. Paesano, A. Perotti, A. Buschini, C. Carubbi, M. Marmiroli, E. Maestri, S. Iannotta, N. Marmiroli, Data on HepG2 cells changes following exposure to cadmium sulphide quantum dots (CdS QDs), Data Br. 11 (2017). https://doi.org/10.1016/j.dib.2016.12.051.

[33] L. Pagano, F. Pasquali, S. Majumdar, R. De La Torre-Roche, N. Zuverza-Mena, M. Villani, A. Zappettini, R.E. Marra, S.M. Isch, M. Marmiroli, E. Maestri, O.P. Dhankher, J.C. White, N. Marmiroli, Exposure of Cucurbita pepo to binary combinations of engineered nanomaterials: Physiological and molecular response, Environ. Sci. Nano. 4 (2017) 1579–1590. https://doi.org/10.1039/c7en00219j.

[34] J. O'Brien, I. Wilson, T. Orton, F. Pognan, Investigation of the Alamar Blue (resazurin) fluorescent dye for the assessment of mammalian cell cytotoxicity, Eur. J. Biochem. 267 (2000) 5421–5426. https://doi.org/10.1046/j.1432-1327.2000.01606.x.

[35] E. Oh, R. Liu, A. Nel, K.B. Gemill, M. Bilal, Y. Cohen, I.L. Medintz, Meta-analysis of cellular toxicity for cadmium-containing quantum dots, Nat Nano. (2016) doi:10.1038/nnano.2015.338. https://doi.org/10.1038/nnano.2015.338.

[36] L. Peng, M. He, B. Chen, Q. Wu, Z. Zhang, D. Pang, Y. Zhu, B. Hu, Cellular

761 uptake, elimination and toxicity of CdSe/ZnS quantum dots in HepG2 cells,
762 Biomaterials. 34 (2013) 9545–9558.
763 https://doi.org/10.1016/j.biomaterials.2013.08.038.

764 [37] K.J. Livak, T.D. Schmittgen, Analysis of relative gene expression data using
765 real-time quantitative PCR and the 2(-Delta Delta C(T)) Method., Methods. 25
766 (2001) 402–408. https://doi.org/10.1006/meth.2001.1262.

767 [38] M.G. Bianchi, M. Allegri, A.L. Costa, M. Blosi, D. Gardini, C. Del Pivo, A. Prina-
768 Mello, L. Di Cristo, O. Bussolati, E. Bergamaschi, Titanium dioxide
769 nanoparticles enhance macrophage activation by LPS through a TLR4-
770 dependent intracellular pathway, Toxicol. Res. (Camb). 4 (2015) 385–398.
771 https://doi.org/10.1039/c4tx00193a.

772 [39] I.S. Vlachos, M.D. Paraskevopoulou, D. Karagkouni, G. Georgakilas, T.
773 Vergoulis, I. Kanellos, I.-L. Anastasopoulos, S. Maniou, K. Karathanou, D.
774 Kalfakakou, A. Fevgas, T. Dalamagas, A.G. Hatzigeorgiou, DIANA-TarBase
775 v7.0: indexing more than half a million experimentally supported miRNA:mRNA
776 interactions., Nucleic Acids Res. 43 (2015) D153-9.
777 https://doi.org/10.1093/nar/gku1215.

778 [40] I.S. Vlachos, K. Zagganas, M.D. Paraskevopoulou, G. Georgakilas, D.
779 Karagkouni, T. Vergoulis, T. Dalamagas, A.G. Hatzigeorgiou, DIANA-miRPath
780 v3.0: deciphering microRNA function with experimental support, Nucleic Acids
781 Res. 43 (2015) W460–W466. https://doi.org/10.1093/nar/gkv403.

782 [41] S.-D. Hsu, Y.-T. Tseng, S. Shrestha, Y.-L. Lin, A. Khaleel, C.-H. Chou, C.-F.
783 Chu, H.-Y. Huang, C.-M. Lin, S.-Y. Ho, T.-Y. Jian, F.-M. Lin, T.-H. Chang, S.-L.
784 Weng, K.-W. Liao, I.-E. Liao, C.-C. Liu, H.-D. Huang, miRTarBase update

2014: an information resource for experimentally validated miRNA-target interactions., Nucleic Acids Res. 42 (2014) D78-85. https://doi.org/10.1093/nar/gkt1266.

[42] T. Brzicova, E. Javorkova, K. Vrbova, A. Zajicova, V. Holan, D. Pinkas, V. Philimonenko, J. Sikorova, J. Klema, J. Topinka, P. Rossner, Molecular responses in THP-1 macrophage-like cells exposed to diverse nanoparticles, Nanomaterials. 9 (2019). https://doi.org/10.3390/nano9050687.

[43] M.M. Haque, H. Im, J. Seo, M. Hasan, K. Woo, O.-S. Kwon, Acute toxicity and tissue distribution of CdSe/CdS-MPA quantum dots after repeated intraperitoneal injection to mice, J. Appl. Toxicol. 33 (2013) 940–950. https://doi.org/10.1002/jat.2775.

[44] C. Urani, P. Melchioretto, C. Canevali, G.F. Crosta, Cytotoxicity and induction of protective mechanisms in HepG2 cells exposed to cadmium., Toxicol. In Vitro. 19 (2005) 887–892. https://doi.org/10.1016/j.tiv.2005.06.011.

[45] S. Oh, S. Lim, A rapid and transient ROS generation by cadmium triggers apoptosis via caspase-dependent pathway in HepG2 cells and this is inhibited through N-acetylcysteine-mediated catalase upregulation, Toxicol. Appl. Pharmacol. 212 (2006) 212–223. https://doi.org/10.1016/j.taap.2005.07.018.

[46] K.G. Li, J.T. Chen, S.S. Bai, X. Wen, S.Y. Song, Q. Yu, J. Li, Y.Q. Wang, Intracellular oxidative stress and cadmium ions release induce cytotoxicity of unmodified cadmium sulfide quantum dots, Toxicol. Vitr. 23 (2009) 1007–1013. https://doi.org/10.1016/j.tiv.2009.06.020.

[47] F. Pasquali, C. Agrimonti, L. Pagano, A. Zappettini, M. Villani, M. Marmiroli,

808 J.C. White, N. Marmiroli, Nucleo-mitochondrial interaction of yeast in response
809 to cadmium sulfide quantum dot exposure, J. Hazard. Mater. 324 (2017) 744–
810 752. https://doi.org/10.1016/J.JHAZMAT.2016.11.053.

811 [48] S.W. Funkhouser, O. Martinezmaza, D.L. Vredevoe, Cadmium Inhibits IL-6
812 Production and IL-6 mRNA Expression in a Human Monocytic Cell Line, THP-
813 1, Environ. Res. 66 (1994) 77–86. https://doi.org/10.1006/ENRS.1994.1045.

814 [49] J. Li, Y. Zhang, Q. Xiao, F. Tian, X. Liu, R. Li, G. Zhao, F. Jiang, Y. Liu,
815 Mitochondria as target of Quantum dots toxicity, J. Hazard. Mater. 194 (2011)
816 440–444. https://doi.org/10.1016/j.jhazmat.2011.07.113.

817 [50] Y. Wang, M. Tang, Dysfunction of various organelles provokes multiple cell
818 death after quantum dot exposure, Int. J. Nanomedicine. 13 (2018) 2729–2742.
819 https://doi.org/10.2147/IJN.S157135.

820 [51] M. Yan, Y. Zhang, H. Qin, K. Liu, M. Guo, Y. Ge, M. Xu, Y. Sun, X. Zheng,
821 Cytotoxicity of CdTe quantum dots in human umbilical vein endothelial cells:
822 The involvement of cellular uptake and induction of pro-apoptotic endoplasmic
823 reticulum stress, Int. J. Nanomedicine. 11 (2016) 529–542.
824 https://doi.org/10.2147/IJN.S93591.

825 [52] L. Paesano, M. Marmiroli, M.G. Bianchi, J.C. White, O. Bussolati, A. Zappettini,
826 M. Villani, N. Marmiroli, Data on miRNome changes in human cells exposed to
827 nano- or ionic- form of Cd, Data Br. (submitted).

828 [53] D.J. Klionsky, F.C. Abdalla, H. Abeliovich, R.T. Abraham, A. Acevedo-Arozena,
829 K. Adeli, L. Agholme, M. Agnello, P. Agostinis, J.A. Aguirre-Ghiso, et al.,
830 Guidelines for the use and interpretation of assays for monitoring autophagy,

831 Autophagy. 8 (2012) 445–544. https://doi.org/10.4161/auto.19496.

832 [54] M. Komatsu, Y. Ichimura, Physiological significance of selective degradation of
833 p62 by autophagy, FEBS Lett. 584 (2010) 1374–1378.
834 https://doi.org/10.1016/j.febslet.2010.02.017.

835 [55] K.C. Nguyen, W.G. Willmore, A.F. Tayabali, Cadmium telluride quantum dots
836 cause oxidative stress leading to extrinsic and intrinsic apoptosis in
837 hepatocellular carcinoma HepG2 cells, Toxicology. 306 (2013) 114–123.
838 https://doi.org/10.1016/j.tox.2013.02.010.

839 [56] Z. Su, Z. Yang, Y. Xu, Y. Chen, Q. Yu, Z. Su, Z. Yang, Y. Xu, Y. Chen, Q. Yu,
840 MicroRNAs in apoptosis, autophagy and necroptosis, Oncotarget. 6 (2015)
841 8474–8490. https://doi.org/10.18632/oncotarget.3523.

842 [57] V. Pileczki, R. Cojocneanu-Petric, M. Maralani, I.B. Neagoe, R. Sandulescu,
843 MicroRNAs as regulators of apoptosis mechanisms in cancer., Clujul Med. 89
844 (2016) 50–5. https://doi.org/10.15386/cjmed-512.

845 [58] K. Cuk, D. Madhavan, A. Turchinovich, B. Burwinkel, Plasma microRNAs as
846 Biomarkers of Human Diseases, in: S.C. Sahu (Ed.), MicroRNAs Toxicol. Med.,
847 John Wiley & Sons, Ltd, Chichester, UK, 2013: pp. 389–418.
848 https://doi.org/10.1002/9781118695999.

849 [59] K.A. Bailey, R.C. Fry, Environmental Toxicants and Perturbation of miRNA
850 Signaling, in: S.C. Sahu (Ed.), MicroRNAs Toxicol. Med., John Wiley & Sons,
851 Ltd, Chichester, UK, 2013: pp. 5–22. https://doi.org/10.1002/9781118695999.

852 [60] B. Boyerinas, S.M. Park, A. Hau, A.E. Murmann, M.E. Peter, The role of let-7 in
853 cell differentiation and cancer, Endocr. Relat. Cancer. 17 (2010) 19–36.

https://doi.org/10.1677/ERC-09-0184.

[61] C.-J. Guo, Q. Pan, D.-G. Li, H. Sun, B.-W. Liu, miR-15b and miR-16 are implicated in activation of the rat hepatic stellate cell: An essential role for apoptosis, J. Hepatol. 50 (2009) 766–778. https://doi.org/10.1016/j.jhep.2008.11.025.

[62] P. Schulte, V. Leso, M. Niang, I. Iavicoli, Biological monitoring of workers exposed to engineered nanomaterials, Toxicol. Lett. 298 (2018) 112–124. https://doi.org/10.1016/j.toxlet.2018.06.003.

[63] A.A. Mansur, H.S. Mansur, S.M. de Carvalho, Z.I. Lobato, M.I. Guedes, M.F. Leite, Surface biofunctionalized CdS and ZnS quantum dot nanoconjugates for nanomedicine and oncology: to be or not to be nanotoxic?, Int. J. Nanomedicine. 11 (2016) 4669–4690. https://doi.org/10.2147/ijn.s115208.

[64] J.R. Roberts, J.M. Antonini, D.W. Porter, R.S. Chapman, J.F. Scabilloni, S.H. Young, D. Schwegler-Berry, V. Castranova, R.R. Mercer, Lung toxicity and biodistribution of Cd/Se-ZnS quantum dots with different surface functional groups after pulmonary exposure in rats., Part. Fibre Toxicol. 10 (2013). https://doi.org/10.1186/1743-8977-10-5.

[65] C.-C. Ho, H. Chang, H.-T. Tsai, M.-H. Tsai, C.-S. Yang, Y.-C. Ling, P. Lin, Quantum dot 705, a cadmium-based nanoparticle, induces persistent inflammation and granuloma formation in the mouse lung, Nanotoxicology. 7 (2013) 105–115. https://doi.org/10.3109/17435390.2011.635814.

[66] M. Olejniczak, A. Kotowska-Zimmer, W. Krzyzosiak, Stress-induced changes in miRNA biogenesis and functioning, Cell. Mol. Life Sci. 75 (2018) 177–191.

https://doi.org/10.1007/s00018-017-2591-0.

[67] D. Castanotto, X. Zhang, J. Alluin, X. Zhang, J. Rüger, B. Armstrong, J. Rossi, A. Riggs, C.A. Stein, A stress-induced response complex (SIRC) shuttles miRNAs, siRNAs, and oligonucleotides to the nucleus, Proc. Natl. Acad. Sci. U. S. A. 115 (2018) E5756–E5765. https://doi.org/10.1073/pnas.1721346115.

[68] L.A. McConnachie, C.C. White, D. Botta, M.E. Zadworny, D.P. Cox, R.P. Beyer, X. Hu, D.L. Eaton, X. Gao, T.J. Kavanagh, Heme oxygenase expression as a biomarker of exposure to amphiphilic polymer-coated CdSe/ZnS quantum dots, Nanotoxicology. 7 (2013) 181–191. https://doi.org/10.3109/17435390.2011.648224.

[69] K.D. Neibert, D. Maysinger, Mechanisms of cellular adaptation to quantum dots – the role of glutathione and transcription factor EB, Nanotoxicology. 6 (2012) 249–262. https://doi.org/10.3109/17435390.2011.572195.

[70] J. Fan, Y. Sun, S. Wang, Y. Li, X. Zeng, Z. Cao, P. Yang, P. Song, Z. Wang, Z. Xian, H. Gao, Q. Chen, D. Cui, D. Ju, Inhibition of autophagy overcomes the nanotoxicity elicited by cadmium-based quantum dots, Biomaterials. 78 (2016) 102–114. https://doi.org/10.1016/j.biomaterials.2015.11.029.

[71] P. Rodríguez-Fragoso, J. Reyes-Esparza, A. León-Buitimea, L. Rodríguez-Fragoso, Synthesis, characterization and toxicological evaluation of maltodextrin capped cadmium sulfide nanoparticles in human cell lines and chicken embryos., J. Nanobiotechnology. 10 (2012) 47. https://doi.org/10.1186/1477-3155-10-47.

[72] L. Lai, J.C. Jin, Z.Q. Xu, P. Mei, F.L. Jiang, Y. Liu, Necrotic cell death induced

by the protein-mediated intercellular uptake of CdTe quantum dots, Chemosphere. 135 (2015) 240–249. https://doi.org/10.1016/j.chemosphere.2015.04.044.

[73] S. Li, Y. Wang, H. Wang, Y. Bai, G. Liang, Y. Wang, N. Huang, Z. Xiao, MicroRNAs as participants in cytotoxicity of CdTe quantum dots in NIH/3T3 cells, Biomaterials. 32 (2011) 3807–3814. https://doi.org/10.1016/j.biomaterials.2011.01.074.

[74] V. Bravo, S. Rosero, C. Ricordi, R.L. Pastori, Instability of miRNA and cDNAs derivatives in RNA preparations, Biochem. Biophys. Res. Commun. 353 (2007) 1052–1055. https://doi.org/10.1016/j.bbrc.2006.12.135.

[75] T. Nolan, R.E. Hands, S.A. Bustin, Quantification of mRNA using real-time RT-PCR, Nat. Protoc. 1 (2006) 1559. http://dx.doi.org/10.1038/nprot.2006.236.

[76] S. Tang, Q. Cai, H. Chibli, V. Allagadda, J.L. Nadeau, G.D. Mayer, Cadmium sulfate and CdTe-quantum dots alter DNA repair in zebrafish (Danio rerio) liver cells, Toxicol. Appl. Pharmacol. 272 (2013) 443–452. https://doi.org/https://doi.org/10.1016/j.taap.2013.06.004.

[77] B. Sun, F. Yang, F.H. Hu, N.P. Huang, Z.D. Xiao, Comprehensive annotation of microRNA expression profiles, BMC Genet. 14 (2013) 1–9. https://doi.org/10.1186/1471-2156-14-120.

[78] J. Fan, S. Wang, X. Zhang, W. Chen, Y. Li, P. Yang, Z. Cao, Y. Wang, W. Lu, D. Ju, Quantum Dots Elicit Hepatotoxicity through Lysosome-Dependent Autophagy Activation and Reactive Oxygen Species Production, ACS Biomater. Sci. Eng. 4 (2018) 1418–1427.

https://doi.org/10.1021/acsbiomaterials.7b00824.

[79] E.Y. Lee, H.C. Bae, H. Lee, Y. Jang, Y.-H. Park, J.H. Kim, W.-I. Ryu, B.H. Choi, J.H. Kim, S.H. Jeong, S.W. Son, Intracellular ROS levels determine the apoptotic potential of keratinocyte by Quantum Dot via blockade of AKT Phosphorylation, Exp. Dermatol. 26 (2017) 1046–1052. https://doi.org/10.1111/exd.13365.

[80] F. Wei, Y. Duan, Crosstalk between Autophagy and Nanomaterials: Internalization, Activation, Termination, Adv. Biosyst. 3 (2019) 1800259. https://doi.org/10.1002/adbi.201800259.

[81] S.T. Stern, P.P. Adiseshaiah, R.M. Crist, Autophagy and lysosomal dysfunction as emerging mechanisms of nanomaterial toxicity, Part. Fibre Toxicol. 9 (2012) 20. https://doi.org/10.1186/1743-8977-9-20.

[82] J. Zhang, X. Qin, B. Wang, G. Xu, Z. Qin, J. Wang, L. Wu, X. Ju, D.D. Bose, F. Qiu, H. Zhou, Z. Zou, Zinc oxide nanoparticles harness autophagy to induce cell death in lung epithelial cells, Cell Death Dis. 8 (2017) e2954. https://doi.org/10.1038/cddis.2017.337.

[83] L. Sripada, D. Tomar, R. Singh, Mitochondria: One of the destinations of miRNAs, Mitochondrion. 12 (2012) 593–599. https://doi.org/10.1016/j.mito.2012.10.009.

[84] M.J. Axtell, Lost in translation? microRNAs at the rough ER, Trends Plant Sci. 22 (2017) 273–274. https://doi.org/10.1016/j.tplants.2017.03.002.

[85] P. Li, J. Jiao, G. Gao, B.S. Prabhakar, Control of mitochondrial activity by miRNAs, J. Cell. Biochem. 113 (2012) 1104–1110.

https://doi.org/10.1002/jcb.24004.

[86] K.C. Nguyen, P. Rippstein, a. F. Tayabali, W.G. Willmore, Mitochondrial Toxicity of Cadmium Telluride Quantum Dot Nanoparticles in Mammalian Hepatocytes, Toxicol. Sci. 146 (2015) 31–42. https://doi.org/10.1093/toxsci/kfv068.

[87] I. Armenia, G.L. Marcone, F. Berini, V.T. Orlandi, C. Pirrone, E. Martegani, R. Gornati, G. Bernardini, F. Marinelli, Magnetic Nanoconjugated Teicoplanin: A Novel Tool for Bacterial Infection Site Targeting, Front. Microbiol. 9 (2018). https://doi.org/10.3389/fmicb.2018.02270.

[88] M.C. Johnston, C.J. Scott, Antibody conjugated nanoparticles as a novel form of antibody drug conjugate chemotherapy, Drug Discov. Today Technol. 30 (2018) 63–69. https://doi.org/10.1016/J.DDTEC.2018.10.003.

[89] K.J. McHugh, L. Jing, S.Y. Severt, M. Cruz, M. Sarmadi, H.S.N. Jayawardena, C.F. Perkinson, F. Larusson, S. Rose, S. Tomasic, T. Graf, S.Y. Tzeng, J.L. Sugarman, D. Vlasic, M. Peters, N. Peterson, L. Wood, W. Tang, J. Yeom, J. Collins, P.A. Welkhoff, A. Karchin, M. Tse, M. Gao, M.G. Bawendi, R. Langer, A. Jaklenec, Biocompatible near-infrared quantum dots delivered to the skin by microneedle patches record vaccination, Sci. Transl. Med. 11 (2019) eaay7162. https://doi.org/10.1126/scitranslmed.aay7162.

[90] J. Choi, Y. Rui, J. Kim, N. Gorelick, D.R. Wilson, K. Kozielski, A. Mangraviti, E. Sankey, H. Brem, B. Tyler, J.J. Green, E.M. Jackson, Nonviral polymeric nanoparticles for gene therapy in pediatric CNS malignancies, Nanomedicine Nanotechnology, Biol. Med. 23 (2020). https://doi.org/10.1016/j.nano.2019.102115.

Figure captions

Fig. 1 *The effect of CdS QDs and Cd(II) treatment on mitochondrial membrane potential, as quantified by JC-1 staining.* Cells were exposed for 24 h to Cd in the form of either CdS QDs or Cd(II). The data report the ratio between aggregated and monomeric forms of JC1, and are representative of three independent experiments. The concentrations of CdS QDs and Cd(II) shown are for the Cd in the material. Asterisks ***. ****: p<0.001, <0.0001 vs. values obtained from non-treated cells.

Fig. 2 *The effect on THP-1 cell morphology of exposure to Cd in the form of either CdS QDs or* Cd(II)*.* After a 24 h exposure to a high or low dose of either stressor, cell monolayers were labelled with JC-1 to assay mitochondrial function or with DRAQ5 to assay nuclear morphology. CdS QDs, 6.4 μg ml^{-1} equivalent to 5 μg ml^{-1} Cd, induced a modest increase in the amount of JC-1 monomers, suggesting some alteration in mitochondrial function but there was no evidence of marked changes in cell morphology. Cd in the form of Cd(II), 11.4 μg ml^{-1} equivalent to 5 μg ml^{-1} Cd, not only substantially increased the abundance of JC-1 monomers, but also caused loss of the red signal, suggesting a significant alteration in mitochondrial function. In addition, Cd(II) treatment also changed the typical elongated shape into a more rounded form. When THP-1 cells were exposed to a high dose of CdS QDs, 50 μg ml^{-1} equivalent to 39 μg ml^{-1} Cd, most of the CdS QDs aggregated and the presence of JC-1 monomeric forms was only slightly increased. Cell morphology appeared to be substantially unaffected. Bar: 20 μm. The images illustrate representative microscope fields where at least 100 cells were present.

Fig. 3 *The uptake of CdS QDs into THP-1 cells as measured using a cytofluorimetric assay.* Cells were exposed to 39 μg ml^{-1} Cd as 50 μg ml^{-1} CdS QDs for 0 - 24 h. Typical scatter plots are shown, obtained from a representative experiment performed three times with comparable results. FS, forward scatter; SS, side scatter

Fig. 4 *Venn diagram representation of the effect of exposure to Cd on the miRNome.* **a**, HepG2 cells exposed to 2.3 μg ml^{-1} Cd as 3 μg ml^{-1} CdS QDs or 5.2 μg ml^{-1} Cd(II). The number of miRNAs increased in abundance were 34 and 29, respectively, while number of miRNAs decreased in abundance were 32 and 102, respectively. Only 11 and 13 miRNAs were increased or reduced in abundance by both treatments, respectively. **b**, THP-1 cells exposed to 5 μg ml^{-1} Cd as 6.4 μg ml^{-1} CdS QDs or 11.4 μg ml^{-1} Cd(II). Exposure to CdS QDs increased the abundance of 136 miRNAs, whereas only 15 were reduced. **c**, Comparison between HepG2 cells exposed to 2.3 μg ml^{-1} Cd as 3 μg ml^{-1} CdS QDs and THP-1 cells exposed to 5 μg ml^{-1} Cd as 6.4 μg ml^{-1} CdS QDs. Ten miRNAs responded positively and 2 responded negatively in both cell types. Eight miRNAs responded in opposite directions. **d**, Comparison between HepG2 cells exposed to 2.3 μg ml^{-1} Cd as 5.2 μg ml^{-1} Cd(II) and THP-1 cells exposed to 5 μg ml^{-1} Cd as 11.4 μg ml^{-1} Cd(II). Thirty nine miRNAs responded negatively in both cell types, while no miRNA responded positively; 16 miRNAs responded in opposite manner.

Fig. 5 *A heatmap-based illustration of the HepG2 and THP-1 cell responses to Cd exposure*. The heatmaps show only those miRNAs which were increased or decreased in both cell types or with either treatment. Positively responding miRNAs are shown in red and negatively responding ones in green. **a**, Differentially abundant

1019 miRNAs present in HepG2 cells exposed to 2.3 μg ml^{-1} Cd as 3 μg ml^{-1} CdS QDs or
1020 5.2 μg ml^{-1} Cd(II). For a large number of miRNAs abundance is reduced when the
1021 cells are treated with Cd(II) as compared with cells treated with CdS QDs. **b**,
1022 Differentially abundant miRNAs present in HepG2 and THP-1 cells exposed to 2.3
1023 and 5 μg ml^{-1} Cd as 5.2 μg ml^{-1} and 11.4 μg ml^{-1} Cd(II). **c**, Differentially abundant
1024 miRNAs present in HepG2 and THP-1 cells exposed to 2.3 and 5 μg ml^{-1} Cd as 3 μg
1025 ml^{-1} and 6.4 μg ml^{-1} CdS QDs.
1026
1027 **Fig. 6** *The effect on the miRNome of exposure to Cd, illustrated by a Venn diagram.*
1028 **a**, miRNAs induced in THP-1 cells in response to exposure to either 39 μg ml^{-1} Cd as
1029 50 μg ml^{-1} CdS QDs or 5 μg ml^{-1} Cd as 11.4 μg ml^{-1} Cd(II). The abundances of totals
1030 of 9 and 18 miRNAs were increased by CdS QDs and Cd(II) treatment, respectively.
1031 miRNAs decreased in response to the two treatments were 237 and 129
1032 respectively; of these, 124 responded negatively to both treatments, while 5 miRNAs
1033 were decreased by Cd(II) treatment but increased in the presence of CdS QDs. **b**,
1034 miRNAs induced in either HepG2 or THP-1 cells in response to exposure to,
1035 respectively, 2.3 μg ml^{-1} Cd as 3 μg ml^{-1} CdS QDs and 39 μg ml^{-1} Cd as 50 μg ml^{-1}
1036 CdS QDs; **c**, miRNAs induced in either HepG2 or THP-1 cells in response to
1037 exposure to CdS QDs (all treatments).
1038
1039 **Fig. 7** *The core autophagy pathway and its regulation by miRNAs in THP-1 cells*
1040 *exposed to 39 μg ml^{-1} Cd as 50 μg ml^{-1} CdS QDs..* The entire pathway was divided
1041 into five steps: induction, vesicle nucleation, elongation, retrieval and fusion. Arrows
1042 indicate increase or decrease of miRNA. A green arrow indicated a decrease with

lack of repression of its specific targets. The overall effect seems to bring the cell towards autophagosome formation and autophagy.

Fig. 8 *The effect of exposure to Cd on autophagy markers in THP-1 and HepG2 cells.* THP-1 and HepG2 cells were incubated for 24h in the presence of different doses of Cd: 2.3 µg ml^{-1} as 3 µg ml^{-1} CdS QDs, 5 µg ml^{-1} as 6.4 µg ml^{-1} CdS QDs or as 11.4 µg ml^{-1} Cd(II) and 39 µg ml^{-1} as 50 µg ml^{-1} CdS QDs. Cells were then extracted and Western Blot analysis of p62 and LC3II was performed as described in Materials and Methods. Tubulin was used for loading control. *Pos* indicates THP-1 cells, treated with rapamycin, 10 nM, 3h, and cloroquine, 100 µM, 2h, exploited as positive controls for autophagy.

Fig. 9 *The core apoptotic pathway and its regulation by miRNAs in HepG2 cells exposed to 2.3 µg ml^{-1} Cd as 3 µg ml^{-1} CdS QDs.* The figure depicts events of the intrinsic and extrinsic apoptotic pathways. Arrows indicate increase or decrease of miRNA or gene. A red arrow indicates increased abundance of a specific gene. A green arrow indicates a decrease which permits the expression of its specific target. In this system the activation of the intrinsic pathway leads to apoptosis. At the dose of CdS QDs considered and under the experimental conditions adopted, the proportion of cells which effectively completed apoptosis was limited, as shown by morphological observation (see Fig. A.2).

Table

Table 1 Differentially abundant miRNAs in response to Cd exposure and their principal cellular targets, pathways and related diseases

		THP-1			HepG2			
		39 μg ml^{-1} Cd	5 μg ml^{-1} Cd		2.3 μg ml^{-1} Cd			
Processes[1]	**miRNA involved**[2]	QDs[3] 50 μg ml^{-1}	QDs[3] 6.4 μg ml^{-1}	Cd(II)[3] 11.4 μg ml^{-1}	QDs[3] 3 μg ml^{-1}	Cd(II)[3] 5.2 μg ml^{-1}	**Target protein**[4]	**Diseases**[5]
Apoptosis	miR-34a	/	/	/	/	↓	BCL-2	Cancer
	miR-195	↓	/	/	↓	↓		
	miR-143	↓	/	↓	/	↓		
	miR-155	↓	↑	↓	↓	/		
	miR-125	↓	↑	↓	/	/		
	miR-29a	↓	/	/	/	↓	CDC42, p58α	Cancer/ Huntington's disease
	miR-125b	↓	/	↓	/	/	p53	Cancer/ Psoriasis
	miR-221	↓	/	↓	/	/	p27 (KIP1)	
	miR-222	↑	↑	↓	/	↓		
	miR-181a	↑	↑	/	/	/	BIM	Cancer
	miR-32	↓	/	↓	↓	↓		
	miR-25	↓	/	↓	/	/		
DNA Repair	miR-16	↓	↑	↓	/	/	UNG2	Cancer
	miR-199	↓	↑	↓	/	/		
	miR-21	↓	/	↓	/	↓	hMSH2	
	miR-192	↓	/	↓	/	↓	ERCC3, ERCC4	Toxicant exposure biomarker
	miR-101	↓	↑	↓	/	/	DNA-PKcs	
	miR-24	↓	↑	↓	/	/	H2AX	Cancer
	miR-96	↓	/	/	/	/	RAD51	/
Cell cycle	miR-16	↓	↑	↓	/	/	CDK2	Cancer
	miR-449a/b	↓	↑/↓	↓	/	/	CDK6, CDC25A	/
	miR-15	↓	/	/	↑	/	WEE1, CHK1	Cancer
	miR-125	↓	↑	↓	/	/	Cyclin A2	
	let-7b	↓	/	↓	/	↓	Cyclin A	
Xenobiotic metabolism	miR-27b	↓	/	/	/	↓	CYP1B1	Diabetes
	miR-126	↓	↑	/	↓	↓	CYP2A3	Cancer/ Cardiovascular diseases
	miR-378	↓	/	/	↓	↓	CYP2E1	Cancer
	miR-133a	↓	↑	/	↑	↑	GSTP1	
Autophagy/ Phagocytosis	let-7a	↓	/	↓	/	↓	several chemokines	Cancer
	miR-146a	↓	/	/	/	/		Inflammatory diseases

	miR-25	↓	/	↓	/	/		Cancer
	miR-26a	↓	/	↓	/	↑		
Autophagy/ Phagocytosis	miR-132	↓	↑	↓	/	↑	several chemokines	Alzheimer's disease
	miR-140	↓	↑	↓	/	↓		Cancer
	miR-146b	↓	/	/	/	/		Inflammatory diseases
	miR-155	↓	↑	↓	↓	/		Cancer
	miR-210	↓	↑	↓	/	/		
	miR-21	↓	/	↓	/	/		
	miR-142-3p	↓	/	/	↓	/		Cardiovascular diseases
	miR-125b	↓	/	↓	/	/		Cancer
	miR-17-5p	↓	/	↓	/	↓		
	miR-24	↓	↑	↓	/	/		
	miR-30b	↓	↑	↓	/	↓		
	miR-101	↓	↑	↓	/	/		Toxicant exposure biomarker
	miR-652-3p	↓	/	↓	/	↓		/
	miR-1275	↓	↑	↓	/	↓		/
	miR-7	/	↑	/	↓	/	mTOR	/
	miR-199a	↓	↑	↓	/	/		Cancer
	miR-30a	↓	↑	/	↓	↓	Beclin	Cancer

Note. [1] The more relevant processes emerging from analysis by DIANA-mirPath software.
[2] The miRNAs evaluated here represent the more significant variations, which have commonalities between different cell types and different treatments. The same were also suggested as exposure biomarkers for different environmental or health related clues [58,59].
[3] The red and green arrows indicate the miRNA is increased or decreased in abundance.
[4,5] Main target proteins and diseases were taken from literature [58,59].

Differences in toxicity, mitochondrial function and miRNome in human cells exposed *in vitro* to Cd as CdS quantum dots or ionic Cd

Laura Paesano[a], *Marta Marmiroli*[a], *Massimiliano G. Bianchi*[b], *Jason C. White*[c], *Ovidio Bussolati*[b], *Andrea Zappettini*[d], *Marco Villani*[d], *Nelson Marmiroli*[a,e]*

[a]University of Parma, Department of Chemistry, Life Sciences and Environmental Sustainability, Parco Area delle Scienze 11/A, 43124 Parma, Italy

[b]University of Parma, Department of Medicine and Surgery, Laboratory of General Pathology, Via Volturno 39, 43125 Parma, Italy

[c]Department of Analytical Chemistry, The Connecticut Agricultural Experiment Station (CAES), New Haven, Connecticut 06504, United States

[d]Institute of Materials for Electronics and Magnetism (IMEM-CNR), Parco Area delle Scienze 37/A, 43124 Parma, Italy

[e]National Interuniversity Consortium for Environmental Sciences (CINSA), Parco Area delle Scienze 93/A, 43124 Parma, Italy Parma, Italy

[*]*Corresponding Author*:

Email address: nelson.marmiroli@unipr.it

Phone: +39 0521 905606

ABSTRACT

Cadmium is toxic to humans, although Cd-based quantum dots exerts less toxicity. Human hepatocellular carcinoma cells (HepG2) and macrophages (THP-1) were exposed to ionic Cd, Cd(II), and cadmium sulfide quantum dots (CdS QDs), and cell viability, cell integrity, Cd accumulation, mitochondrial function and miRNome profile were evaluated.

Cell-type and Cd form-specific responses were found: CdS QDs affected cell viability more in HepG2 than in THP-1; respective IC_{20} values were ~ 3 and ~ 50 µg ml^{-1}. In both cell types, Cd(II) exerted greater effects on viability.

Mitochondrial membrane function in HepG2 cells was reduced 70% with 40 µg ml^{-1} CdS QDs but was totally inhibited by Cd(II) at corresponding amounts. In THP-1 cells, CdS QDs has less effect on mitochondrial function; 50 µg ml^{-1} CdS QDs or equivalent Cd(II) caused 30% reduction or total inhibition, respectively. The different *in vitro* effects of CdS QDs were unrelated to Cd uptake, which was greater in THP-1 cells.

For both cell types, changes in the expression of miRNAs (miR-222, miR-181a, miR-142-3p, miR-15) were found with CdS QDs, which may be used as biomarkers of hazard nanomaterial exposure. The cell-specific miRNome profiles were indicative of a more conservative autophagic response in THP-1 and as apoptosis as in HepG2.

Keywords. miRNA; quantum dot; HepG2; THP-1; cadmium.

Abbreviations.

Δψm, mitochondrial membrane potential;

Cd(II), $CdSO_4$ 8/3 -hydrate;

CdS QDs, cadmium sulfide quantum dots;

DMEM, Dulbecco's Modified Eagle's Medium;

ENMs, engineered nanomaterials;

FBS, fetal bovine serum;

FCCP, carbonyl cyanide 4-(trifluoromethoxy) phenylhydrazone;

JC1, tetraethylbenzimidazolylcarbocyanine iodide;

PMA, phorbol 12-myristate 13-acetate;

QDs, quantum dots;

SS, side scatter.

1. Introduction

Quantum dots (QDs) have medical applications including fluorescence imaging, biosensing and targeted drug delivery to treat inflammation or drug-resistant cancer cells [1–3]; QDs conjugated with antibodies have been used to distinguish normal from cancerous cells [4]. There is an increasing interest in developing nano-theranostic platforms for simultaneous sensing, imaging and therapy [5]. Given the growing demand for and use of QDs, there is a clear need to understand potential toxicity for organisms and the environment [6]. The likely hazards posed by QDs in the biomedical field are not yet fully understood, although some studies have sought to address this issue [7]. The toxicity associated with cadmium (Cd)-containing QDs has been shown to be higher than for other QDs. This has been assumed to be related to the presence of Cd, leading to the production of excessive reactive oxygen species (ROS), indirectly affecting integrity of proteins, nucleic acid and membranes [8–10]. HepG2 cells, a human hepatocellular carcinoma cell line used as a model for human hepatic tissue [11], have been shown to respond to cadmium sulfide quantum

dots (CdS QDs) exposure by altering the abundance of gene transcripts encoding products associated with apoptosis, oxidative stress response and autophagy [12]. The transcriptomic approach has allowed for the identification of molecular mechanisms of CdS QDs exposure, highlighting potential candidates for exposure biomarkers. This paper describes the miRNA profiles as a consequence of exposure to either ionic Cd or CdS QDs and reveals several miRNAs that have the potential to be early biomarkers of exposure to these toxicants [13,14].

MiRNAs are short (19 - 23 nucleotides) non-coding sequences that are ubiquitous in all life forms. Their biological significance lies in their regulatory control over a wide range of cellular processes, achieved either by targeting the degradation of complementary mRNAs or by repressing the process of translation. There is also evidence to suggest that certain miRNAs can interact with sequences in the 5' and 3' untranslated region of their target mRNA, resulting in an enhancement rather than a reduction in translation [15]. Changes in cellular miRNA profiles have been associated with a number of conditions in humans, including cancer, viral infection, immune disorders and cardiovascular diseases [16–18]. In the plant kingdom, miRNA involvement has been described in the response to heavy metal exposure, including Cd and Cu [19,20]. In yeast (*Saccharomyces cerevisiae*), several miRNAs have been associated with the expression of Cd tolerance [21]. A number of epigenetic effects have been shown to be induced by Cd exposure, including DNA methylation, the post-translational modification of histone tails, and the packaging of DNA around the nucleosome; all have been correlated with the abundances of specific miRNAs [22]. Increasing evidence indicates that *in vitro* and *in vivo* exposure of human cells to environmental organic contaminants and metals can alter miRNA expression [23]. It has been demonstrated that the relative abundance of certain miRNAs is responsive

to nanomaterials, although the global effect of this exposure is not understood [24]. For example, titanium dioxide, zinc oxide and gold nanoparticles change miRNAs expression [25,26].

This study examined the changes in the miRNome of two widely studied human cell lines exposed to various levels of Cd, presented as either CdS QDs or Cd(II). The cell lines used were HepG2, hepatocellular carcinoma cells, and THP-1, human macrophage-like cells. While the literature contains numerous descriptions of therapeutic uses of miRNAs [16], their potential as biomarkers for xenobiotic exposure remains unknown; this is in spite of the fact that miRNAs have been reported to be mediators of cellular responses to environmental contaminants [27]. Moreover, the US Food and Drug Administration (USFDA) considers changes in miRNA levels as a possible genome biomarker [13,14]. MiRNAs could be useful not only as potential biomarkers of several diseases but also as key mediators of the mechanisms linking environmental exposure to toxicity and disease development [28]. The present toxicogenomic study on human cell lines was carried out to assess an *in vitro* (non-animal) test for health risk assessment [29] for exposure to ionic- and nanoscale-Cd. In addition, the study was intended to determine whether CdS QDs could represent a less toxic form of Cd in diagnostic medicine [30].

2. Materials and methods

2.1 Preparation of CdS QDs suspension medium

CdS QDs were synthesized at IMEM-CNR (Parma, Italy), as described elsewhere [31]. They were characterized in deionized water by transmission electron microscopy (Hitachi HT7700, Hitachi High Technologies America, Pleasanton, CA). Major details are described in Paesano *et al.* [32]. Their structure is crystalline with a

mean static diameter of 5 nm with approximately 78% Cd. Average particle size (d_h) of the aggregates and zeta potential in deionized water were estimated 178.7 nm and +15.0 mV, respectively (Zetasizer Nano Series ZS90, Malvern Instruments, Malvern, UK) [33]. The zeta potential of CdS QDs were comparable in water and in the culture medium used: QDs have approximately neutral charge. For hydrodynamic diameters, difference observed in the experimental systems is due to the presence of divalent cations and serum protein that characterizes the culture medium. Characterization details are given in Appendix A. The CdS QDs were suspended in Milli-Q water at a concentration of 100 µg ml^{-1}, and pulsed probe sonication was used to minimize aggregation. For cell treatment, the stock particle suspension was vortexed and sonicated for 30 min, and then diluted as appropriate into complete culture medium.

2.2 Cell Culture, Treatments and Cell Viability Assay

Cells were cultured in Dulbecco's Modified Eagle's Medium (DMEM) containing 10% fetal bovine serum (FBS), 100 µg ml^{-1} streptomycin, 100 U ml^{-1} penicillin, 4 mM glutamine; for THP-1 cells, the glutamine concentration was reduced to 2 mM. Cells were cultured in 10-cm Petri dishes under a humidified atmosphere in the presence of 5% CO_2. Prior to treatment, THP-1 cells were differentiated into macrophages through an incubation with 0.1 µM of phorbol 12-myristate 13-acetate (PMA) for 3 days.

Cells in complete culture medium were seeded into either 96-well plates, at a density of 15×10^3 cells/well, or 10-cm diameter dishes at 3×10^6 cells/dish. The medium was replaced after 24 h with fresh medium containing either CdS QDs or Cd(II) (as $CdSO_4$ 8/3 -hydrate). HepG2 cells were treated with a range of Cd concentration, either as CdS QDs or Cd(II), from 0 to 93.6 µg ml^{-1}; the THP-1 cells were treated with

149 a range of Cd doses from 0 to 124.8 µg ml^{-1}. Details of all the Cd treatments are
150 given in Table A.1. Each treatment was carried out in triplicate (biological replicates)
151 and each replicate was measured three times (technical replicates). Cell viability was
152 evaluated after 24 h of incubation in the presence of Cd using the resazurin method
153 [34]. Briefly, the culture medium was replaced with a solution of resazurin (44 µM,
154 Sigma-Aldrich, Saint Louis, MO, USA) in serum-free medium. After 30 min,
155 fluorescence was measured at 572 nm with a multimode plate reader (Perkin Elmer
156 Enspire, Waltham, MA, USA). Potential interference in this assay was excluded by
157 measuring fluorescence of the dye mixed with CdS QDs. The treatment time of 24 h
158 was chosen from literature reports about the internalisation time of QDs [35].
159
160 *2.3 Mitochondrial Membrane Function Assay*
161 Mitochondrial membrane potential (Δψm) was estimated using the JC-1 kit (Abcam
162 Ltd, Cambridge, UK) according to the manufacturer's instructions. The assay relies
163 on the accumulation of the cationic dye tetraethylbenzimidazolylcarbocyanine iodide
164 (JC-1) in energized mitochondria. When the Δψm is low, JC-1 is present mostly in
165 monomeric form, which can be detected through its emission of green fluorescence
166 (530±15 nm). Conversely, when the Δψm is high, the dye polymerizes, resulting in
167 the emission of red to orange fluorescence (590±17.5 nm). Therefore, a decrease in
168 red fluorescence and an increase in green fluorescence are indicative of
169 depolarization in the mitochondrial membrane. Carbonyl cyanide 4-
170 trifluoromethoxyphenylhydrazone (FCCP), an H^+ ionophore uncoupler of oxidative
171 phosphorylation, was used as a Δψm-depolarization positive control. HepG2 or THP-
172 1 cells were seeded into 96-well plates at a density of 7.5×10^4 cells per well and
173 were incubated for 24 h to allow adhesion. Cells were then exposed to a range of Cd

174 treatments (Table A.1) for 24 h in the form of either CdS QDs or Cd(II). After
175 extensive washing in phosphate buffered saline (PBS) to remove adherent particles
176 or QDs aggregates, cells were incubated in the JC-1 solution for 30 min at 37°C in
177 the dark. Following a further PBS rinse, fluorescence emitted by the cells was
178 determined by a multimode plate reader (Perkin Elmer Enspire). Individual
179 experiments were run in triplicate; data were expressed as the relative fluorescence
180 unit (RFU) with respect to the control.
181
182 *2.4 Confocal Microscopy*
183 HepG2 and THP-1 cells were seeded into four-well chamber slides at a density of 5 ×
184 10^4 cells ml^{-1}. After treatment with either CdS QDs or Cd(II) (see Table A.1), cells
185 were transferred to a medium containing 5 µM JC-1 for 30 minutes. Following the
186 staining procedure, the cells were rinsed in complete culture medium, incubated at
187 37°C and 5% CO_2 in a Kit Cell Observer (Carl Zeiss, Jena, Germany) and imaged
188 using an inverted LSM 510 Meta laser scanning microscope (Carl Zeiss). Excitation
189 at 633 nm and reflectance were used to visualize CdS QDs. The status of the JC-1
190 dye was recorded by excitation at 480 nm and the emission was passed through a
191 535-595 nm filter. In selected experiments, nuclei were counterstained with
192 DRAQ5™ (Alexis Biochemicals, San Diego, California, USA). In these instances, 5
193 µM DRAQ5™ was added together with JC-1 and cells were visualized with excitation
194 at 633 nm with emission through a 670 nm long pass filter.
195 The cytoplasm of THP-1 cells exposed to 50 µg ml^{-1} CdS QDs for 24 h was
196 visualized by incubation with 1 µM calcein-AM (Millipore Merck, Burlington, MA, USA)
197 for 2 h; calcein-loaded cells were excited at 488 nm and fluorescence was measured
198 through a 515-540 nm band pass filter.

199

200 *2.5 Cellular Uptake of Cadmium*

201 The entry of CdS QDs into THP-1 cells exposed to 50 µg ml^{-1} of the nanomaterial for
202 either 4 and 24 h was estimated with a cytofluorimetric assay [12]. After exposure,
203 cells were first harvested by trypsin treatment and centrifugation (800 x *g*, 5 min),
204 after which they were suspended in PBS containing 1% (v/v) FBS. The presence of
205 CdS QDs was revealed by flow cytometry (NovoCyte, ACEA Biosciences, San
206 Diego, CA, USA); specifically, CdS QDs uptake was associated with a higher side
207 scatter (SS) intensity. The experiment involved three biological replicates, each
208 represented by three technical replicates. A similar analysis of Cd entry into HepG2
209 cells has been reported previously [12]. The cells were thoroughly washed to remove
210 any surface-attached agglomerates of CdS QDs and quantification of Cd
211 accumulated by the cells was then obtained using inductively coupled plasma mass
212 spectrometry (ICP-MS) as described by Peng *et al.* [36]. Confocal microscopy
213 showed that agglomerates of CdS QDs were absent from these preparations. HepG2
214 or THP-1 cells, exposed to various doses of CdS QDs or Cd(II) (Table A.1) for 24 h,
215 were rinsed three times in PBS, harvested by trypsinization prior to counting, and
216 then digested with 67% HNO_3 at 165°C for 3 h. The solution obtained was diluted by
217 adding 2 volumes of water prior to ICP-MS analysis.

218

219 *2.6 RNA Isolation and miRNAs Quantification*

220 To avoid compromising RNA integrity, extractions from HepG2 and THP-1 cells
221 exposed to Cd in the form of either CdS QDs or Cd(II) were performed using a
222 mirVANA™ column-based kit (Life Technologies, Carlsbad, CA, USA). RNA
223 concentration and integrity were monitored by spectrophotometry and gel

electrophoresis, respectively. The abundance of each miRNA was obtained using a TaqMan® Array Human MicroRNA A+B Card Set v3.0 (Applied Biosystems, Foster City, CA, USA), which quantifies 754 miRNAs. A 1-µg aliquot of RNA was reverse-transcribed using Megaplex™ RT Primers (Applied Biosystems), and the subsequent PCR array was run using a 7900HT Fast Real Time PCR system (Applied Biosystems) following the MegaPlex™ Pool Protocol (PN 4399721 RevC). Each sample was analyzed in duplicate. The raw data were analyzed using RQ Manager 1.2 software (Applied Biosystems) and relative abundances were calculated using the $2^{-\Delta\Delta Ct}$ method [37]. The selected reference sequence was non-coding U6 small nuclear RNA. The fold-change threshold applied to define significant changes in abundance was 2 (for increased miRNAs) and 0.5 (for decreased miRNAs).

2.7 In vitro analysis of autophagy: Western blot assay

Total cell lysates were obtained as described elsewhere [38]. The monolayers were rinsed with ice-cold PBS and then covered with 60 µl of Lysis buffer (20 mM Tris–HCl, pH 7.5, 150 mM NaCl, 1 mM EDTA, 1 mM EGTA, 1% Triton, 2.5 mM sodium pyrophosphate, 1 mM β-glycerophosphate, 1 mM Na_3VO_4, 1 mM NaF, 2 mM imidazole) supplemented with a protease inhibitor cocktail (Complete, Mini, EDTA-free, Roche, Monza, Italy). Equal amounts of proteins from each sample were separated by 4-20% SDS-polyacrylamide gels and transferred to PVDF membranes (Immobilon-P, Millipore, Millipore Merck Corporation, MA, USA); membranes were then incubated in TBS with 10% blocking solution (Western Blocking Reagent, Roche) for 1h and exposed overnight at 4°C to primary antibodies against LC3II (microtubule–associated protein light chain 3, Cell Signaling Technology, Danvers, MA, USA), p62 (ubiquitin-binding protein p62, Abcam Ltd) or tubulin (Sigma-Aldrich)

diluted in TBS-T with 5% BSA. After three washes of 10 min each in TBS-T (50mM Tris Base, 150mM NaCl, pH 7.5), membranes were exposed to the HRP-conjugated secondary anti-rabbit or anti-mouse IgG antibodies for 1h at room temperature (HRP, Cell Signaling Technology). Visualization of protein bands was performed using Immobilon Western Chemiluminescent HRP Substrate (Millipore, Merck). The expression of tubulin was used for loading control. Individual experiment were run in triplicate.

2.8 Statistic and Bioinformatics Analysis

The software package SPSS Statistics® v.21 (IBM, Armonk, NY, USA) was used to compare control and treatment effects. Levene, Shapiro-Wilk and Kolmogorov-Smirnov tests were applied to ascertain data normality and variance homogeneity. One-way analysis of variance, followed by the Tukey test was used to identify and order means differing significantly from one another. The significance threshold probability was set at 0.05. To visualize transcriptomic data, hierarchical clustering was performed using the heatmap.2 routine implemented in the R software (www.R-project.org/). Genes targeted by differentially abundant miRNAs were identified using the DIANA-Tarbase v.7 database (diana.imis.athena-innovation.gr/DianaTools/index.php?r=tarbase/index)[39]. The KEGG pathway enrichment of these target genes was derived from an analysis based on DIANA-mirPath software [40]. The p-value threshold was set 0.05 and FDR correction was applied. miRTargetLink [41] was used to identify interaction networks among the target genes using information documented in the miRTarBase. Only strong interactions (backed up by strong experimental methods such as the 'reporter gene assay') were taken into consideration. PANTHER (pantherdb.org/) software was used

to search for gene enrichment, and the Gene Ontology database provided functional annotation for the genes targeted by differentially abundant miRNAs.

3. Results and Discussion

Experiments were designed to compare the responses of HepG2 and THP-1 cells to Cd exposure in the form of either CdS QDs or Cd(II). Some of the distinguishing features of the two cell types are listed in Table A.2. THP-1 were compared with HepG2 cells because of their different role relative to *in vivo* exposure to Cd. In the body, engineered nanoparticles may be recognized and processed by immune cells, among which macrophages play a crucial role. Macrophages act as the first line of defense against invading agents, including QDs [42]. Hepatocytes are instead involved in the attempt to dispose the eventual toxicant in the liver, which is the major human organ which accumulates both Cd^{2+} and Cd-containing QDs [43].

3.1 Cell viability

When exposed to Cd(II), the viability of both cell types was dose-dependent, as reported elsewhere [44,45]. Specifically, the estimated IC_{50} for HepG2 cells was ~ 4 μg ml^{-1} Cd as Cd(II) and ~ 15 μg ml^{-1} Cd as CdS QDs (corresponding to ~ 20 μg ml^{-1} CdS QDs) (Fig. A.1a). The IC_{20} for CdS QDs was calculated at 3 μg ml^{-1} (~ 2.3 μg ml^{-1} Cd). Measurements taken after a 14-day immersion of CdS QDs in the growth medium showed that the release of Cd^{2+} into solution reached a maximum of approximately 1 – 2%, consistent with previous reports [46,47]. This value occurs for all the growth and treatment conditions reported throughout the paper.

For THP-1 cells, the susceptibility to Cd(II) was comparable, whereas the IC_{20} for CdS QDs was nearly 50 μg ml^{-1}, and at ~ 120 μg ml^{-1} viability was still more than

299 60% (Fig. A.1b). Thus, the sub-toxic dose (IC_{20}) of CdS QDs for THP-1 cells was
300 established at 50 µg ml^{-1} (39 µg ml^{-1} Cd). From the literature and from our study, an
301 equivalent dose of Cd^{2+} drastically reduces cell viability [48].
302
303 *3.2 Mitochondrial Function and Cell Morphology*
304 Mitochondrial function is one of the main targets of QDs [49,50]. In HepG2 cells, 2.3
305 µg ml^{-1} of Cd as CdS QDs at IC_{20} (3 µg ml^{-1} CdS QDs) had a minimal effect on
306 mitochondrial membrane potential; an inhibition of ~ 50% was observed at 31.2 µg
307 ml^{-1} of Cd (40 µg ml^{-1} CdS QDs) (Fig. 1a). In contrast, mitochondrial function was
308 significantly inhibited in the presence of 2.3 µg ml^{-1} Cd as Cd(II) (Fig. 1b). THP-1
309 cells responded in similar fashion but were largely unaffected by CdS QDs exposure
310 even at 50 µg ml^{-1} (39 µg ml^{-1} Cd) (Fig. 1c), although they were quite susceptible to
311 Cd(II), the dose totally inhibiting mitochondrial membrane potential being 7.8 µg ml^{-1}
312 Cd as Cd(II) (Fig. 1d). Therefore, Cd strongly inhibited mitochondrial function in both
313 cell lines when present as Cd(II) but not as CdS QDs, which caused only a partial
314 inhibition.
315 Confocal images of JC-1-labeled HepG2 cells exposed to 3 µg ml^{-1} of CdS QDs are
316 shown in Fig. A.2. This condition (IC_{20}) failed to induce any significant reduction in
317 JC-1 aggregation; the amount of JC-1 monomer was not altered (Fig. A.2), indicating
318 that mitochondrial function was unaffected by the treatment. In this condition, the cell
319 shapes were also normal. Treatment with 2.3 µg ml^{-1} Cd as Cd(II) led to a significant
320 decrease in JC-1 aggregates (data not shown). In contrast, micrographs of THP-1
321 cells exposed to 5 µg ml^{-1} Cd in the form of either Cd(II) or CdS QDs (Fig. 2), show a
322 significant alteration in mitochondrial function after exposure to Cd(II). When THP-1
323 cells were exposed to 50 µg ml^{-1} of CdS QDs, a more significant reduction in JC-1

aggregates was observed (Fig. 2), but cell morphology appeared to be substantially unaffected.

3.3 Cd Uptake

Internalization of QDs in human cells occurs *in vitro* within 24 h from exposure [51]. A cytofluorimetric assay was used to demonstrate the capacity of HepG2 and THP-1 cells to accumulate CdS QDs. CdS QDs uptake by HepG2 cells was reported in a previous paper [12]. The same method was applied here for the THP-1 cell line. A significant increase in side scatter (SS) was observed when cells were exposed to 50 μg ml^{-1} of CdS QDs for 4 h and 24 h (Fig. 3), consistent with QDs entry. Separate ICP-MS measurements of cells exposed to CdS QDs for 24 h, with subsequent thorough washing to remove any CdS QDs remaining on the surface, demonstrated a dose-dependent increase in cellular Cd levels (Table A.3). Interestingly, HepG2 cells accumulated greater amounts of Cd upon exposure to CdS QDs than to equivalent amounts of Cd as Cd(II). THP-1 cells accumulated more Cd than HepG2 cells, possibly a result of their phagocytic competence. Also in this case the uptake of Cd as CdS QDs was higher than for Cd as Cd(II). Therefore, the larger negative impacts on viability and mitochondrial function reported for Cd(II) are not due to a greater uptake of Cd.

To evaluate the interaction of THP-1 cells with CdS QDs, calcein-loaded macrophages were treated with 50 μg ml^{-1} of CdS QDs: the majority of the CdS QDs formed aggregates that were clearly evident in reflectance mode (see the grey pseudocolor in the confocal images in Fig. A.3a). The orthogonal projections and 3-D reconstruction indicate that the CdS QDs were grouped in aggregates in close

contact with the cell surface, with images indicating the formation of deep, shallow invaginations in the cell membrane, highly suggestive of internalization (Fig. A.3b).

3.4 miRNAs Expression Profiling: Comparison Between CdS QDs and Cd(II)

Significant changes have been reported for miRNAs of human cells exposed to engineered nanomaterials (ENMs) [25]. Table A.4 gives a summary of the effect of Cd exposure on HepG2 and THP-1 miRNomes (the number of assayed miRNAs was 754). For HepG2 cells exposed to 3 μg ml^{-1} CdS QDs or 5.2 μg ml^{-1} Cd(II), the number of miRNAs with significantly increased or decreased abundance are reported in Fig. 4a as Venn diagrams. Heatmaps showed the abundances of three miRNAs (miR-1267, miR-200a-5p, 26b-3p) which were increased by CdS QDs, but reduced by Cd(II); the opposite trend was evident for three other miRNAs (miR-218-5p, miR-548b-3p, miR-589-3p) (Fig. 5a). A more extensive heatmap is presented in Fig. 1 in Paesano *et al.* (Data in Brief). The analysis demonstrates that exposure to CdS QDs or to Cd(II) had markedly different effects on the HepG2 miRNome. The response of THP-1 cells was more complex, with markedly different effects of high dose CdS QDs (39 μg ml^{-1} Cd) or Cd(II) (5 μg ml^{-1} Cd) on miRNAs abundance (Fig. 6a). Heatmap representations of these data are given in Fig. 2a in Paesano *et al.* (Data in Brief). When THP-1 cells were exposed to lower doses of Cd (5 μg ml^{-1}), equivalent to 6.4 μg ml^{-1} CdS QDs or 11.4 μg ml^{-1} Cd(II), the effects on miRNAs levels were different: only six common miRNAs were found up-modulated while one down-modulated (Fig. 4b). CdS QDs induced a general increase in miRNAs levels, while Cd(II) produced a decrease (heatmap with individual variations is reported in Fig. 2b in Paesano *et al.* (Data in Brief)). Thus, at this lower level of stress, the two forms of

372 Cd also had very different effects on the miRNome in THP-1 and HepG2 cells; Cd(II)
373 led to more dramatic consequences as compared with CdS QDs.
374
375 *3.5 Comparison between the Cell Line Responses to Cd*
376 Figs 4c, d and 5b, c show a comparison of the miRNomes for HepG2 and THP-1
377 cells when exposed to CdS QDs and Cd(II).
378 Exposure of THP-1 cells to 50 μg ml^{-1} CdS QDs had a similar suppressive effect on
379 cell viability as did exposure of 3 μg ml^{-1} CdS QDs on HepG2 cells (Fig. A.1).
380 However, there was little similarity with respect to the effect of the exposure on the
381 miRNome. Specifically, there was no overlap between the sets of miRNAs that
382 increased in abundance, although there were 17 suppressed miRNAs in common
383 between the two cell types (Fig. 6b). Conversely, 13 of the miRNAs responded
384 differentially, either increasing in abundance in THP-1 cells while decreasing in
385 HepG2 cells, or *vice versa*. Analysis of the relevant heatmaps (Fig. 5b and Fig. 3a in
386 Paesano *et al.* (Data in Brief)) suggests that the two cell types deployed different
387 strategies to maintain viability in response to Cd exposure. Molecular responses to a
388 comparable level of CdS QDs-imposed stress (3 μg ml^{-1} for HepG2 and 6.4 μg ml^{-1}
389 for THP-1 cells) were also quite distinct: 10 miRNAs increased in both cell types, and
390 2 decreased (Fig. 4c). In THP-1 cells, exposure to the lower dose of CdS QDs mostly
391 increased miRNAs levels. When the stress was imposed by Cd(II), the responses of
392 the two cell types were similar in the number of miRNAs down-modulated, with 39 of
393 these in common (Fig. 4d). The heatmaps presented in Figs 5b, c presents an
394 overview of the effect of the lower dose of CdS QDs and Cd(II) on the miRNome. A
395 comparison between the two cell lines each challenged with CdS QDs at lower (3 or
396 6.4 μg ml^{-1}) and THP-1 at higher dose (50 μg ml^{-1}) is shown in Fig. 3b in Paesano *et*

al. (Data in Brief). For both THP-1 and HepG2 the lower doses result primarily in up-modulation, whereas THP-1 at 50 μg ml^{-1} is largely down-modulated. A global comparison between the responses of the two cell lines to CdS QDs-imposed stress is also given in Fig. 6c. For THP-1 cells, 130 miRNAs were modulated exclusively in response to 50 μg ml^{-1} of CdS QDs treatment but at 6.4 μg ml^{-1}, that value was only 45. For HepG2 cells, 26 miRNAs responded exclusively to 3 μg ml^{-1} CdS QDs. In conclusion, the miRNomes of the two cell lines reacted differently to QDs exposure; however, exposure to Cd(II) caused mainly a reduction in miRNA abundances in both cell lines.

3.6 In silico analysis: Pathways, GO and Networks Analysis

The pathways potentially impacted by miRNA modulation under Cd-induced stress were identified using the DIANA-mirPath algorithm [40]. In the case of the HepG2 cell line, Tables A.5 and A.6 show the cellular pathways more likely affected by 3 μg ml^{-1} CdS QDs or 5.2 μg ml^{-1} Cd(II). An equivalent analysis was conducted for THP-1 cells exposed to either 6.4 μg ml^{-1} CdS QDs or 11.4 μg ml^{-1} Cd(II) (Tables A.7 and A.8). Although a rather similar set of pathways was impacted in the two cell types, it is noteworthy that the miRNAs involved were markedly different for the two forms of Cd. An *in silico* analysis on the biological significance of the differentially abundant miRNAs was also performed using miRTargetLink and PANTHER software. Gene ontology (GO) enrichment analysis from PANTHER gave results shown summarized below and reported in details in Fig. 4 in Paesano *et al.* (Data in Brief) for HepG2 cells, treated with either CdS QDs or Cd(II). Fig. 5 in Paesano *et al.* (Data in Brief) shows results for THP-1 cells treated with 50 μg ml^{-1} CdS QDs, and Fig. 6 in Paesano *et al.* (Data in Brief) reports THP-1 cells exposed to the lower dose of CdS

422 QDs or to Cd(II). A comparison for HepG2 showed that in the treatment with CdS
423 QDs the major GO categories involved were: ‘miRNA mediated inhibition of
424 translation’, ‘regulation of RNA polymerase II transcriptional preinitiation complex
425 assembly’ and ‘regulation of gene silencing by miRNA’. In the case of Cd(II) the
426 major target genes were associated with apoptosis, stress response, gene silencing
427 and mitochondrial depolarization.
428 For THP-1 exposed to the lower dose of CdS QDs (6.4 µg ml^{-1}), the main GO
429 categories were ‘positive regulation of cell-cycle phase transition’, ‘regulation of cell-
430 cycle G1/S phase transition’ and ‘positive regulation of production of miRNAs
431 involved in gene silencing by miRNA’. In the case of Cd(II) the gene targets belonged
432 to: ‘regulation of B cell apoptotic process’, ‘release of cytochrome c from
433 mitochondria’, ‘positive regulation of protein insertion into mitochondrial membrane
434 involved in programmed cell death’ and ‘leukocyte apoptotic process’. For THP-1,
435 GO categories related to mitochondrial function were more evident when treated with
436 Cd(II) or with CdS QDs at the higher dose. Indeed, when THP-1 were treated with
437 the higher dose of CdS QDs (50 µg ml^{-1}) most of the regulated miRNA belonged to
438 GO categories: ‘regulation of production of miRNAs involved in gene silencing by
439 miRNA’, ‘extrinsic apoptotic signaling pathway in absence of ligand’, ‘regulation of
440 mitochondrial membrane potential’ and ‘cellular response to mechanical stimulus’. A
441 comparison of the GO categories of the target genes in the two cell types revealed
442 for treatment with CdS QDs some commonalities, notably 'epidermal growth factor
443 receptor signaling', 'positive regulation of mitotic cell cycle phase transition' and
444 'negative regulation of extrinsic apoptosis' (see Fig. 7 in Paesano *et al.* (Data in
445 Brief)). Some common categories were also evident from comparison between the
446 response of cells exposed to CdS QDs and those exposed to Cd(II) (see Fig. 7 in

447 Paesano *et al.* (Data in Brief)). Although the two cell lines responded differently to
448 CdS QDs, this analysis has highlighted that some targets of regulated miRNAs
449 belong to the same classes of GO, suggesting that they are involved in the same
450 cellular processes. All similarities and differences in response to CdS QDs and to
451 Cd(II) was markedly different both in HepG2 and in THP-1 are shown in Fig. 7 in
452 Paesano *et al.* (Data in Brief).
453 miRTargetLink software was used to generate regulatory networks using miRNAs
454 modulated in response to CdS QDs in HepG2 and THP-1 cells. From these data, a
455 network was created considering mainly autophagic and apoptotic pathways. The
456 network summarized the response of the two cell types to CdS QDs. Overall, the
457 autophagic pathway seemed activated in THP-1 cells exposed to the higher, but not
458 to the lower dose of CdS QDs. In contrast, in HepG2 cells, exposure to QDs led to
459 activation of the apoptotic process. These networks are illustrated in Figs 8a, b in
460 Paesano *et al.* (Data in Brief).
461
462 *3.7 Activation of miRNA Response*
463 One notable feature of the response of THP-1 cells to 50 μg ml^{-1} CdS QDs was the
464 high number of miRNAs with a decreased abundance. The major pathways likely
465 affected by this response were apoptosis, DNA repair, cell cycling, xenobiotic
466 metabolism and autophagy. In particular, Fig. 7 illustrates a reconstruction *in silico* of
467 miRNAs involved in the regulation of autophagy in the response of THP-1 to the
468 higher dose of CdS QDs (50 μg ml^{-1}); however, the same pathway appears to be
469 largely unaffected in THP-1 cells exposed to the lower dose of CdS QDs (6.4 μg ml^{-1},
470 Fig. 9 in Paesano *et al.* (Data in Brief)). *MTOR* transcript was likely repressed, given
471 that the abundance of miR-101, miR-199a, miR-30a and miR-7 was enhanced. At the

same time, the vesicle elongation phase could be repressed by up-regulated miRNAs including miR-101, miR-30a, miR-885-3p and miR-181a. Moreover, miR-30a, which is involved in the repression of Beclin-1, was up-regulated, thus pointing to autophagy suppression. Several other miRNAs that responded positively to exposure also have gene targets that encode proteins involved in autophagy (Fig. 9 in Paesano *et al.* (Data in Brief)). This hypothesis is confirmed by *in vitro* analysis with autophagy markers (LC3II and p62). LC3II is recruited from the cytosol and associates with the phagophore early in autophagy. This localization serves as a general marker for autophagic membranes and for monitoring the process as it develops [53]. p62 is a receptor for cargo destined to be degraded by autophagy, including ubiquitinated protein aggregates destined for clearance. The p62 protein is able to bind ubiquitin and also to LC3II, thereby targeting the autophagosome and facilitating clearance of ubiquitinated proteins [54]. As shown in Fig. 8, the induction of autophagy in THP-1 cells treated with Cd as CdS QDs was confirmed by an increase in LC3II and a constant p62 levels, while the increase in p62 and LC3II levels after exposure to 5 μg ml^{-1} of Cd as Cd(II) (11.4 μg ml^{-1}) suggests a blockage of the autophagic flow. Conversely, the miRNAs responding in the CdS QDs-exposed HepG2 cells had little or no association with the regulation of autophagy but were, instead, associated with apoptosis (Fig. 9). In this case, the exposure to QDs does not cause an increase in LC3II, suggesting a normal condition of the autophagic flow (Fig. 8). Thus, autophagy seemed to be preferentially activated over apoptosis in THP-1 cells exposed to the highest dose of Cd (Fig. 10 in Paesano *et al.* (Data in Brief)). Instead, THP-1 cells exposed to the lower dose of CdS QDs did not activate the apoptotic process (Fig. 11 in Paesano *et al.* (Data in Brief)), which was, however,

triggered by the exposure to the equivalent dose of Cd as Cd(II) (Fig. 12 in Paesano *et al.* (Data in Brief)).

A previous analysis of the HepG2 response to CdS QDs exposure had suggested that a number of genes associated with apoptosis were among those up-regulated by the stress [12,55]. The current work demonstrates that exposure to CdS QDs reduced the abundance of both miR-32 and miR-149, which would have favored the release of cytochrome c, mitochondria-related apoptosis inducing factor and endonuclease G and, hence, promoted apoptosis [56,57]. The response to Cd(II) suggests that both the intrinsic and the extrinsic apoptotic pathways were activated, pointing to a larger alteration and damage of cell viability (Fig. 13 in Paesano *et al.* (Data in Brief)). The response of THP-1 cells to CdS QDs exposure was quite different in term of cell viability, mitochondrial function and in the number of miRNAs up- or down-modulated. This may explain why these cells appeared to be less susceptible to the stress than HepG2 cells: autophagy is obviously less clearly indicative of a death process than the triggering of apoptosis. Moreover, at the lower dose of CdS QDs, THP-1 cells do not activate either autophagy or apoptosis, relying on subtler rescue mechanisms (see Figs 9 and 10 in Paesano *et al.* (Data in Brief)).

An overview of the differences and commonalities between the miRNomes of the two cell types in response to the lower or to the higher level of CdS QDs is shown in Table 1 and in Figs 14a, b in Paesano *et al.* (Data in Brief). Of note, two cancer-associated miRNAs, miR-191-3p and miR-133a-3p, are increased in abundance.

Table 1 catalogs the miRNAs that were most responsive to the various treatments, including Cd(II), along with functional information regarding their likely target genes [58,59]. miRNAs belonging to the let-7 family were particularly responsive to Cd exposure; these miRNAs have been described as tumor suppressors, given that their

521 abundance is often much lower in cancerous than in healthy tissues [29,60]. In the
522 THP-1 cells, seven let-7 miRNAs were reduced in abundance after exposure to 50 µg
523 ml^{-1} CdS QDs, whereas there was no effect in cells exposed to the lower dose.
524 Meanwhile, exposure to 11.4 µg ml^{-1} Cd(II) reduced the abundance of eight let-7
525 miRNAs. Note that in HepG2 cells exposed to 5.2 µg ml^{-1} Cd(II), only three let-7
526 miRNAs were reduced. In THP-1 cells, miR-15b, which has also been implicated as a
527 tumor suppressor because it affects apoptosis through its targeting of gene *BCL-2*
528 [61], was also reduced by 50 µg ml^{-1} CdS QDs. A low dose of CdS QDs in HepG2
529 cells reduced expression of miR-15b in HepG2 cells but a comparable dose had no
530 effect on THP-1 cells.
531
532 **4. Conclusion**
533 *In vitro* studies on cellular models have clearly shown the molecular effects of ENMs
534 such as QDs and suggested possible modes of action in relation to their intrinsic
535 physico-chemical properties [62]. This information may be important for defining their
536 hazardous properties, a critical step in the identification of suitable biomarkers of
537 exposure. For similar QDs the metal (e.g. Cd) is largely responsible for the toxicity
538 [63]. *In vivo* evidence shows QDs cause pulmonary inflammation and hepatic toxicity
539 [64,65]. MiRNAs have been suggested as potential biomarkers of exposure to toxins
540 with some having important roles in multiple signaling pathways and apoptosis [28].
541 One function of miRNAs seems to cover a critical aspect of the general stress
542 response [66] with involvement in the formation of stress-induced response complex
543 (SIRC) which shuttles miRNAs into the nucleus [67]. Some proteins responsive to
544 metal-containing QDs, including metallothionein 1A, cytochrome P450 1A and heme
545 oxygenase, can be used as sensitivity biomarkers [68], but other events and

546 molecules would be useful to track exposure to QDs. After the oxidative stress which
547 follows ROS production and mitochondrial stress, additional glutathione is
548 synthesized and redistributed via MPAK-Nrf2. In addition TFEB is activated which
549 may promote lysosome formation and stabilization, helping to clear damaged
550 organelles [69]. If the stress continues there can be different types of cell damage
551 [10] including autophagy [70], apoptosis [71] and necrosis [72].
552 Different studies propose miRNAs as biomarkers of adverse exposure to metal-
553 based nanomaterials [25]. Moreover, the USFDA has recently accepted the use of
554 miRNAs as ‘genome biomarkers’.
555 Although miRNA profiling has been used to detect the response of different types of
556 cells and organisms to metals and to nanomaterials such as CdTe QDs [73], no
557 available study reports a direct comparison between exposure to the same
558 metal/element as a salt and as a QD constituent. A number of studies have
559 correlated the level of toxicant exposure to the induction of miRNAs in blood [13,14]
560 but there are several potential drawbacks of using miRNA changes to detect any
561 possible ‘genome biomarkers’ of exposure, including molecular instability [74]. The
562 assay of miRNAs expression we used here was based on 'array' quantitative PCR
563 with specific primers and TaqMan probes, which constitutes a gold-standard method
564 for quantitative transcriptional analysis [75]. Exposure to cadmium-based QDs and
565 changes in miRNAs have been correlated and used to explain cytotoxicity in
566 mammalian NIH/3T3 cells [73], in zebrafish liver cells [76], and in the brain of
567 Alzheimer's disease patients [77]. Altering the level of a single miRNA can trigger a
568 cascade of signaling events, potentially culminating in a major effect, either
569 stimulatory or inhibitory, on cell proliferation, apoptosis or other processes. In
570 principle, this raises the possibility of clinical interventions based on the modulation of

571 specific miRNAs by exposure to inhibitors or enhancers. The data presented here
572 showed that nanosized Cd, rather than ionic Cd, has a ‘soft’ regulatory effect on
573 miRNomes in human cells that is quite different from the ‘toxic’ inhibitory impact of
574 ionic Cd. There are three possible levels of response of human cells to nanomaterials
575 such as CdS QDs. The first of these is cell-type specific, as evidenced in a meta-
576 analysis of Cd-containing QDs [35]. Macrophages appear to be less susceptible to
577 toxicity than hepatocytes, even though they accumulate QDs more readily. The
578 second is physiological, as exemplified by differences in the capacity to maintain
579 mitochondrial structure and function when exposed to the stress agent. The final
580 level relates to the response of the miRNome, which has an impact on the
581 expression of various genes associated with defense or response to damage. It is
582 known that CdS QDs enter HepG2 cells. Previous studies had shown this was
583 followed by entry into lysosomes, triggering lysosomal enzymes with production of
584 ROS and initiation of autophagy [78] or apoptosis [79]. In our work HepG2 cells seem
585 to be programmed for apoptosis when exposed to CdS QDs, whereas for THP-1 cells
586 the outcome is autophagy. Some nanomaterials induce autophagy in cancer cells
587 which could lead to cancer cell death, enabling specific cancer therapies [80].
588 Autophagy induced by QDs can be seen as an attempt to degrade what is perceived
589 as foreign [81], but, in some instances, as for HepG2 cells, it can lead to apoptosis
590 and cell death [82]. MiRNAs associated with mitochondria [83,84] and cytosolic
591 miRNAs can be transferred into the mitochondria (or generated inside) and initiate
592 this deregulation processes [85]. Mitochondria are known as ROS generators and
593 also targets of ROS [49]. ROS cause mitochondrial swelling, inhibition of respiration
594 and mitochondrial permeability transition [86]. In the cells we studied, mitochondrial
595 function was particularly sensitive to Cd(II) but less sensitive to QDs. In particular, the

relative tolerance of THP-1 cells favors the idea that this cell type is more capable to maintain a stable level of cellular homeostasis employing autophagy. Another potentially significant impact is the activation of miRNAs of the tumor-suppressing let-7 family which were down-regulated by Cd(II) but not by equivalent doses of Cd QDs. The relative low cytotoxicity exhibited by CdS QDs could be of interest in the context of their potential use as carriers of clinically active compounds such as antibiotics [87] or antibodies [88] or in gene delivery, as in gene therapy [89, 90].

Appendix A. Supplementary data

Acknowledgments

This work has been supported by the CINSA (National Interuniversity Consortium for Environmental Sciences). The University of Parma, Local Founds (FIL) has also supported OB. Institute of Materials for Electronics and Magnetism – National Research Council (IMEM-CNR) has supported the work of AZ and MV in the preparation analysis and characterization of CdS QDs utilized in this paper. The confocal images were obtained in the Laboratory of Confocal Microscopy of the Department of Medicine and Surgery of the University of Parma. Real Time-PCR analysis were performed using an equipment of SITEIA-Parma, Region Emilia Romagna Tecnopole (Interdepartmental Center on Safety and Technology in the Agro-Food Industry).

Declaration of Competing Interest

The authors declare no competing financial interest.

Author Contributions

The manuscript was written with contributions from all authors who have given approval to the final version of the manuscript.

References

[1] Y.P. Zhang, P. Sun, X.R. Zhang, W.L. Yang, C.S. Si, Synthesis of CdTe quantum dot-conjugated CC49 and their application for in vitro imaging of gastric adenocarcinoma cells, Nanoscale Res. Lett. 8 (2013) 1–9. https://doi.org/10.1186/1556-276X-8-294.

[2] K. V. Chakravarthy, B.A. Davidson, J.D. Helinski, H. Ding, W.C. Law, K.T. Yong, P.N. Prasad, P.R. Knight, Doxorubicin-conjugated quantum dots to target alveolar macrophages and inflammation, Nanomedicine Nanotechnology, Biol. Med. 7 (2011) 88–96. https://doi.org/10.1016/j.nano.2010.09.001.

[3] G. Zhang, L. Shi, M. Selke, X. Wang, CdTe quantum dots with daunorubicin induce apoptosis of multidrug-resistant human hepatoma HepG2/ADM cells: in vitro and in vivo evaluation, 2011. https://doi.org/10.1186/1556-276X-6-418.

[4] Y. Wang, M. Tang, Review of in vitro toxicological research of quantum dot and potentially involved mechanisms, Sci. Total Environ. 625 (2018) 940–962. https://doi.org/10.1016/j.scitotenv.2017.12.334.

[5] C.T. Matea, T. Mocan, F. Tabaran, T. Pop, O. Mosteanu, C. Puia, C. Iancu, L. Mocan, Quantum dots in imaging, drug delivery and sensor applications, Int. J. Nanomedicine. 12 (2017) 5421–5431. https://doi.org/10.2147/IJN.S138624.

[6] D. Mo, L. Hu, G. Zeng, G. Chen, J. Wan, Z. Yu, Z. Huang, K. He, C. Zhang, M. Cheng, Cadmium-containing quantum dots: properties, applications, and toxicity, Appl. Microbiol. Biotechnol. 101 (2017) 2713–2733. https://doi.org/10.1007/s00253-017-8140-9.

[7] B.B. Manshian, J. Jiménez, U. Himmelreich, S.J. Soenen, Personalized medicine and follow-up of therapeutic delivery through exploitation of quantum dot toxicity, Biomaterials. 127 (2017) 1–12. https://doi.org/10.1016/j.biomaterials.2017.02.039.

[8] N. Chen, Y. He, Y. Su, X. Li, Q. Huang, H. Wang, X. Zhang, R. Tai, C. Fan, The cytotoxicity of cadmium-based quantum dots, Biomaterials. 33 (2012) 1238–1244. https://doi.org/10.1016/j.biomaterials.2011.10.070.

[9] T. Zhang, Y. Hu, M. Tang, L. Kong, J. Ying, T. Wu, Y. Xue, Y. Pu, Liver Toxicity of Cadmium Telluride Quantum Dots (CdTe QDs) Due to Oxidative Stress in Vitro and in Vivo., Int. J. Mol. Sci. 16 (2015) 23279–99. https://doi.org/10.3390/ijms161023279.

[10] K. He, X. Liang, T. Wei, N. Liu, Y. Wang, L. Zou, J. Lu, Y. Yao, L. Kong, T. Zhang, Y. Xue, T. Wu, M. Tang, DNA damage in BV-2 cells: An important supplement to the neurotoxicity of CdTe quantum dots, J. Appl. Toxicol. 39 (2019) 525–539. https://doi.org/10.1002/jat.3745.

[11] S. Kato, K. Itoh, T. Yaoi, T. Tozawa, Y. Yoshikawa, H. Yasui, N. Kanamura, A. Hoshino, N. Manabe, K. Yamamoto, S. Fushiki, Organ distribution of quantum dots after intraperitoneal administration, with special reference to area-specific distribution in the brain, Nanotechnology. 21 (2010) 335103. https://doi.org/10.1088/0957-4484/21/33/335103.

[12] L. Paesano, A. Perotti, A. Buschini, C. Carubbi, M. Marmiroli, E. Maestri, S. Iannotta, N. Marmiroli, Markers for toxicity to HepG2 exposed to cadmium sulphide quantum dots; damage to mitochondria, Toxicology. 374 (2016) 18–28. https://doi.org/10.1016/j.tox.2016.11.012.

[13] H. Food and Drug Administration, International Conference on Harmonisation; Guidance on E15 Pharmacogenomics Definitions and Sample Coding; Availability. Notice., Fed. Regist. 73 (2008) 19074–6. http://www.ncbi.nlm.nih.gov/pubmed/18677821 (accessed September 4, 2018).

[14] H. Food and Drug Administration, International Conference on Harmonisation; Guidance on E16 Biomarkers Related to Drug or Biotechnology Product Development: Context, Structure, and Format of Qualification Submissions; availability. Notice., Fed. Regist. 76 (2011) 49773–4. http://www.ncbi.nlm.nih.gov/pubmed/21834216 (accessed September 4, 2018).

[15] Y. Bai, Y. Xue, X. Xie, T. Yu, Y. Zhu, Q. Ge, Z. Lu, The RNA expression signature of the HepG2 cell line as determined by the integrated analysis of miRNA and mRNA expression profiles, Gene. 548 (2014) 91–100. https://doi.org/10.1016/j.gene.2014.07.016.

[16] Y. Chen, D.-Y. Gao, L. Huang, In vivo delivery of miRNAs for cancer therapy: challenges and strategies., Adv. Drug Deliv. Rev. 81 (2015) 128–41. https://doi.org/10.1016/j.addr.2014.05.009.

[17] F. Bignami, E. Pilotti, L. Bertoncelli, P. Ronzi, M. Gulli, N. Marmiroli, G. Magnani, M. Pinti, L. Lopalco, C. Mussini, R. Ruotolo, M. Galli, A. Cossarizza, C. Casoli, Stable changes in CD4+ T lymphocyte miRNA expression after exposure to HIV-1, Blood. 119 (2012) 6259–6267.

https://doi.org/10.1182/blood-2011-09-379503.

[18] L.A. Genovesi, D. Anderson, K.W. Carter, K.M. Giles, P.B. Dallas, Identification of suitable endogenous control genes for microRNA expression profiling of childhood medulloblastoma and human neural stem cells, BMC Res. Notes. 5 (2012). https://doi.org/10.1186/1756-0500-5-507.

[19] A. Tripathi, K. Goswami, N. Sanan-Mishra, Role of bioinformatics in establishing microRNAs as modulators of abiotic stress responses: the new revolution., Front. Physiol. 6 (2015) 286. https://doi.org/10.3389/fphys.2015.00286.

[20] A.B. Mendoza-Soto, F. Sánchez, G. Hernández, MicroRNAs as regulators in plant metal toxicity response., Front. Plant Sci. 3 (2012) 105. https://doi.org/10.3389/fpls.2012.00105.

[21] D. Hosiner, S. Gerber, H. Lichtenberg-Frané, W. Glaser, C. Schüller, E. Klipp, Impact of Acute Metal Stress in Saccharomyces cerevisiae, PLoS One. 9 (2014) e83330. https://doi.org/10.1371/journal.pone.0083330.

[22] B. Wang, Y. Li, C. Shao, Y. Tan, L. Cai, Cadmium and Its Epigenetic Effects, Curr. Med. Chem. 19 (2012) 2611–2620. https://doi.org/10.2174/092986712800492913.

[23] M.A. Burgos-Aceves, A. Cohen, G. Paolella, M. Lepretti, Y. Smith, C. Faggio, L. Lionetti, Modulation of mitochondrial functions by xenobiotic-induced microRNA: From environmental sentinel organisms to mammals, Sci. Total Environ. 645 (2018) 79–88. https://doi.org/10.1016/j.scitotenv.2018.07.109.

[24] H.J. Eom, N. Chatterjee, J. Lee, J. Choi, Integrated mRNA and micro RNA

715 profiling reveals epigenetic mechanism of differential sensitivity of Jurkat T
716 cells to AgNPs and Ag ions, Toxicol. Lett. 229 (2014) 311–318.
717 https://doi.org/10.1016/j.toxlet.2014.05.019.

718 [25] J. Ndika, U. Seemab, W.L. Poon, V. Fortino, H. El-Nezami, P. Karisola, H.
719 Alenius, Silver, titanium dioxide, and zinc oxide nanoparticles trigger
720 miRNA/isomiR expression changes in THP-1 cells that are proportional to their
721 health hazard potential, Nanotoxicology. (2019).
722 https://doi.org/10.1080/17435390.2019.1661040.

723 [26] Y. Huang, X. Lü, Y. Qu, Y. Yang, S. Wu, MicroRNA sequencing and molecular
724 mechanisms analysis of the effects of gold nanoparticles on human dermal
725 fibroblasts, Biomaterials. 37 (2015) 13–24.
726 https://doi.org/10.1016/j.biomaterials.2014.10.042.

727 [27] K. Vrijens, V. Bollati, T.S. Nawro, MicroRNAs as Potential Signatures of
728 Environmental Exposure or Effect:, Env. Heal. Perspect. 123 (2015) 399–411.
729 https://doi.org/http://dx.doi.org/10.1289/ehp.1408459.

730 [28] R. Machtinger, V. Bollati, A.A. Baccarelli, miRNAs and lncRNAs as Biomarkers
731 of Toxicant Exposure, in: Toxicoepigenetics, Elsevier, 2019: pp. 237–247.
732 https://doi.org/10.1016/b978-0-12-812433-8.00010-1.

733 [29] M. Fabbri, C. Urani, M.G. Sacco, C. Procaccianti, L. Gribaldo, Whole genome
734 analysis and microRNAs regulation in HepG2 cells exposed to cadmium.,
735 ALTEX. 29 (2012) 173–82. https://doi.org/10.14573/altex.2012.2.173.

736 [30] Z. Liu, W. Jiang, J. Nam, J.J. Moon, B.Y.S. Kim, Immunomodulating
737 Nanomedicine for Cancer Therapy, Nano Lett. 18 (2018) 6655–6659.

https://doi.org/10.1021/acs.nanolett.8b02340.

[31] M. Villani, D. Calestani, L. Lazzarini, L. Zanotti, R. Mosca, A. Zappettini, Extended functionality of ZnO nanotetrapods by solution-based coupling with CdS nanoparticles, J. Mater. Chem. 22 (2012) 5694. https://doi.org/10.1039/c2jm16164h.

[32] L. Paesano, A. Perotti, A. Buschini, C. Carubbi, M. Marmiroli, E. Maestri, S. Iannotta, N. Marmiroli, Data on HepG2 cells changes following exposure to cadmium sulphide quantum dots (CdS QDs), Data Br. 11 (2017). https://doi.org/10.1016/j.dib.2016.12.051.

[33] L. Pagano, F. Pasquali, S. Majumdar, R. De La Torre-Roche, N. Zuverza-Mena, M. Villani, A. Zappettini, R.E. Marra, S.M. Isch, M. Marmiroli, E. Maestri, O.P. Dhankher, J.C. White, N. Marmiroli, Exposure of Cucurbita pepo to binary combinations of engineered nanomaterials: Physiological and molecular response, Environ. Sci. Nano. 4 (2017) 1579–1590. https://doi.org/10.1039/c7en00219j.

[34] J. O'Brien, I. Wilson, T. Orton, F. Pognan, Investigation of the Alamar Blue (resazurin) fluorescent dye for the assessment of mammalian cell cytotoxicity, Eur. J. Biochem. 267 (2000) 5421–5426. https://doi.org/10.1046/j.1432-1327.2000.01606.x.

[35] E. Oh, R. Liu, A. Nel, K.B. Gemill, M. Bilal, Y. Cohen, I.L. Medintz, Meta-analysis of cellular toxicity for cadmium-containing quantum dots, Nat Nano. (2016) doi:10.1038/nnano.2015.338. https://doi.org/10.1038/nnano.2015.338.

[36] L. Peng, M. He, B. Chen, Q. Wu, Z. Zhang, D. Pang, Y. Zhu, B. Hu, Cellular

761 uptake, elimination and toxicity of CdSe/ZnS quantum dots in HepG2 cells,
762 Biomaterials. 34 (2013) 9545–9558.
763 https://doi.org/10.1016/j.biomaterials.2013.08.038.

764 [37] K.J. Livak, T.D. Schmittgen, Analysis of relative gene expression data using
765 real-time quantitative PCR and the 2(-Delta Delta C(T)) Method., Methods. 25
766 (2001) 402–408. https://doi.org/10.1006/meth.2001.1262.

767 [38] M.G. Bianchi, M. Allegri, A.L. Costa, M. Blosi, D. Gardini, C. Del Pivo, A. Prina-
768 Mello, L. Di Cristo, O. Bussolati, E. Bergamaschi, Titanium dioxide
769 nanoparticles enhance macrophage activation by LPS through a TLR4-
770 dependent intracellular pathway, Toxicol. Res. (Camb). 4 (2015) 385–398.
771 https://doi.org/10.1039/c4tx00193a.

772 [39] I.S. Vlachos, M.D. Paraskevopoulou, D. Karagkouni, G. Georgakilas, T.
773 Vergoulis, I. Kanellos, I.-L. Anastasopoulos, S. Maniou, K. Karathanou, D.
774 Kalfakakou, A. Fevgas, T. Dalamagas, A.G. Hatzigeorgiou, DIANA-TarBase
775 v7.0: indexing more than half a million experimentally supported miRNA:mRNA
776 interactions., Nucleic Acids Res. 43 (2015) D153-9.
777 https://doi.org/10.1093/nar/gku1215.

778 [40] I.S. Vlachos, K. Zagganas, M.D. Paraskevopoulou, G. Georgakilas, D.
779 Karagkouni, T. Vergoulis, T. Dalamagas, A.G. Hatzigeorgiou, DIANA-miRPath
780 v3.0: deciphering microRNA function with experimental support, Nucleic Acids
781 Res. 43 (2015) W460–W466. https://doi.org/10.1093/nar/gkv403.

782 [41] S.-D. Hsu, Y.-T. Tseng, S. Shrestha, Y.-L. Lin, A. Khaleel, C.-H. Chou, C.-F.
783 Chu, H.-Y. Huang, C.-M. Lin, S.-Y. Ho, T.-Y. Jian, F.-M. Lin, T.-H. Chang, S.-L.
784 Weng, K.-W. Liao, I.-E. Liao, C.-C. Liu, H.-D. Huang, miRTarBase update

2014: an information resource for experimentally validated miRNA-target interactions., Nucleic Acids Res. 42 (2014) D78-85. https://doi.org/10.1093/nar/gkt1266.

[42] T. Brzicova, E. Javorkova, K. Vrbova, A. Zajicova, V. Holan, D. Pinkas, V. Philimonenko, J. Sikorova, J. Klema, J. Topinka, P. Rossner, Molecular responses in THP-1 macrophage-like cells exposed to diverse nanoparticles, Nanomaterials. 9 (2019). https://doi.org/10.3390/nano9050687.

[43] M.M. Haque, H. Im, J. Seo, M. Hasan, K. Woo, O.-S. Kwon, Acute toxicity and tissue distribution of CdSe/CdS-MPA quantum dots after repeated intraperitoneal injection to mice, J. Appl. Toxicol. 33 (2013) 940–950. https://doi.org/10.1002/jat.2775.

[44] C. Urani, P. Melchioretto, C. Canevali, G.F. Crosta, Cytotoxicity and induction of protective mechanisms in HepG2 cells exposed to cadmium., Toxicol. In Vitro. 19 (2005) 887–892. https://doi.org/10.1016/j.tiv.2005.06.011.

[45] S. Oh, S. Lim, A rapid and transient ROS generation by cadmium triggers apoptosis via caspase-dependent pathway in HepG2 cells and this is inhibited through N-acetylcysteine-mediated catalase upregulation, Toxicol. Appl. Pharmacol. 212 (2006) 212–223. https://doi.org/10.1016/j.taap.2005.07.018.

[46] K.G. Li, J.T. Chen, S.S. Bai, X. Wen, S.Y. Song, Q. Yu, J. Li, Y.Q. Wang, Intracellular oxidative stress and cadmium ions release induce cytotoxicity of unmodified cadmium sulfide quantum dots, Toxicol. Vitr. 23 (2009) 1007–1013. https://doi.org/10.1016/j.tiv.2009.06.020.

[47] F. Pasquali, C. Agrimonti, L. Pagano, A. Zappettini, M. Villani, M. Marmiroli,

808 J.C. White, N. Marmiroli, Nucleo-mitochondrial interaction of yeast in response
809 to cadmium sulfide quantum dot exposure, J. Hazard. Mater. 324 (2017) 744–
810 752. https://doi.org/10.1016/J.JHAZMAT.2016.11.053.

811 [48] S.W. Funkhouser, O. Martinezmaza, D.L. Vredevoe, Cadmium Inhibits IL-6
812 Production and IL-6 mRNA Expression in a Human Monocytic Cell Line, THP-
813 1, Environ. Res. 66 (1994) 77–86. https://doi.org/10.1006/ENRS.1994.1045.

814 [49] J. Li, Y. Zhang, Q. Xiao, F. Tian, X. Liu, R. Li, G. Zhao, F. Jiang, Y. Liu,
815 Mitochondria as target of Quantum dots toxicity, J. Hazard. Mater. 194 (2011)
816 440–444. https://doi.org/10.1016/j.jhazmat.2011.07.113.

817 [50] Y. Wang, M. Tang, Dysfunction of various organelles provokes multiple cell
818 death after quantum dot exposure, Int. J. Nanomedicine. 13 (2018) 2729–2742.
819 https://doi.org/10.2147/IJN.S157135.

820 [51] M. Yan, Y. Zhang, H. Qin, K. Liu, M. Guo, Y. Ge, M. Xu, Y. Sun, X. Zheng,
821 Cytotoxicity of CdTe quantum dots in human umbilical vein endothelial cells:
822 The involvement of cellular uptake and induction of pro-apoptotic endoplasmic
823 reticulum stress, Int. J. Nanomedicine. 11 (2016) 529–542.
824 https://doi.org/10.2147/IJN.S93591.

825 [52] L. Paesano, M. Marmiroli, M.G. Bianchi, J.C. White, O. Bussolati, A. Zappettini,
826 M. Villani, N. Marmiroli, Data on miRNome changes in human cells exposed to
827 nano- or ionic- form of Cd, Data Br. (submitted).

828 [53] D.J. Klionsky, F.C. Abdalla, H. Abeliovich, R.T. Abraham, A. Acevedo-Arozena,
829 K. Adeli, L. Agholme, M. Agnello, P. Agostinis, J.A. Aguirre-Ghiso, et al.,
830 Guidelines for the use and interpretation of assays for monitoring autophagy,

831 Autophagy. 8 (2012) 445–544. https://doi.org/10.4161/auto.19496.

832 [54] M. Komatsu, Y. Ichimura, Physiological significance of selective degradation of
833 p62 by autophagy, FEBS Lett. 584 (2010) 1374–1378.
834 https://doi.org/10.1016/j.febslet.2010.02.017.

835 [55] K.C. Nguyen, W.G. Willmore, A.F. Tayabali, Cadmium telluride quantum dots
836 cause oxidative stress leading to extrinsic and intrinsic apoptosis in
837 hepatocellular carcinoma HepG2 cells, Toxicology. 306 (2013) 114–123.
838 https://doi.org/10.1016/j.tox.2013.02.010.

839 [56] Z. Su, Z. Yang, Y. Xu, Y. Chen, Q. Yu, Z. Su, Z. Yang, Y. Xu, Y. Chen, Q. Yu,
840 MicroRNAs in apoptosis, autophagy and necroptosis, Oncotarget. 6 (2015)
841 8474–8490. https://doi.org/10.18632/oncotarget.3523.

842 [57] V. Pileczki, R. Cojocneanu-Petric, M. Maralani, I.B. Neagoe, R. Sandulescu,
843 MicroRNAs as regulators of apoptosis mechanisms in cancer., Clujul Med. 89
844 (2016) 50–5. https://doi.org/10.15386/cjmed-512.

845 [58] K. Cuk, D. Madhavan, A. Turchinovich, B. Burwinkel, Plasma microRNAs as
846 Biomarkers of Human Diseases, in: S.C. Sahu (Ed.), MicroRNAs Toxicol. Med.,
847 John Wiley & Sons, Ltd, Chichester, UK, 2013: pp. 389–418.
848 https://doi.org/10.1002/9781118695999.

849 [59] K.A. Bailey, R.C. Fry, Environmental Toxicants and Perturbation of miRNA
850 Signaling, in: S.C. Sahu (Ed.), MicroRNAs Toxicol. Med., John Wiley & Sons,
851 Ltd, Chichester, UK, 2013: pp. 5–22. https://doi.org/10.1002/9781118695999.

852 [60] B. Boyerinas, S.M. Park, A. Hau, A.E. Murmann, M.E. Peter, The role of let-7 in
853 cell differentiation and cancer, Endocr. Relat. Cancer. 17 (2010) 19–36.

https://doi.org/10.1677/ERC-09-0184.

[61] C.-J. Guo, Q. Pan, D.-G. Li, H. Sun, B.-W. Liu, miR-15b and miR-16 are implicated in activation of the rat hepatic stellate cell: An essential role for apoptosis, J. Hepatol. 50 (2009) 766–778. https://doi.org/10.1016/j.jhep.2008.11.025.

[62] P. Schulte, V. Leso, M. Niang, I. Iavicoli, Biological monitoring of workers exposed to engineered nanomaterials, Toxicol. Lett. 298 (2018) 112–124. https://doi.org/10.1016/j.toxlet.2018.06.003.

[63] A.A. Mansur, H.S. Mansur, S.M. de Carvalho, Z.I. Lobato, M.I. Guedes, M.F. Leite, Surface biofunctionalized CdS and ZnS quantum dot nanoconjugates for nanomedicine and oncology: to be or not to be nanotoxic?, Int. J. Nanomedicine. 11 (2016) 4669–4690. https://doi.org/10.2147/ijn.s115208.

[64] J.R. Roberts, J.M. Antonini, D.W. Porter, R.S. Chapman, J.F. Scabilloni, S.H. Young, D. Schwegler-Berry, V. Castranova, R.R. Mercer, Lung toxicity and biodistribution of Cd/Se-ZnS quantum dots with different surface functional groups after pulmonary exposure in rats., Part. Fibre Toxicol. 10 (2013). https://doi.org/10.1186/1743-8977-10-5.

[65] C.-C. Ho, H. Chang, H.-T. Tsai, M.-H. Tsai, C.-S. Yang, Y.-C. Ling, P. Lin, Quantum dot 705, a cadmium-based nanoparticle, induces persistent inflammation and granuloma formation in the mouse lung, Nanotoxicology. 7 (2013) 105–115. https://doi.org/10.3109/17435390.2011.635814.

[66] M. Olejniczak, A. Kotowska-Zimmer, W. Krzyzosiak, Stress-induced changes in miRNA biogenesis and functioning, Cell. Mol. Life Sci. 75 (2018) 177–191.

https://doi.org/10.1007/s00018-017-2591-0.

[67] D. Castanotto, X. Zhang, J. Alluin, X. Zhang, J. Rüger, B. Armstrong, J. Rossi, A. Riggs, C.A. Stein, A stress-induced response complex (SIRC) shuttles miRNAs, siRNAs, and oligonucleotides to the nucleus, Proc. Natl. Acad. Sci. U. S. A. 115 (2018) E5756–E5765. https://doi.org/10.1073/pnas.1721346115.

[68] L.A. McConnachie, C.C. White, D. Botta, M.E. Zadworny, D.P. Cox, R.P. Beyer, X. Hu, D.L. Eaton, X. Gao, T.J. Kavanagh, Heme oxygenase expression as a biomarker of exposure to amphiphilic polymer-coated CdSe/ZnS quantum dots, Nanotoxicology. 7 (2013) 181–191. https://doi.org/10.3109/17435390.2011.648224.

[69] K.D. Neibert, D. Maysinger, Mechanisms of cellular adaptation to quantum dots – the role of glutathione and transcription factor EB, Nanotoxicology. 6 (2012) 249–262. https://doi.org/10.3109/17435390.2011.572195.

[70] J. Fan, Y. Sun, S. Wang, Y. Li, X. Zeng, Z. Cao, P. Yang, P. Song, Z. Wang, Z. Xian, H. Gao, Q. Chen, D. Cui, D. Ju, Inhibition of autophagy overcomes the nanotoxicity elicited by cadmium-based quantum dots, Biomaterials. 78 (2016) 102–114. https://doi.org/10.1016/j.biomaterials.2015.11.029.

[71] P. Rodríguez-Fragoso, J. Reyes-Esparza, A. León-Buitimea, L. Rodríguez-Fragoso, Synthesis, characterization and toxicological evaluation of maltodextrin capped cadmium sulfide nanoparticles in human cell lines and chicken embryos., J. Nanobiotechnology. 10 (2012) 47. https://doi.org/10.1186/1477-3155-10-47.

[72] L. Lai, J.C. Jin, Z.Q. Xu, P. Mei, F.L. Jiang, Y. Liu, Necrotic cell death induced

by the protein-mediated intercellular uptake of CdTe quantum dots, Chemosphere. 135 (2015) 240–249. https://doi.org/10.1016/j.chemosphere.2015.04.044.

[73] S. Li, Y. Wang, H. Wang, Y. Bai, G. Liang, Y. Wang, N. Huang, Z. Xiao, MicroRNAs as participants in cytotoxicity of CdTe quantum dots in NIH/3T3 cells, Biomaterials. 32 (2011) 3807–3814. https://doi.org/10.1016/j.biomaterials.2011.01.074.

[74] V. Bravo, S. Rosero, C. Ricordi, R.L. Pastori, Instability of miRNA and cDNAs derivatives in RNA preparations, Biochem. Biophys. Res. Commun. 353 (2007) 1052–1055. https://doi.org/10.1016/j.bbrc.2006.12.135.

[75] T. Nolan, R.E. Hands, S.A. Bustin, Quantification of mRNA using real-time RT-PCR, Nat. Protoc. 1 (2006) 1559. http://dx.doi.org/10.1038/nprot.2006.236.

[76] S. Tang, Q. Cai, H. Chibli, V. Allagadda, J.L. Nadeau, G.D. Mayer, Cadmium sulfate and CdTe-quantum dots alter DNA repair in zebrafish (Danio rerio) liver cells, Toxicol. Appl. Pharmacol. 272 (2013) 443–452. https://doi.org/https://doi.org/10.1016/j.taap.2013.06.004.

[77] B. Sun, F. Yang, F.H. Hu, N.P. Huang, Z.D. Xiao, Comprehensive annotation of microRNA expression profiles, BMC Genet. 14 (2013) 1–9. https://doi.org/10.1186/1471-2156-14-120.

[78] J. Fan, S. Wang, X. Zhang, W. Chen, Y. Li, P. Yang, Z. Cao, Y. Wang, W. Lu, D. Ju, Quantum Dots Elicit Hepatotoxicity through Lysosome-Dependent Autophagy Activation and Reactive Oxygen Species Production, ACS Biomater. Sci. Eng. 4 (2018) 1418–1427.

https://doi.org/10.1021/acsbiomaterials.7b00824.

[79] E.Y. Lee, H.C. Bae, H. Lee, Y. Jang, Y.-H. Park, J.H. Kim, W.-I. Ryu, B.H. Choi, J.H. Kim, S.H. Jeong, S.W. Son, Intracellular ROS levels determine the apoptotic potential of keratinocyte by Quantum Dot via blockade of AKT Phosphorylation, Exp. Dermatol. 26 (2017) 1046–1052. https://doi.org/10.1111/exd.13365.

[80] F. Wei, Y. Duan, Crosstalk between Autophagy and Nanomaterials: Internalization, Activation, Termination, Adv. Biosyst. 3 (2019) 1800259. https://doi.org/10.1002/adbi.201800259.

[81] S.T. Stern, P.P. Adiseshaiah, R.M. Crist, Autophagy and lysosomal dysfunction as emerging mechanisms of nanomaterial toxicity, Part. Fibre Toxicol. 9 (2012) 20. https://doi.org/10.1186/1743-8977-9-20.

[82] J. Zhang, X. Qin, B. Wang, G. Xu, Z. Qin, J. Wang, L. Wu, X. Ju, D.D. Bose, F. Qiu, H. Zhou, Z. Zou, Zinc oxide nanoparticles harness autophagy to induce cell death in lung epithelial cells, Cell Death Dis. 8 (2017) e2954. https://doi.org/10.1038/cddis.2017.337.

[83] L. Sripada, D. Tomar, R. Singh, Mitochondria: One of the destinations of miRNAs, Mitochondrion. 12 (2012) 593–599. https://doi.org/10.1016/j.mito.2012.10.009.

[84] M.J. Axtell, Lost in translation? microRNAs at the rough ER, Trends Plant Sci. 22 (2017) 273–274. https://doi.org/10.1016/j.tplants.2017.03.002.

[85] P. Li, J. Jiao, G. Gao, B.S. Prabhakar, Control of mitochondrial activity by miRNAs, J. Cell. Biochem. 113 (2012) 1104–1110.

https://doi.org/10.1002/jcb.24004.

[86] K.C. Nguyen, P. Rippstein, a. F. Tayabali, W.G. Willmore, Mitochondrial Toxicity of Cadmium Telluride Quantum Dot Nanoparticles in Mammalian Hepatocytes, Toxicol. Sci. 146 (2015) 31–42. https://doi.org/10.1093/toxsci/kfv068.

[87] I. Armenia, G.L. Marcone, F. Berini, V.T. Orlandi, C. Pirrone, E. Martegani, R. Gornati, G. Bernardini, F. Marinelli, Magnetic Nanoconjugated Teicoplanin: A Novel Tool for Bacterial Infection Site Targeting, Front. Microbiol. 9 (2018). https://doi.org/10.3389/fmicb.2018.02270.

[88] M.C. Johnston, C.J. Scott, Antibody conjugated nanoparticles as a novel form of antibody drug conjugate chemotherapy, Drug Discov. Today Technol. 30 (2018) 63–69. https://doi.org/10.1016/J.DDTEC.2018.10.003.

[89] K.J. McHugh, L. Jing, S.Y. Severt, M. Cruz, M. Sarmadi, H.S.N. Jayawardena, C.F. Perkinson, F. Larusson, S. Rose, S. Tomasic, T. Graf, S.Y. Tzeng, J.L. Sugarman, D. Vlasic, M. Peters, N. Peterson, L. Wood, W. Tang, J. Yeom, J. Collins, P.A. Welkhoff, A. Karchin, M. Tse, M. Gao, M.G. Bawendi, R. Langer, A. Jaklenec, Biocompatible near-infrared quantum dots delivered to the skin by microneedle patches record vaccination, Sci. Transl. Med. 11 (2019) eaay7162. https://doi.org/10.1126/scitranslmed.aay7162.

[90] J. Choi, Y. Rui, J. Kim, N. Gorelick, D.R. Wilson, K. Kozielski, A. Mangraviti, E. Sankey, H. Brem, B. Tyler, J.J. Green, E.M. Jackson, Nonviral polymeric nanoparticles for gene therapy in pediatric CNS malignancies, Nanomedicine Nanotechnology, Biol. Med. 23 (2020). https://doi.org/10.1016/j.nano.2019.102115.

Figure captions

Fig. 1 *The effect of CdS QDs and Cd(II) treatment on mitochondrial membrane potential, as quantified by JC-1 staining.* Cells were exposed for 24 h to Cd in the form of either CdS QDs or Cd(II). The data report the ratio between aggregated and monomeric forms of JC1, and are representative of three independent experiments. The concentrations of CdS QDs and Cd(II) shown are for the Cd in the material. Asterisks ***. ****: p<0.001, <0.0001 vs. values obtained from non-treated cells.

Fig. 2 *The effect on THP-1 cell morphology of exposure to Cd in the form of either CdS QDs or* Cd(II)*.* After a 24 h exposure to a high or low dose of either stressor, cell monolayers were labelled with JC-1 to assay mitochondrial function or with DRAQ5 to assay nuclear morphology. CdS QDs, 6.4 μg ml^{-1} equivalent to 5 μg ml^{-1} Cd, induced a modest increase in the amount of JC-1 monomers, suggesting some alteration in mitochondrial function but there was no evidence of marked changes in cell morphology. Cd in the form of Cd(II), 11.4 μg ml^{-1} equivalent to 5 μg ml^{-1} Cd, not only substantially increased the abundance of JC-1 monomers, but also caused loss of the red signal, suggesting a significant alteration in mitochondrial function. In addition, Cd(II) treatment also changed the typical elongated shape into a more rounded form. When THP-1 cells were exposed to a high dose of CdS QDs, 50 μg ml^{-1} equivalent to 39 μg ml^{-1} Cd, most of the CdS QDs aggregated and the presence of JC-1 monomeric forms was only slightly increased. Cell morphology appeared to be substantially unaffected. Bar: 20 μm. The images illustrate representative microscope fields where at least 100 cells were present.

Fig. 3 *The uptake of CdS QDs into THP-1 cells as measured using a cytofluorimetric assay.* Cells were exposed to 39 μg ml^{-1} Cd as 50 μg ml^{-1} CdS QDs for 0 - 24 h. Typical scatter plots are shown, obtained from a representative experiment performed three times with comparable results. FS, forward scatter; SS, side scatter

Fig. 4 *Venn diagram representation of the effect of exposure to Cd on the miRNome.* **a**, HepG2 cells exposed to 2.3 μg ml^{-1} Cd as 3 μg ml^{-1} CdS QDs or 5.2 μg ml^{-1} Cd(II). The number of miRNAs increased in abundance were 34 and 29, respectively, while number of miRNAs decreased in abundance were 32 and 102, respectively. Only 11 and 13 miRNAs were increased or reduced in abundance by both treatments, respectively. **b**, THP-1 cells exposed to 5 μg ml^{-1} Cd as 6.4 μg ml^{-1} CdS QDs or 11.4 μg ml^{-1} Cd(II). Exposure to CdS QDs increased the abundance of 136 miRNAs, whereas only 15 were reduced. **c**, Comparison between HepG2 cells exposed to 2.3 μg ml^{-1} Cd as 3 μg ml^{-1} CdS QDs and THP-1 cells exposed to 5 μg ml^{-1} Cd as 6.4 μg ml^{-1} CdS QDs. Ten miRNAs responded positively and 2 responded negatively in both cell types. Eight miRNAs responded in opposite directions. **d**, Comparison between HepG2 cells exposed to 2.3 μg ml^{-1} Cd as 5.2 μg ml^{-1} Cd(II) and THP-1 cells exposed to 5 μg ml^{-1} Cd as 11.4 μg ml^{-1} Cd(II). Thirty nine miRNAs responded negatively in both cell types, while no miRNA responded positively; 16 miRNAs responded in opposite manner.

Fig. 5 *A heatmap-based illustration of the HepG2 and THP-1 cell responses to Cd exposure*. The heatmaps show only those miRNAs which were increased or decreased in both cell types or with either treatment. Positively responding miRNAs are shown in red and negatively responding ones in green. **a**, Differentially abundant

1019 miRNAs present in HepG2 cells exposed to 2.3 μg ml^{-1} Cd as 3 μg ml^{-1} CdS QDs or
1020 5.2 μg ml^{-1} Cd(II). For a large number of miRNAs abundance is reduced when the
1021 cells are treated with Cd(II) as compared with cells treated with CdS QDs. **b**,
1022 Differentially abundant miRNAs present in HepG2 and THP-1 cells exposed to 2.3
1023 and 5 μg ml^{-1} Cd as 5.2 μg ml^{-1} and 11.4 μg ml^{-1} Cd(II). **c**, Differentially abundant
1024 miRNAs present in HepG2 and THP-1 cells exposed to 2.3 and 5 μg ml^{-1} Cd as 3 μg
1025 ml^{-1} and 6.4 μg ml^{-1} CdS QDs.
1026
1027 **Fig. 6** *The effect on the miRNome of exposure to Cd, illustrated by a Venn diagram.*
1028 **a**, miRNAs induced in THP-1 cells in response to exposure to either 39 μg ml^{-1} Cd as
1029 50 μg ml^{-1} CdS QDs or 5 μg ml^{-1} Cd as 11.4 μg ml^{-1} Cd(II). The abundances of totals
1030 of 9 and 18 miRNAs were increased by CdS QDs and Cd(II) treatment, respectively.
1031 miRNAs decreased in response to the two treatments were 237 and 129
1032 respectively; of these, 124 responded negatively to both treatments, while 5 miRNAs
1033 were decreased by Cd(II) treatment but increased in the presence of CdS QDs. **b**,
1034 miRNAs induced in either HepG2 or THP-1 cells in response to exposure to,
1035 respectively, 2.3 μg ml^{-1} Cd as 3 μg ml^{-1} CdS QDs and 39 μg ml^{-1} Cd as 50 μg ml^{-1}
1036 CdS QDs; **c**, miRNAs induced in either HepG2 or THP-1 cells in response to
1037 exposure to CdS QDs (all treatments).
1038
1039 **Fig. 7** *The core autophagy pathway and its regulation by miRNAs in THP-1 cells*
1040 *exposed to 39 μg ml^{-1} Cd as 50 μg ml^{-1} CdS QDs..* The entire pathway was divided
1041 into five steps: induction, vesicle nucleation, elongation, retrieval and fusion. Arrows
1042 indicate increase or decrease of miRNA. A green arrow indicated a decrease with

lack of repression of its specific targets. The overall effect seems to bring the cell towards autophagosome formation and autophagy.

Fig. 8 *The effect of exposure to Cd on autophagy markers in THP-1 and HepG2 cells.* THP-1 and HepG2 cells were incubated for 24h in the presence of different doses of Cd: 2.3 µg ml^{-1} as 3 µg ml^{-1} CdS QDs, 5 µg ml^{-1} as 6.4 µg ml^{-1} CdS QDs or as 11.4 µg ml^{-1} Cd(II) and 39 µg ml^{-1} as 50 µg ml^{-1} CdS QDs. Cells were then extracted and Western Blot analysis of p62 and LC3II was performed as described in Materials and Methods. Tubulin was used for loading control. *Pos* indicates THP-1 cells, treated with rapamycin, 10 nM, 3h, and cloroquine, 100 µM, 2h, exploited as positive controls for autophagy.

Fig. 9 *The core apoptotic pathway and its regulation by miRNAs in HepG2 cells exposed to 2.3 µg ml^{-1} Cd as 3 µg ml^{-1} CdS QDs.* The figure depicts events of the intrinsic and extrinsic apoptotic pathways. Arrows indicate increase or decrease of miRNA or gene. A red arrow indicates increased abundance of a specific gene. A green arrow indicates a decrease which permits the expression of its specific target. In this system the activation of the intrinsic pathway leads to apoptosis. At the dose of CdS QDs considered and under the experimental conditions adopted, the proportion of cells which effectively completed apoptosis was limited, as shown by morphological observation (see Fig. A.2).

Table

Table 1 Differentially abundant miRNAs in response to Cd exposure and their principal cellular targets, pathways and related diseases

		THP-1			HepG2			
		39 μg ml^{-1} Cd	5 μg ml^{-1} Cd		2.3 μg ml^{-1} Cd			
Processes[1]	**miRNA involved**[2]	QDs[3] 50 μg ml^{-1}	QDs[3] 6.4 μg ml^{-1}	Cd(II)[3] 11.4 μg ml^{-1}	QDs[3] 3 μg ml^{-1}	Cd(II)[3] 5.2 μg ml^{-1}	**Target protein**[4]	**Diseases**[5]
Apoptosis	miR-34a	/	/	/	/	↓	BCL-2	Cancer
	miR-195	↓	/	/	↓	↓		
	miR-143	↓	/	↓	/	↓		
	miR-155	↓	↑	↓	↓	/		
	miR-125	↓	↑	↓	/	/		
	miR-29a	↓	/	/	/	↓	CDC42, p58α	Cancer/ Huntington's disease
	miR-125b	↓	/	↓	/	/	p53	Cancer/ Psoriasis
	miR-221	↓	/	↓	/	/	p27 (KIP1)	
	miR-222	↑	↑	↓	/	↓		
	miR-181a	↑	↑	/	/	/	BIM	Cancer
	miR-32	↓	/	↓	↓	↓		
	miR-25	↓	/	↓	/	/		
DNA Repair	miR-16	↓	↑	↓	/	/	UNG2	Cancer
	miR-199	↓	↑	↓	/	/		
	miR-21	↓	/	↓	/	↓	hMSH2	
	miR-192	↓	/	↓	/	↓	ERCC3, ERCC4	Toxicant exposure biomarker
	miR-101	↓	↑	↓	/	/	DNA-PKcs	
	miR-24	↓	↑	↓	/	/	H2AX	Cancer
	miR-96	↓	/	/	/	/	RAD51	/
Cell cycle	miR-16	↓	↑	↓	/	/	CDK2	Cancer
	miR-449a/b	↓	↑/↓	↓	/	/	CDK6, CDC25A	/
	miR-15	↓	/	/	↑	/	WEE1, CHK1	Cancer
	miR-125	↓	↑	↓	/	/	Cyclin A2	
	let-7b	↓	/	↓	/	↓	Cyclin A	
Xenobiotic metabolism	miR-27b	↓	/	/	/	↓	CYP1B1	Diabetes
	miR-126	↓	↑	/	↓	↓	CYP2A3	Cancer/ Cardiovascular diseases
	miR-378	↓	/	/	↓	↓	CYP2E1	Cancer
	miR-133a	↓	↑	/	↑	↑	GSTP1	
Autophagy/ Phagocytosis	let-7a	↓	/	↓	/	↓	several chemokines	Cancer
	miR-146a	↓	/	/	/	/		Inflammatory diseases

	miR-25	↓	/	↓	/	/		Cancer
	miR-26a	↓	/	↓	/	↑		
Autophagy/ Phagocytosis	miR-132	↓	↑	↓	/	↑	several chemokines	Alzheimer's disease
	miR-140	↓	↑	↓	/	↓		Cancer
	miR-146b	↓	/	/	/	/		Inflammatory diseases
	miR-155	↓	↑	↓	↓	/		Cancer
	miR-210	↓	↑	↓	/	/		
	miR-21	↓	/	↓	/	/		
	miR-142-3p	↓	/	/	↓	/		Cardiovascular diseases
	miR-125b	↓	/	↓	/	/		Cancer
	miR-17-5p	↓	/	↓	/	↓		
	miR-24	↓	↑	↓	/	/		
	miR-30b	↓	↑	↓	/	↓		
	miR-101	↓	↑	↓	/	/		Toxicant exposure biomarker
	miR-652-3p	↓	/	↓	/	↓		/
	miR-1275	↓	↑	↓	/	↓		/
	miR-7	/	↑	/	↓	/	mTOR	/
	miR-199a	↓	↑	↓	/	/		Cancer
	miR-30a	↓	↑	/	↓	↓	Beclin	Cancer

Note. [1] The more relevant processes emerging from analysis by DIANA-mirPath software.
[2] The miRNAs evaluated here represent the more significant variations, which have commonalities between different cell types and different treatments. The same were also suggested as exposure biomarkers for different environmental or health related clues [58,59].
[3] The red and green arrows indicate the miRNA is increased or decreased in abundance.
[4,5] Main target proteins and diseases were taken from literature [58,59].

Figure 1

Click here to download high resolution image

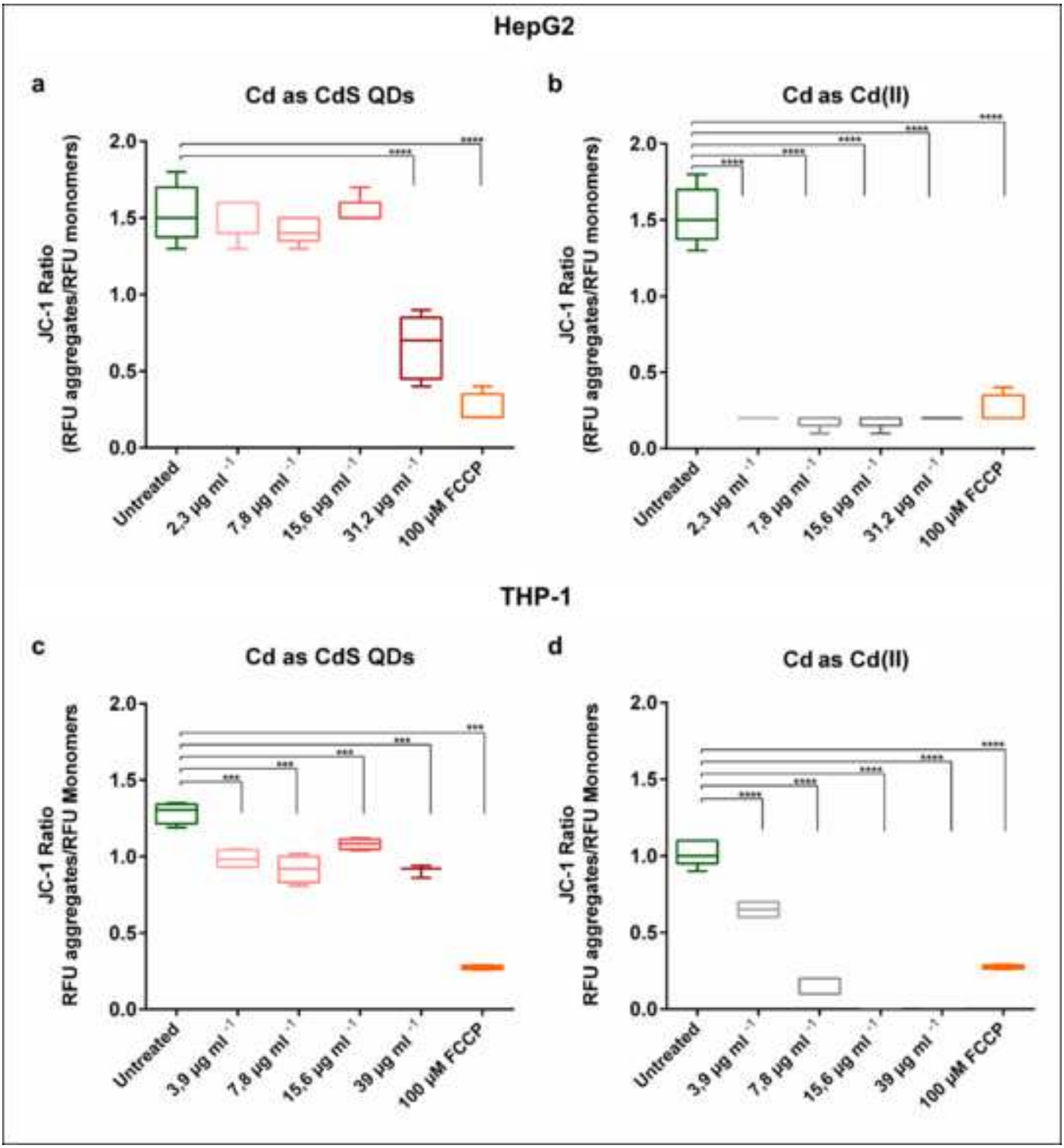

Figure 2

Click here to download high resolution image

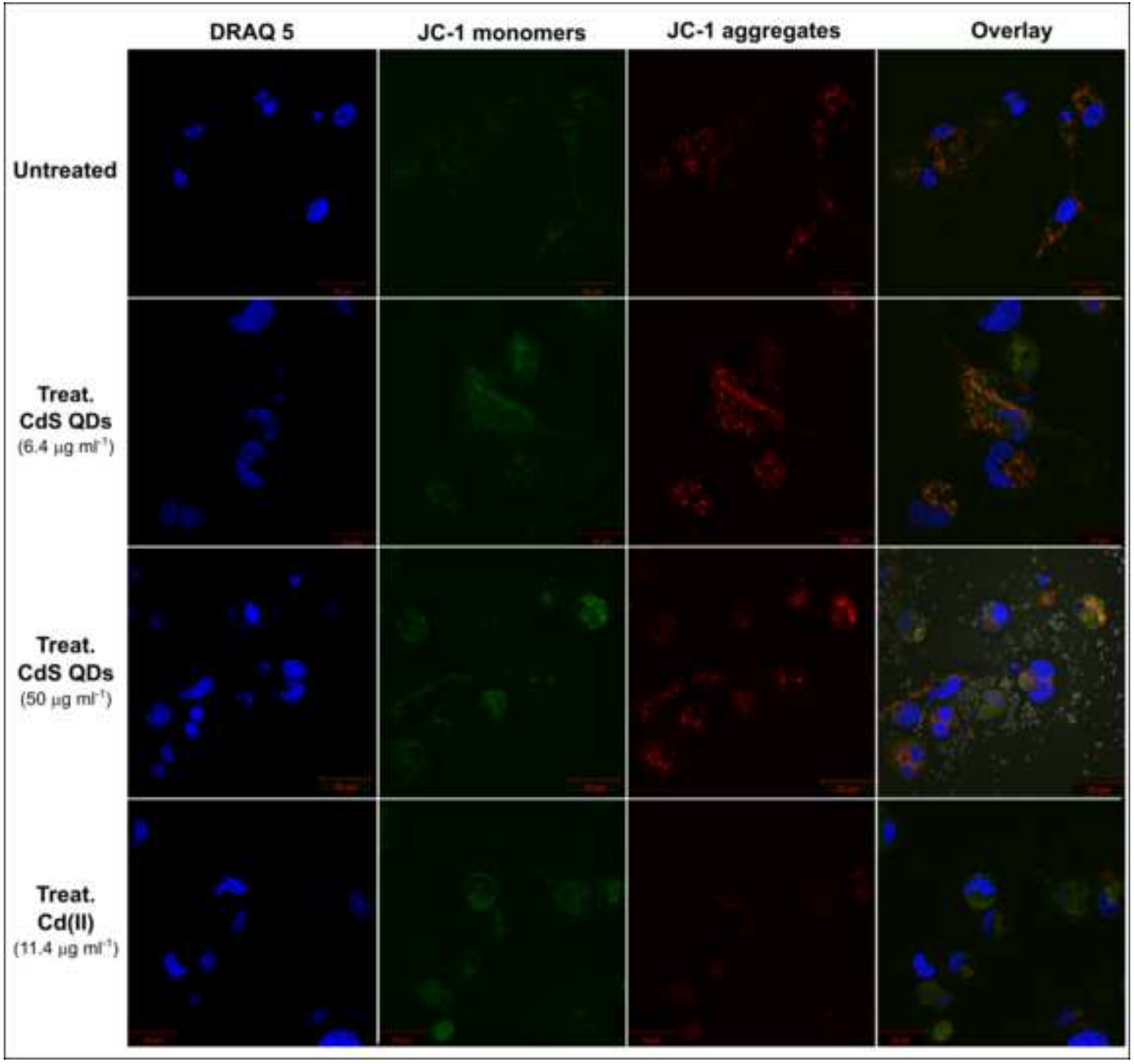

Figure 3

Click here to download high resolution image

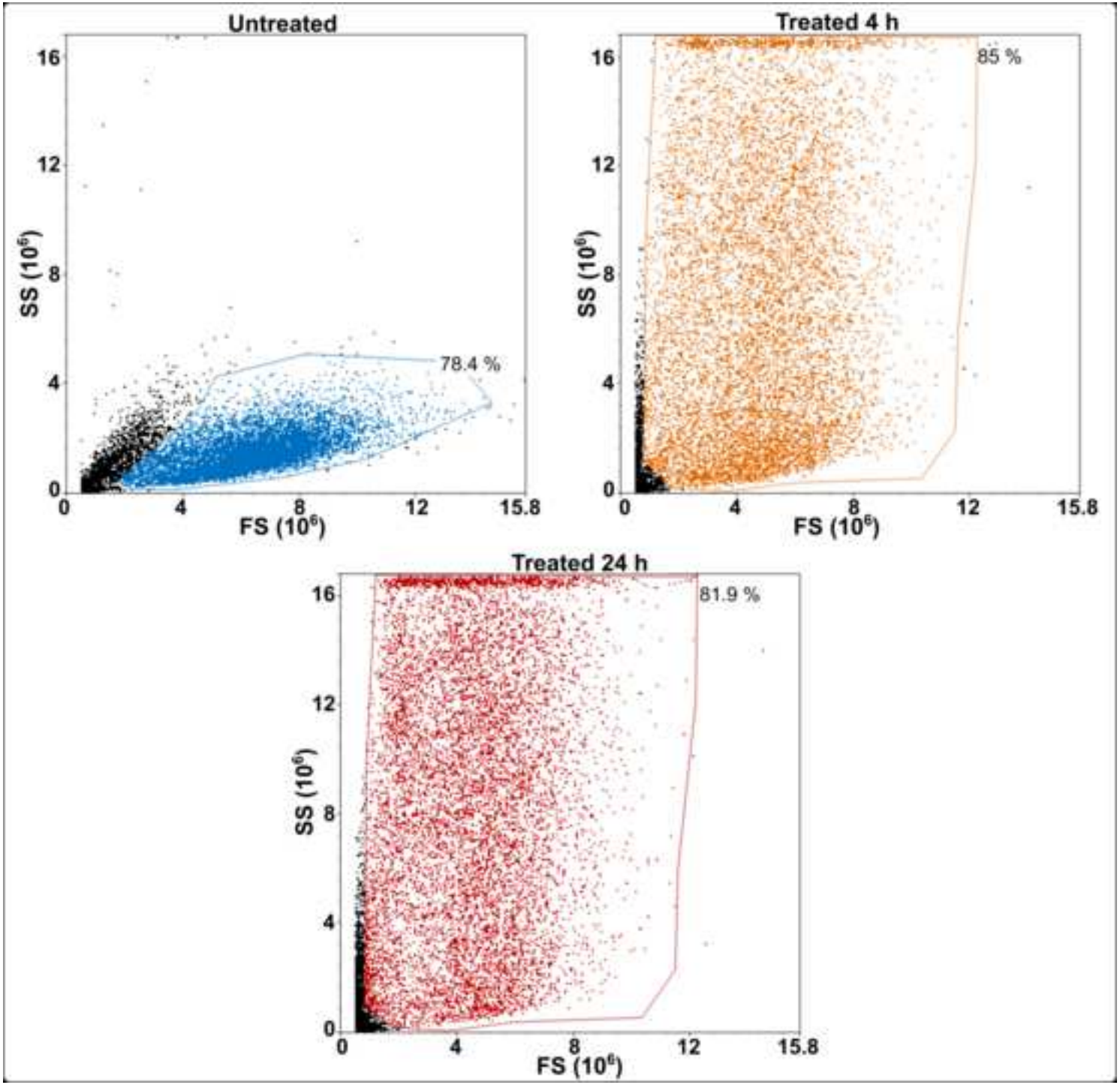

Figure 4

Click here to download high resolution image

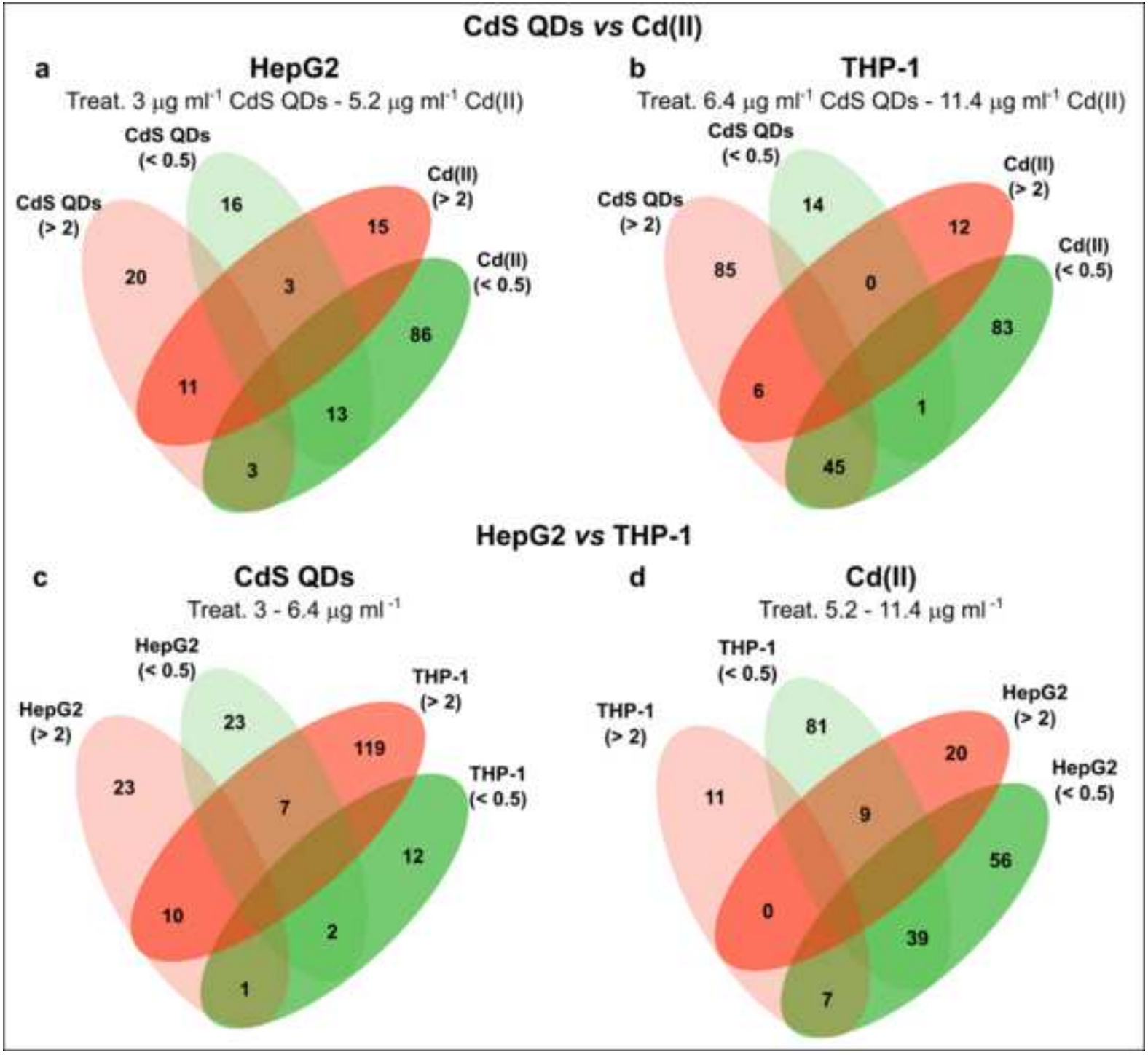

Figure 5

Click here to download high resolution image

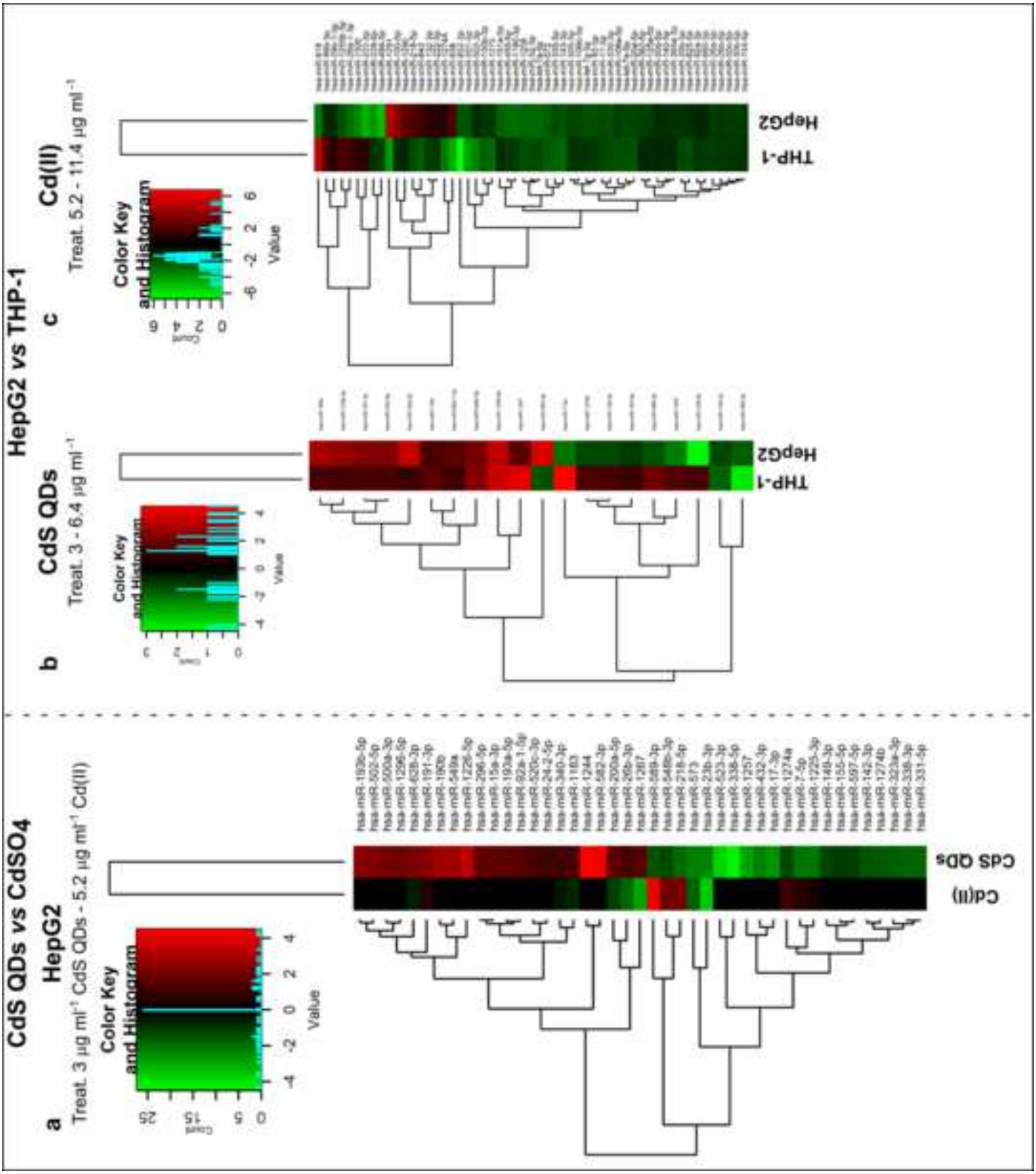

Figure 6

Click here to download high resolution image

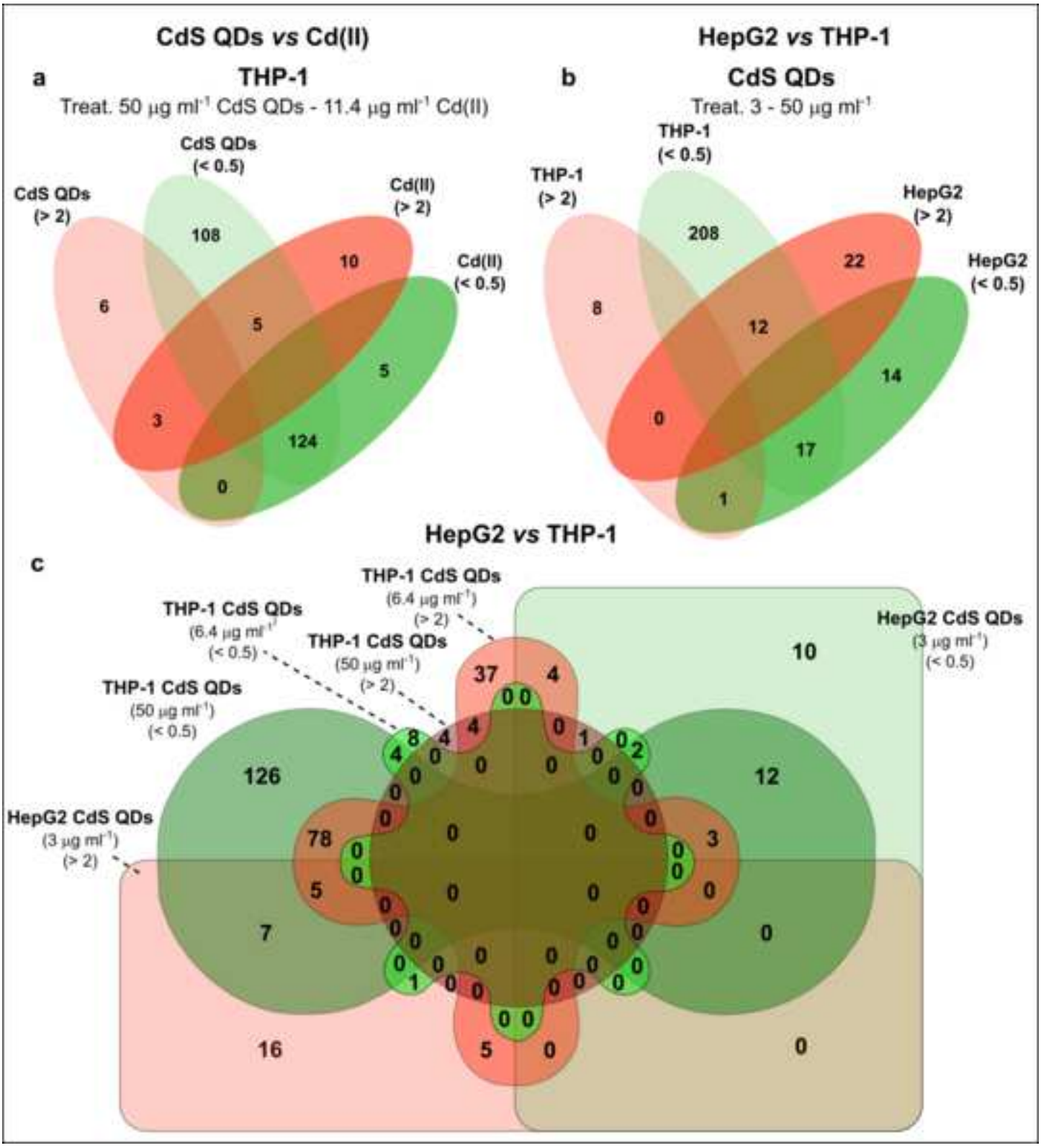

Figure 7

Click here to download high resolution image

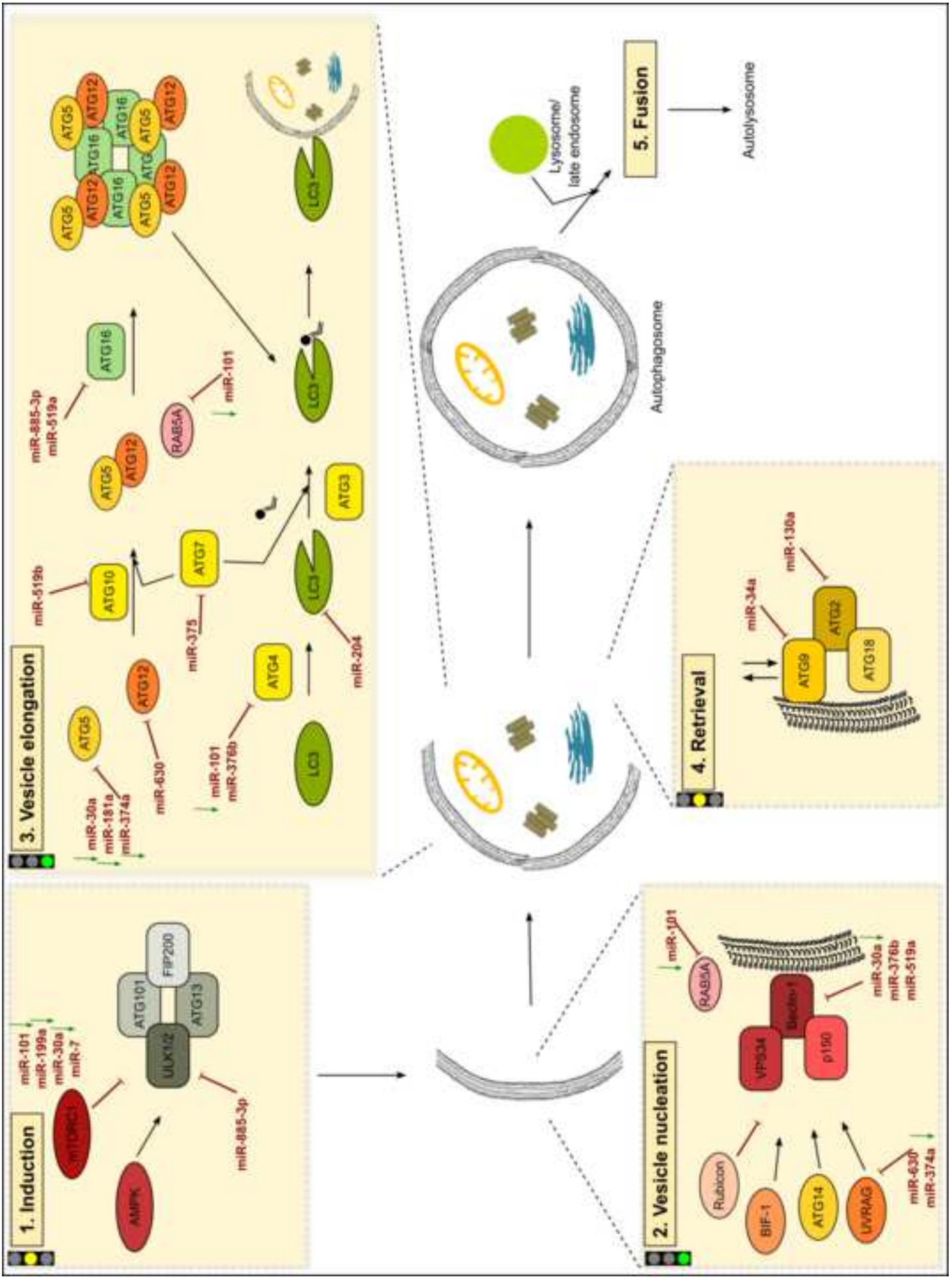

Figure 8

Click here to download high resolution image

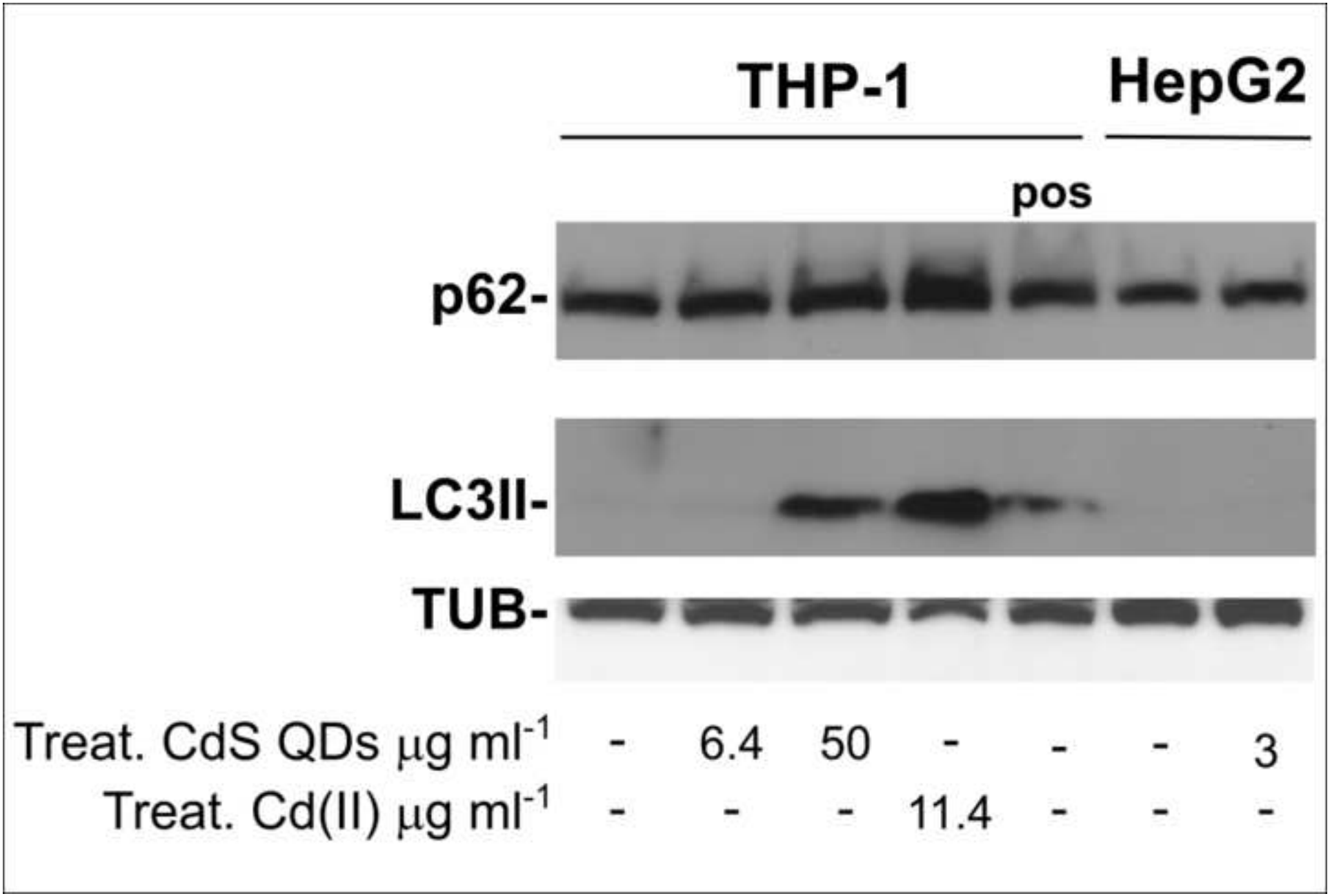

Figure 9

Click here to download high resolution image

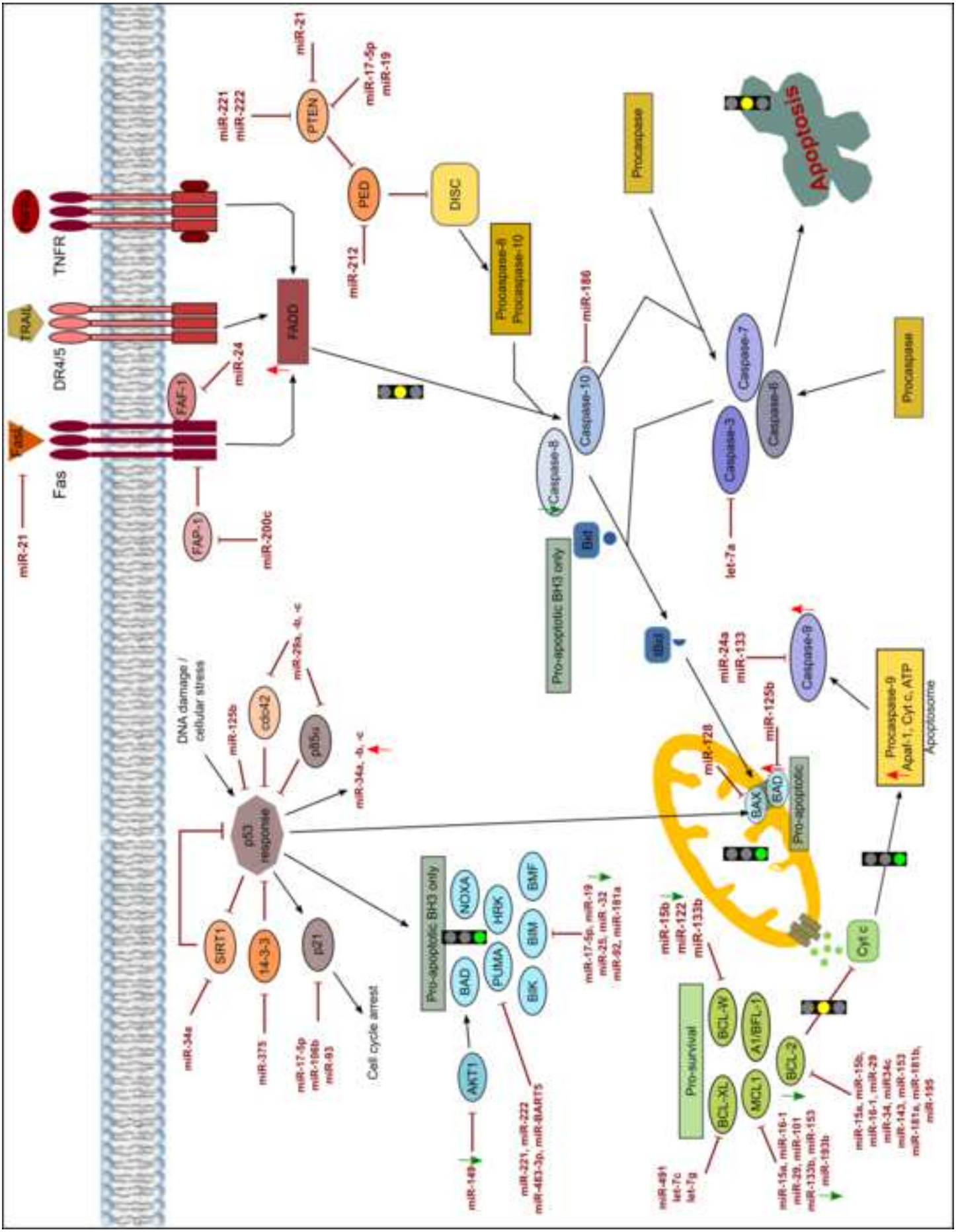

Appendix A

Click here to download Supplementary Material: Revisioned_Appendix A.docx

Data in Brief

Click here to download Data in Brief: Data in Brief.zip

ABSTRACT

Cadmium is toxic to humans, although Cd-based quantum dots exerts less toxicity. Human hepatocellular carcinoma cells (HepG2) and macrophages (THP-1) were exposed to ionic Cd, Cd(II), and cadmium sulfide quantum dots (CdS QDs), and cell viability, cell integrity, Cd accumulation, mitochondrial function and miRNome profile were evaluated.

Cell-type and Cd form-specific responses were found: CdS QDs affected cell viability more in HepG2 than in THP-1; respective IC_{20} values were ~ 3 and ~ 50 μg ml^{-1}. In both cell types, Cd(II) exerted greater effects on viability.

Mitochondrial membrane function in HepG2 cells was reduced 70% with 40 μg ml^{-1} CdS QDs but was totally inhibited by Cd(II) at corresponding amounts. In THP-1 cells, CdS QDs has less effect on mitochondrial function; 50 μg ml^{-1} CdS QDs or equivalent Cd(II) caused 30% reduction or total inhibition, respectively. The different *in vitro* effects of CdS QDs were unrelated to Cd uptake, which was greater in THP-1 cells.

For both cell types, changes in the expression of miRNAs (miR-222, miR-181a, miR-142-3p, miR-15) were found with CdS QDs, which may be used as biomarkers of hazard nanomaterial exposure. The cell-specific miRNome profiles were indicative of a more conservative autophagic response in THP-1 and as apoptosis as in HepG2.

HIGHLIGHTS

- In two human cell lines, Cd toxicity varied depending on its form: nano or ionic.
- Cells were more sensitive to ionic Cd than to Cd as quantum dots.
- HepG2 cells were more sensitive than THP-1 but this did not correlate to Cd uptake.
- Cell-type and Cd-type responses were correlated with the miRNome.
- *In silico* and *in vitro* pathway analysis suggests apoptosis (HepG2) or autophagy (THP-1).

Graphical Abstract

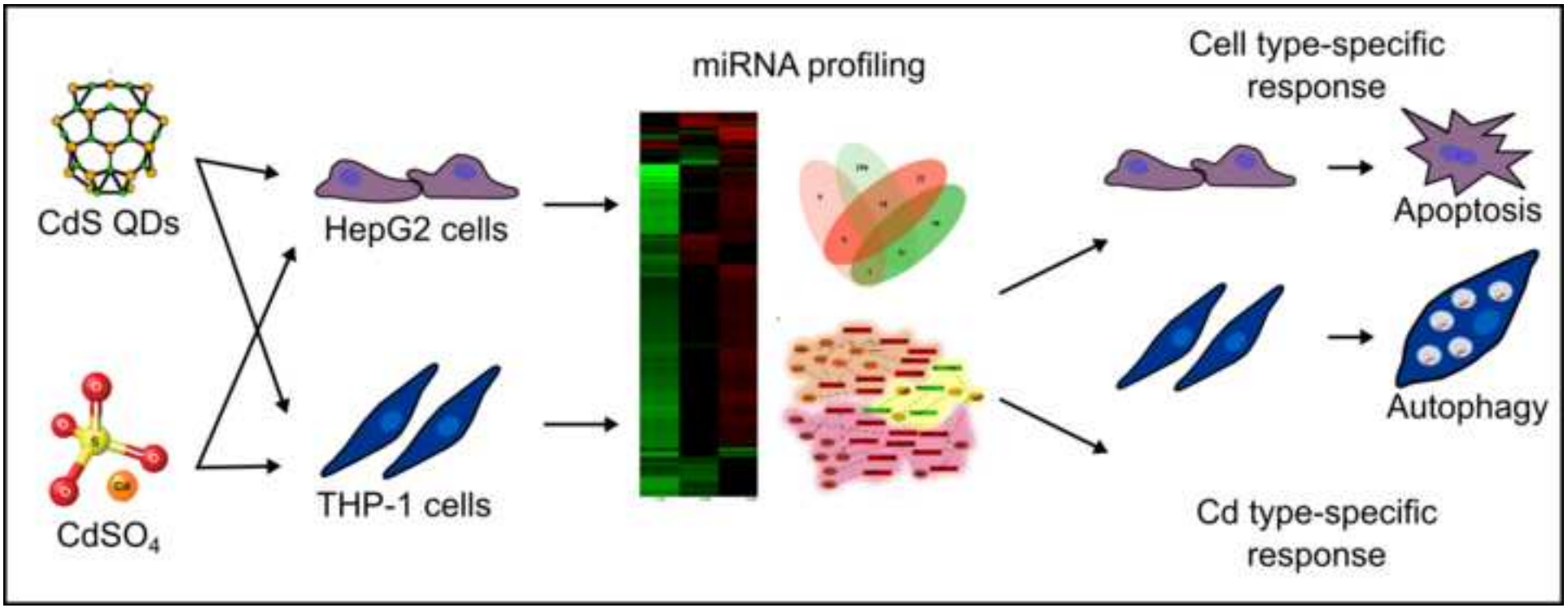

Novelty Statement

This paper describes a novel application of the miRNome to the risk assessment of engineered nanomaterials. Our results show that cadmium induced different effects on HepG2 and THP-1 cells viability and mitochondrial function in nano and ionic forms. The miRNome was found to be specific to both cell type and Cd form, suggesting great potential as a tool to identify biomarkers for environmental and health risk assessment. *In silico* miRNomes analysis suggested HepG2 cells exposed to a low concentration of quantum dots were subject to apoptosis. At a similar concentration, THP-1 cells were little affected but at higher levels, they tended towards autophagy.

***Credit Author Statement**

CRediT author statement

The manuscript was written with contributions from all authors

***Declaration of Interest Statement**

Declaration of interests

☒ The authors declare that they have no known competing financial interests or personal relationships that could have appeared to influence the work reported in this paper.

☐The authors declare the following financial interests/personal relationships which may be considered as potential competing interests: